Density and tracer statistics in compressible turbulence: Phase transition to multifractality

Itzhak Fouxon[*] and Michael Mond[†]
Department of Mechanical Engineering, Ben-Gurion University of the Negev, P.O. Box 653, Beer-Sheva 84105, Israel

(Received 1 April 2019; published 20 August 2019)

We study the statistics of fluid (gas) density and concentration of passive tracer particles (dust) in compressible turbulence. As Ma increases from small or moderate values, the density and the concentration in the inertial range go through a phase transition from a finite continuous smooth distribution to a singular multifractal spatial distribution. Multifractality is associated with scaling, which would not hold if the solenoidal and the potential components of the flow scaled differently, producing transport which is not self-similar. Thus, we propose that the transition occurs when the difference of the scaling exponents of the components, decreasing with Ma, becomes small. Under the smallness assumption, the particles' volumes obey a power-law evolution. That, by the use of conservation of the total volume of the flow, entails the volumes' shrinking to zero with probability 1 and formation of a singular distribution. We discuss various concepts of multifractality and propose a way to calculate fractal dimensions from numerical or experimental data. We derive a simple expression for the spectrum of fractal dimensions of isothermal turbulence and describe limitations of lognormality. The expression depends on a single parameter: the scaling exponent of the density spectrum. We demonstrate that the pair-correlation function of the tracer concentration has the Markov property. This implies applicability of the compressible version of the Kraichnan turbulence model. We use the model to derive an explicit expression for the tracer pair correlation that demonstrates their smooth transition to multifractality and confirms the transition's mechanism. The obtained fractal dimension explains previous numerical observations. Our results have potentially important implications for astrophysical problems such as star formation as well as technological applications such as supersonic combustion. As an example, we demonstrate the strong increase of planetesimal formation rate at the transition. We prove that finiteness of internal energy implies vanishing of the sum of Lyapunov exponents in the dissipation range. Our study leads to the question of whether the fluid density which is an active field that reacts back on the transporting flow and the passive concentration of tracers must coincide in the steady state. This is demonstrated to be crucial both theoretically and experimentally. The fields' coincidence is provable at small Mach numbers; however, at finite Mach numbers, the assumption of mixing is needed, which we demonstrate to be not self-evident because of the possibility of self-organization.

DOI: 10.1103/PhysRevE.100.023111

I. INTRODUCTION

Supersonic turbulence plays a crucial role in processes of fundamental nature such as star formation in dense molecular clouds and density fluctuations in the solar wind as well as in advanced technological applications such as combustion processes in scramjets and drag and stability of supersonically moving bodies in the terrestrial atmosphere. This type of turbulence differs qualitatively from its incompressible counterpart due to the presence of a unique supersonic inertial range. The velocities that characterize the turbulent eddies in this range are larger than the speed of sound so that their compressible and incompressible components are strongly coupled. This causes a transition to another regime: Above a critical Mach number (defined as the ratio of the rms velocity of turbulence and the speed of sound), which is not much larger than 1, the fluid density in the supersonic inertial range becomes a singular field supported on a multifractal set. Thus, the five fluid mechanical fields of mass, momentum, and energy densities are all supported on the multifractal, producing a singular fluid mechanical problem.

The picture becomes even more convoluted and perplexing when the compressible turbulence is seeded with passive tracer particles. These are particles that are carried by the flow but have no back reaction on it. Their spatial distribution can be studied using the methods that proved successful for the investigations of the passive scalar in incompressible turbulence [1]. Since the tracers and the gas satisfy the same continuity equation, then it is tempting to assume that both settle on the same structure in space, and information concerning the latter's spatial distribution may be inferred from following the former. If so, then we could study the density via the tracers, which is a great simplification. Moreover, we would get insight in the dust-to-gas ratio of molecular clouds: When approximating dust particles by tracers, which neglects their inertia and other effects [2], the ratio is constant. This ratio plays a key role in many astrophysical applications, including absorption of light in the interstellar medium, evolution of galactic composition and interstellar medium tracking [3]. Its nonconstancy can have far-reaching consequences [2].

The equality of density and concentration, however, deserves a critical examination. The fluid density is an active

[*]itzhak8@gmail.com
[†]mondmichael@gmail.com

scalar field that reacts back on the transporting flow. Many fluid-mechanical examples of striking difference between active and passive scalars are known; see, e.g., Refs. [1,4] and below. Seemingly, the only (cursory) discussion of the role of back reaction of the density on the transporting compressible flow is found in Ref. [1]. The authors state that density fluctuations do not grow in a statistically steady compressible flow because the pressure provides feedback from the density to the velocity field. This implies that the sum of Lyapunov exponents, defined as the average logarithmic growth rate of infinitesimal volumes of the fluid, is zero for compressible flows. However, the authors of Ref. [5] observed numerically a nonzero sum of Lyapunov exponents of passive tracer particles. This is despite the fact that these particles obey the same equation of motion as the fluid particles representing the active density. These works can be noncontradictory only if the sums of fluid and tracer particles differ. That the difference is possible is probably seen most easily by representing the fluid as a collection of a large number of discrete fluid particles; see Refs. [6,7] for smoothed particle hydrodynamics (SPH). The particles move with the local flow velocity and interact via their back reaction on that velocity. Particles' configurations are then possible that would become stable as a result of the interaction and would not be stable for noninteracting tracers moving with the same local flow velocity (so that the active particles would self-organize). Thus, the tracers would move in the flow field created by the active particles of the fluid; however, they could detach from these particles. The difference of the sums would hold then because of the different stability properties of active and passive fields; cf. Ref. [8].

The issues raised above are currently controversial and unsolved. The assumption of the finite density and zero sum of the Lyapunov exponents faced strong opposition from several of our referees despite the fact that this issue is minor for our paper (it is considered only in Sec. XI and has nothing to do with multifractality in the supersonic inertial range, which is the main object of our studies). Nevertheless, this made us search for a finer formulation. We observe that the fully resolved density field, appearing in the definition of the internal energy, cannot be multifractal since that would produce divergence of that energy at small scales (the internal energy's dependence on the density incorporates the back reaction indirectly). This does not contradict the multifractality in the inertial range, referred to previously. That multifractality is defined by continuation of the behavior of the density in the supersonic inertial range, where the dissipative processes are negligible, to indefinitely small scales. It is that continuation which would produce a singular density supported on a multifractal set. The actual density of the physical fluid is smoothed at a dissipation scale determined by finite values of the dissipation coefficients (the other limitation of the continuation is due to finite speed of sound). Thus, for instance, the density is finite for the shock solutions, which is a typical structure introduced by the compressibility. The density below the shock width is smooth, where the width's value depends on the dissipation coefficients. We demonstrate in Sec. XI that the nonfractal nature of the fully resolved density implies that the sum of Lyapunov exponents vanishes. Our proof is done for isothermal flow since that allows comparison with Ref. [5] and is also most used in the applications. This proof furnishes the conclusion of zero sum under mild assumptions of finite internal energy and flow differentiability in the dissipation range. We remark that for a generic flow, the sum, which is generally nonpositive [9,10], is negative. Thus, compressible fluid flows in this respect differ from the compressible flows describing phase space density of dynamical systems where the sum is generically negative [9]. Finally, we remark that our conclusion that fully resolved density is not multifractal must be compared with the observation of multifractality of passive concentration done in Ref. [5]. That observation, as it stands, is noncontradictory since the concentration is a passive field, of which values are unrestricted by the demand of finite internal energy. However, as above, n and ρ must then differ in the steady state (hereafter concentration n refers to tracers and density ρ to the fluid).

The evolution of initially different distributions of tracers converges at large times to the same unique time-dependent solution of the continuity equation. This solution can be called the natural measure by analogy with time-independent flows [9,11–13]. The convergence holds because of the mixing, similar to the incompressible turbulence. The only difference is that the mixing occurs on the asymptotic attractor of typical trajectories of the tracers and not in the whole volume of the flow.

The evolution to the natural measure holds for generic initial conditions. Nongeneric initial conditions of measure zero can produce other steady-state solutions of the continuity equation [14]. The active density can be a nongeneric steady state. This possibility can be seen by considering the famous difference between the active vorticity $\boldsymbol{w}(t,\boldsymbol{x})$ and the passive magnetic $\boldsymbol{B}(t,\boldsymbol{x})$ fields in incompressible turbulence [1]. If the magnetic resistivity coincides with the fluid viscosity, then the magnetic field obeys the same first order in time evolution equation as the vorticity. This equation is linear if the flow is considered as given. Thus, both $\boldsymbol{w}(t,\boldsymbol{x})$ and $\boldsymbol{B}(t,\boldsymbol{x})$ are obtained from their respective initial conditions, $\boldsymbol{w}(t=0,\boldsymbol{x})$ and $\boldsymbol{B}(t=0,\boldsymbol{x})$, by the same linear integral transformation $B_i(t,\boldsymbol{x})=\int G_{ik}(t,\boldsymbol{x};\boldsymbol{x}')B_k(t=0,\boldsymbol{x}')d\boldsymbol{x}'$ and $w_i(t,\boldsymbol{x})=\int G_{ik}(t,\boldsymbol{x};\boldsymbol{x}')w_k(t=0,\boldsymbol{x}')d\boldsymbol{x}'$, where $G_{ik}(t,\boldsymbol{x};\boldsymbol{x}')$ is the Green's function; see details in Subsec. XII F. This transformation dictates unbounded growth for the magnetic field that exerts no back reaction on the flow, which is the so-called magnetic dynamo; see, e.g., Ref. [15]. The growth holds for a generic initial condition. In contrast, the vorticity is stationary even though it is given by the same transformation. The stationarity holds because the initial condition for the vorticity is nongeneric with respect to the above transformation, which is what the zero measure initial condition is; see details in Subsec. XII F.

The data available at present do not allow us to conclude unequivocally whether $n=\rho$ holds in the steady state; see the next paragraph. The theory also falls short of resolving the issue. Mixing of density that reacts back on the flow demands the study of a strongly nonlinear problem, which is probably unfeasible. It is known that in the case of mixing by incompressible flow the back reaction changes the statistics significantly [4]. Thus, in this work, we derive results on n and ρ that do not depend on their equality. The theory is mainly possible for the passive concentration which obeys

the linear equation; cf. this with the similar situation in the incompressible case [1]. We propose that further progress demands numerical comparison of the statistics of n and ρ. We provide a number of testable predictions that would help to make the comparison and describe the subtle points that could bring erroneous conclusions in future studies.

The currently existing numerical data, although inconclusive, indicate a finite difference between the fields. Spatial distribution of tracers for three different values of the Mach number Ma was studied in Ref. [5]. Multifractal distribution in the inertial range of turbulence was conclusively found at $\mathrm{Ma} = 4.6$ and thus holds also at higher Mach numbers. At the same time, the observations of Ref. [16] revealed that the density spectrum's decay is faster than k^{-1} at $\mathrm{Ma} = 6$. This decay corresponds to nonfractal distribution in space, as we prove in detail below (the data of Ref. [17] demonstrate that at $\mathrm{Ma} \simeq 7$ the decay is slower than k^{-1} and thus the density is multifractal). Thus, seemingly multifractality can hold earlier in Ma for the concentration than for the density. This implies a finite difference of n and ρ. The difference was observed also in the simulations of Ref. [6], where it was attributed to numerical artifacts. However, a definite conclusion needs a purposeful comparison of n and ρ in the same flow that is yet to be done.

In this paper, we present theoretical results that indicate that concentration must be multifractal under the conditions of the simulations of Ref. [16]. We demonstrate in three different ways that if the scalings of the solenoidal and the potential components of the velocity are approximately equal, then the concentration is multifractal. In fact, this seems necessary: Multifractality implies scaling, which demands scaling of the transporting flow. This provides a simple view of the concentration's transition to multifractality. The scalings' difference is of order 1 at $\mathrm{Ma} \lesssim 1$ where the concentration is a large-scale nonfractal field, which is approximately constant in the inertial range. The Mach number's increase closes the scaling gaps (see, e.g., Ref. [16]), resulting in a multifractal distribution (the Mach number at which the scalings become identical with considered accuracy will be designated below by Ma_s). This seems to be the situation of Ref. [16], where the components' scalings are very similar. We manage to pinpoint which properties of the flow in this situation determine the fractal correlation dimension of the concentration. We propose that similar properties determine the dimension of the density and demonstrate that this explains the observed dependence of the fractal dimension of the density on the compressibility of the forcing [18].

We remark that the question of the difference between the fluid density and the concentration of passively transported particles was previously raised in Ref. [2]. In that case, however, the passively transported dust particles detach from the carrying flow due to inertia and their concentration does not obey the same continuity equation as the fluid density. It was observed that dust particles form a multifractal that is more rugged than that formed by the gas particles; see, however, Ref. [19].

Density multifractality is a qualitative property of supersonic compressible turbulence that holds above a critical Mach number $\mathrm{Ma}_{\mathrm{cr}}$ (considering the question of whether $\mathrm{Ma}_{\mathrm{cr}} = \mathrm{Ma}_s$ open). The phenomenological theory of compressible turbulence existing today has been constructed in Ref. [20] on the basis of Ref. [21]. It assumes that density fluctuations grow at decreasing scale as a power law with negative exponent. This growth is assumed to be self-similar and thus governed by a single scaling exponent α which is the fitting parameter of the theory. This assumption is true for fractal but not multifractal support of the density. A kinetic energy cascade has been further assumed [22], which implies that velocity weighted by the density in power $1/3$ behaves as the velocity of incompressible turbulence. Indeed, it was observed [16,23] that for the weighted velocity the third-order structure function scales linearly with the distance and the spectrum is close to the spectrum of incompressible turbulence [24] if the forcing is solenoidal [25]. However, using these assumptions, α derived from the scaling of the third-order structure function of the velocity would be different by about factor of 2 from that derived from the scaling of the first-order structure function [16]. Introducing the notion of multifractality of the density, due to which α is nonconstant and fluctuates in space, is therefore a necessary step toward unravelling the complex nature of supersonic turbulence.

Despite the crucial role it plays in compressible turbulence, there is currently no consistent description of the multifractal properties of the gas density and tracer concentration. It is unknown what determines the critical Mach number for the transition to multifractality and whether it is independent of the degree of compressibility of the stirring force (universality). Moreover, the physical mechanisms that lead to the transition to multifractality are currently not well understood. The present work aims at filling this gap. To this end, we present a thorough discussion of the spectrum of the multifractal dimensions of density and concentration distributions and propose a viable method to calculate it from numerical and experimental results. In particular, for density of isothermal turbulence, which is characterized by a log-normal probability distribution function, we derive an explicit expression for the multifractal dimension spectrum that depends on a single parameter, the exponent of the pair correlation function. In addition, various physical processes and mechanisms that lead to the transition to multifractality are discussed. In particular, we show by employing a heuristic cascade model that as the scalings of the compressive and solenoidal components of the velocity grow closer as the Mach number is raised, the concentration transforms from a large-scale smooth field to a small-scale multifractal.

Carrying out the calculations that are proposed in the current work, such as multifractal dimensions, following Lagrangian trajectories, and examining the various mechanisms that are introduced and discussed in the next sections pose great challenges because of the essential inability to obtain analytical solutions of the Navier-Stokes equations (NSE) in a turbulent flow regime. We demonstrate that in fact this is unnecessary for the study of pair correlations of tracers. We demonstrate in Sec. VIII that the pair-correlation function of concentration obeys a closed stationarity condition. This is derived by considering the conservation of the pair correlation function in the steady state, which holds at any times, at large times. This brings simplifications. We find that the correlation function must be invariant under the action of integral operator whose kernel is the propagator of the interpair distance, that

is, the transition probability for the distance between a pair of particles separating in the supersonic inertial range. Thanks to considering the invariance at large times, the distance has the Markov property. Therefore, instead of the full solution of the NSE, we can use an effective velocity whose dependence on time is described by white noise. This passage is rigorous and parallels the description of complex molecular forces by the Langevin white-noise terms in the theory of Brownian motion. If we further make an assumption of at least qualitative validity of the eddy diffusivity approximation, then we find that the propagator can be described using the famous Kraichnan's model [1]. We stress that this is the model of turbulent transport valid at large times and not the model of turbulence itself (for models of turbulence, see e.g., Refs. [26,27]). The modeled quantity of the NS flow is the large-time propagator of two tracers and not the NS flow itself, which, of course, is not a white noise in time. These are different conceptually. We also observe the transport's robustness: Many properties of the transported fields hold irrespective of the details of the transporting flow [1]. Here we employ the compressible version of Kraichnan's model in order to shed light on the physical processes that participate in the transition to multifractality. In particular, we show by detailed analytical calculations that the simultaneous convergence of the scalings of the compressible and solenoidal components of the velocity to a single limit does indeed underlie the transition from a large-scale smooth distributions to multifractal measure. Also, we unravel the important role played by the effective attractive force that is generated by negative velocity divergence. Thus, the analytical calculations based on Kraichnan's model reveal that as the Mach number increases the number of times that two tracers collide with each other grows until a critical Mach number is reached, beyond which the number of collisions is infinite (return with probability 1). The relation of this phase transition to the phase transition of the density is yet unclear.

The transition of the tracers' distribution within a gas to multifractality has significance to the chemical interaction between a fuel and an oxidant. The process rate depends naturally on the second power of the various relevant tracers' concentrations. Fluctuations of the latter are significantly enhanced due to the transition to multifractality where clusters and filaments of practically infinite concentration are formed. Therefore, a dramatic increase in the process rate is expected at the transition. As an example, we demonstrate that the transition to multifractality indeed results in a significant decrease of the formation time of planetesimals.

Recent years have seen much research on the long-standing problem of supersonic turbulence [2,16,23,25,28–40]. Progress was previously hampered by the lack of an exact scaling law that would be the counterpart of the four-fifths law of incompressible turbulence [41]. It was unclear whether the concepts of energy cascade and approximate self-similarity that proved indispensable in the theory of incompressible turbulence can be extended to the compressible case [33,35,38]. Despite progress (see the references above), the problem is still unsolved.

Theoretical studies of how the transition to multifractality could arise from models of compressible turbulent transport seemingly were not done before the present work. Previous approaches to the statistics of the density relied significantly on random shocks as elementary structures whose superposition forms the distribution; cf. Refs. [42–45]. Here, we do not consider the derivation of the density statistics (though we do derive fractal dimensions from log normality of the density in isothermal case). We derive the statistics of the concentration field, which is, however, quite similar to the density. It might then look problematic that shocks do not have a separate role in our approach. Thus, we stress that our work does not imply that we rule out the possibility that the statistics could be derived from the shocks. Rather, we take a different approach to the same statistics for the reason that we can provide consistent derivations. Our derivation starts from the continuity equation and observes that pair correlation function of the concentration (equivalent to the usually studied spectrum) can be derived from the asymptotic form of the transition probability of the interpair distance at large times. This probability, which is the object of our modeling, integrates turbulent statistics and contains shock contributions well hidden inside its functional form. Thus, when we use the Kraichnan model, we model the asymptotic transition probability and not the flow. In this model, we use it as given that the gap Δ of the scaling exponents of the solenoidal and potential components closes at increasing Ma, as indicated by the numerical observations (we can define Δ as half of the difference of the scaling exponents of the spectra of solenoidal and potential components). We do not try to construct the theory of the gap's dependence on the Mach number, $\Delta(\mathrm{Ma})$. That theory is highly desirable and would probably demand the study of contributions of the shocks to various statistical quantities. Furthermore, our model does not necessarily produce realizations of concentration that would be similar to those in the Navier-Stokes turbulence. (It must be told, though, that the concentration discontinuities, known as fronts or ramp-cliff structures, exist already in incompressible flows, which do not have shock solutions, and the incompressible Kraichnan model [46,47]. Thus, there is little doubt that shock-type structures would be seen in realizations of compressible Kraichnan model. For comparison of fronts with compressible shocks, see Ref. [48].) However, statistically, the model probably would work well, as is clear from our observation of the Markov property. Thus, we find it highly plausible that our derivation of the transition to multifractality from the model captures the origin of the transition. This approach is not so different from traditional approaches to the phase transitions that employ Ising or other models. In our case, we reinforce this approach by providing a detailed phenomenological description. That demonstrates that multifractal distribution must occur at $\mathrm{Ma} > \mathrm{Ma}_s$, where the scaling exponents' gap is negligible, because the volume compressions scale proportionally to the changes of the interparticle distances. Conversely, at $\mathrm{Ma} < \mathrm{Ma}_s$, where there is no proportionality, the scaling, implied by multifractality, cannot hold. Together, the phenomenological description and the quantitative study of the Kraichnan model provide a convincing picture of the transition. The estimate of Ma_s at which we predict the transition agrees with the Mach numbers at which the transition is observed. Finally, we remark that the measurements of the transition itself and its vicinity are yet to be done: The present data are either above or below the transition. The rms value of the density and/or concentration

can be used as an order parameter. That value undergoes a strong increase over a narrow range of Ma.

We describe the organization of the text below. In the next section, we introduce the fluid mechanical equations and their multifractal properties. In Sec. III, we describe the elementary process of formation of the multifractal concentration. This is power-law growth of volumes of tracers holding at negligible Δ. At large times, the volumes shrink to zero with probability 1, generating a singular distribution. We demonstrate that the evolution of volumes occur by a cascade process. In Sec. IV, we use mass conservation for passing from volumes to concentration and describe the evolution of smooth initial conditions to the multifractal steady state distribution. Section V is devoted to the description of the multifractal formalism and Rényi dimensions, whose use might simplify the measurement of fractal dimensions. Section VI derives the spectrum of fractal dimensions of isothermal turbulence. The result is of high interest because many simulations of this type of turbulence have been performed. We correct some previous misconceptions. We introduce the cascade model of formation of fluctuation of concentration in Sec. VII. This model is closer to being rigorous than similar models for incompressible turbulence [41]. Fully rigorous theory is constructed in Sec. VIII. We derive the stationarity condition on the pair correlation function of concentration, study when it has power-law solutions describing multifractality, and relate the scaling of the higher order correlation functions to the famous zero modes [1,49]. This study is done in a model-independent way. We use the applicability of the Chapman-Kolmogorov equation for introducing the Kraichnan model in Sec. IX. We derive the pair-correlation function and the smooth transition to multifractality. We confirm by concrete calculation the general connection between the properties of pair dispersion in the supersonic inertial range and the correlation dimension of the multifractal. Section X describes the acceleration of formation of planetesimals due to the transition to multifractality. This parallels similar acceleration phenomenon in the rain formation [50]. The properties of the dissipation range are considered in Sec. XI. Section XII is devoted to the study of different arguments that could be used for proving that in the steady state $n = \rho$ and how they all fall short of providing the proof. The final section summarizes our main results and describes open questions. Some more detailed calculations are put in the Appendixes.

II. SETTING

The continuity equations for the fluid density ρ and the tracers' concentration n read

$$\partial_t \rho + \nabla \cdot (\rho \boldsymbol{v}) = 0, \quad \partial_t n + \nabla \cdot (n\boldsymbol{v}) = 0, \tag{1}$$

where $\boldsymbol{v}$ is the same transporting flow that obeys

$$\rho(\partial_t \boldsymbol{v} + (\boldsymbol{v}\cdot\nabla)\boldsymbol{v}) = -\nabla p + \rho \boldsymbol{a} + \nabla\sigma'. \tag{2}$$

Here, $\boldsymbol{a}$ is the (random) driving acceleration and σ'_{ik} is the viscous stress tensor. The coupling of the velocity to the density can be the fifth energy (or entropy) equation of fluid mechanics or the barotropic equation of state $p = p(\rho)$ that describes the dependence of the pressure p on ρ. The case of isothermal fluid,

$$\rho(\partial_t \boldsymbol{v} + (\boldsymbol{v}\cdot\nabla)\boldsymbol{v}) = -c_s^2\nabla\rho + \rho\boldsymbol{a} + \nabla\sigma', \tag{3}$$

where c_s is constant, is of high interest because of its astrophysical applications; see, e.g., Ref. [16] and cf. Ref. [51]. In this case, the equations are invariant with respect to rescaling of the density by a constant; cf. Ref. [42]. The internal energy E is proportional to the Gibbs entropy S,

$$E = -c_s^2 S, \quad S = -\int \rho \ln \rho d\boldsymbol{x} = -\langle \rho \ln \rho\rangle. \tag{4}$$

The entropy's properties imply that E is minimal at the state of constant density $\rho = 1$, where it is zero [10].

We consider stationary homogeneous turbulence. The equations can be characterized by the dimensionless Reynolds number $\mathrm{Re} = UL/\nu$ and the Mach number $\mathrm{Ma} = U/c_s$. Here, U is the rms of the flow where the mean flow is assumed to be zero, L is the scale of the stirring force, ν is the kinematic viscosity, and c_s is the speed of sound. The Reynolds number is assumed to be large. We use units where the volume of the flow is 1 and also $\langle\rho\rangle = \langle n\rangle = 1$. Here and below, angular brackets stand for spatial averaging. Thus, ρ and n are normalized dimensionless non-negative functions. This allows us to consider them as probability density functions, which is useful sometimes.

An explicit formula for density or concentration via $\boldsymbol{v}$ can be provided. These fields evolve due to the combined action of convection, causing the mixing and volume compression or rarefaction. This is described by the solution of the continuity equation,

$$\rho(t, \boldsymbol{q}(t,\boldsymbol{x})) = \rho(\boldsymbol{x}) \exp\left(-\int_0^t w(t', \boldsymbol{q}(t',\boldsymbol{x}))dt'\right), \tag{5}$$

where $t > 0$ or $t < 0$; $w(t,\boldsymbol{x}) = \nabla\cdot\boldsymbol{v}(t,\boldsymbol{x})$; $\boldsymbol{q}(t,\boldsymbol{x})$ are Lagrangian trajectories labeled by their $t = 0$ positions,

$$\partial_t \boldsymbol{q}(t,\boldsymbol{x}) = \boldsymbol{v}(t,\boldsymbol{q}(t,\boldsymbol{x})), \quad \boldsymbol{q}(0,\boldsymbol{x}) = \boldsymbol{x}. \tag{6}$$

Here and below, we use the notation $\rho(\boldsymbol{x}) \equiv \rho(0,\boldsymbol{x})$. The mixing in Eq. (5) is described by the spatial proximity of $\boldsymbol{q}(t,\boldsymbol{x})$ for $\boldsymbol{x}$ from space regions with very different $\rho(\boldsymbol{x})$. The compression is described by the exponential factor. An identical formula holds for the concentration.

We define the supersonic inertial range of scales which is of main interest in this paper. Turbulence is excited at scale L, which is the characteristic scale of acceleration $\boldsymbol{a}$ in Eq. (2). It is assumed that the rms velocity at scale L is larger than the speed of sound. The flow instabilities generate fluctuations (eddies) of velocity and density with scales smaller than L. The characteristic velocity of the eddies decreases, becoming of the order of the speed of sound at the sonic scale l_s. Turbulence below l_s behaves as a low-Mach-number quasi-incompressible turbulence with almost uniform density in the inertial range [2]. In some cases, the dissipative scale l_d, defined by the condition that the local (defined with velocity of eddies with this scale [41]) Reynolds number is of order 1, is larger or comparable with l_s (in simulations $l_s \sim l_d$ holds often [16]). Thus, we define $\eta = \max[l_s, l_d]$. Then, the range of scales between η and L defines the supersonic inertial range. Turbulent eddies with a characteristic scale in this range are weakly influenced by viscosity and are supersonic.

Multifractality of ρ and n holds in the supersonic inertial range, showing that in the steady state

$$\langle \rho_r^k \rangle \sim \left(\frac{L}{r}\right)^{\zeta(k)}, \quad \langle n_r^k \rangle \sim \left(\frac{L}{r}\right)^{\check{\zeta}(k)}; \quad \eta \ll r \ll L, \tag{7}$$

where the angular brackets stand for the usual spatial averages (which use is more standard here than the averages over the stationary measure; see the discussion later). These properties are formulated for the coarse-grained fields, where for any function $F(\boldsymbol{x})$ we define

$$F_l(\boldsymbol{x}) \equiv \frac{3}{4\pi l^3} \int_{|\boldsymbol{x}-\boldsymbol{x}'|<l} F(\boldsymbol{x}') d\boldsymbol{x}'. \tag{8}$$

The fluctuations below η are smoothed by the effective incompressibility of the flow there or the dissipation. It will be often useful to consider the limit $\eta \to 0$, similar to the use of $\nu \to 0$ limit in the study of incompressible turbulence [41].

We remark that having a large supersonic inertial range, $L \gg \eta$, does not necessarily imply that Ma $\gg 1$. Indeed, if we denote the scaling exponent of the velocity in this range by χ, then the sonic scale is determined by the condition $(L/l_s)^{\chi} \sim$ Ma so that $L/l_s \sim \mathrm{Ma}^{1/\chi}$. For instance, for Kolmogorov scaling $\chi = 1/3$, we would have cubic growth of L/l_s with Ma. The real growth is slower because of deviations from the Kolmogorov scaling and must by roughly quadratic using χ from Ref. [16]. Thus, the supersonic inertial range may be well defined already at Ma $\simeq$ 4–5.

III. DEVELOPMENT OF MULTIFRACTALITY: EVOLUTION OF VOLUMES

In this section, we consider the elementary process of development of multifractality in supersonic turbulence. This is the growth of volumes of tracers in the supersonic inertial range starting from initially spherical shape. The concentration, which by mass conservation is inversely proportional to the volume, is inferred from the volumes in later sections. We demonstrate that if the solenoidal and the potential components of the flow scale similarly, then the volumes obey a power-law dependence on the time that is associated with formation of a multifractal structure in space. This has a remarkable implication that in the limit of infinite evolution time the volumes decay to zero with probability 1. Thus, in the steady state the mass concentrates on a set with zero volume. This is the singularity characterizing multifractal distributions (we stress that the fluid itself remains a continuum; this is only an effective description of the supersonic inertial range). This decay does not contradict the conservation of the total volume since the decay is strongly nonuniform in space (intermittency). At any, however large but finite, time there are volumes that expanded, providing for the constant total volume.

We demonstrate that the concept of the sum of Lyapunov exponents can be generalized to the inertial range using a logarithmic time variable. The consideration parallels the consideration of similar facts in smooth flows [1,52], from which review we start. The considerations of this section are mostly phenomenological as in the Richardson law or many other considerations of turbulence. Precise calculations can be done in the frame of the Kraichnan model; see Ref. [1] and below.

A. Introduction: Volumes in smooth flows

We consider behavior of tracers in a generic compressible smooth flow. The smooth flow is mostly not the object of the study of this paper and it is studied here as a known case from which the notions will be transferred to the case of interest. The smooth flow can be a flow of a chaotic system or, in the case of turbulence, the flow below the dissipation scale, similar to the flow below the Kolmogorov scale of incompressible turbulence [41]. We observe that very generally the tracers are attracted to regions with negative divergence. This is because the flux of the particles to any region is proportional to the integral over the region's surface $\int \boldsymbol{v} \cdot d\boldsymbol{S}$ that equals the volume integral $\int \nabla \cdot \boldsymbol{v} d\boldsymbol{x}$. Thus, there is an effective attraction of particles that move to the same regions of the flow. This attraction causes shrinking of volumes of particles to zero and formation of multifractal. This conclusion is rigorously proved as the statement that infinitesimal volumes of the fluid particles decay to zero with probability one; see Refs. [9,10] and Appendix A, where the proof is reproduced (the case with anticorrelations causing the sum to vanish is nongeneric and is not considered here). The decay is exponential and its exponent defines the sum of the Lyapunov exponents $\sum_{i=1}^{3} \lambda_i$; see the next paragraph. How general this conclusion is can be understood by recasting it as a form of the second law of thermodynamics, which in this case is deduced from the microscopic description [10,53].

The evolution of an infinitesimal volume $V_s(t, \boldsymbol{x})$ of tracers initially located near $\boldsymbol{x}$ is determined by the Jacobian of the Lagrangian mapping defined in Eq. (6),

$$\ln V_s(t, \boldsymbol{x}) \propto \ln \det \frac{\partial \boldsymbol{q}(t, \boldsymbol{x})}{\partial x} = \int_0^t w(t', \boldsymbol{q}(t', \boldsymbol{x})) dt', \tag{9}$$

where the subscript stands for smooth. There is a property of the evolution that is described by the time average of the type considered in the ergodic theorem [12,13]. This defines

$$\sum_{i=1}^{3} \lambda_i \equiv \lim_{t\to\infty} \frac{1}{t} \ln \det \frac{\partial \boldsymbol{q}(t, \boldsymbol{x})}{\partial x} = \lim_{t\to\infty} \frac{1}{t} \int_0^t w(t', \boldsymbol{q}(t', \boldsymbol{x})) dt'. \tag{10}$$

The limit by the ergodic theorem is independent of $\boldsymbol{x}$ with exception of a nonempty set Ω of $\boldsymbol{x}$ with zero total volume. The nonemptiness here is necessary. The space-averaged Jacobian $\langle V_s(t, \boldsymbol{x}) \rangle$ is a time-independent quantity equal to 1 due to the conservation of the total volume. At the same time, for a generic flow with $\sum_{i=1}^{3} \lambda_i < 0$, Eq. (10) implies exponential decay of volumes with probability 1. The exponential decay and $\langle V_s(t, \boldsymbol{x}) \rangle = 1$ are noncontradictory since the convergence of the limit in Eq. (10) is strongly nonuniform. Thus, for each $\boldsymbol{x}$ in Eq. (10) we could define time $t^*(\boldsymbol{x})$ as the smallest time beyond which $t^{-1} \ln \det \nabla \boldsymbol{q}(t, \boldsymbol{x})$ is within an ϵ neighborhood of $\sum_{i=1}^{3} \lambda_i$. Spatial distribution of $t^*(\boldsymbol{x}, \epsilon)$ is highly intermittent since points in vicinity of Ω produce arbitrarily large values of t^*. This is a consequence of continuity of $\det \nabla \boldsymbol{q}(t, \boldsymbol{x})$ at any finite t. The issuing statistics

of the volumes can be described assuming that $w(t, \boldsymbol{q}(t, \boldsymbol{x}))$ has a finite correlation time τ_c. This assumption holds for turbulent flows and is also true for many nonrandom chaotic flows described by the ergodic theory [12,13]. At times much larger than the correlation time of $w(t, \boldsymbol{q}(t, \boldsymbol{x}))$, the integral in Eq. (10) is roughly a sum of a large number $\sim t/\tau_s$ of independent random variables (as seen by decomposing the integral into the sum of contributions of intervals with length $\sim\tau_c$). Its cumulants grow linearly with time and we find, using the cumulant expansion theorem,

$$\left\langle V_s^k(t)\right\rangle \sim \exp[\gamma(k)t], \tag{11}$$

that holds for space averages at large times [1,54]. Hölder's inequality implies that $\gamma(k)$ is a convex function. Besides the trivial zero at $k = 0$, this function has also a zero at $k = 1$ because this moment gives the conserved total volume of the flow [53]. Thus, if $\gamma(k)$ is not degenerate, we have $\gamma(k) < 0$ for $0 < k < 1$ and $\gamma(k) > 0$ otherwise. This implies $\gamma'(0) < 0$, which agrees with the previously stated negativity of the sum. In fact, it is readily seen from Eqs. (9)–(11) that $\gamma'(0) = \sum_{i=1}^3 \lambda_i$. Writing the moments of V_s with the help of the PDF $P(\sigma_s, t)$ of $\sigma_s = \ln V_s(t)/t$,

$$\left\langle V_s^k(t)\right\rangle \equiv \int P(\sigma_s, t)\exp(kt\sigma_s)d\sigma_s \sim \exp[\gamma(k)t], \tag{12}$$

can be considered as an equation for $P(\sigma_s, t)$. Its solution is given by [55]

$$P \sim \exp\left[-tS(\sigma_s)\right], \quad \max_x[kx - S(x)] = \gamma(k), \tag{13}$$

where $S(x)$ is called the large deviations or rate function. This function is the Legendre transform of the convex function $\gamma(k)$ and thus also convex. It is readily seen by considering $\gamma(0)$ and $\gamma'(0)$ via $S(x)$ that the rate function is non-negative and has a unique minimum of zero taken at $x = \gamma'(0) = \sum_{i=1}^3 \lambda_i$. These conclusions could also be obtained directly from Eq. (9); see Refs. [1,52].

It is seen from Eq. (13) using the properties of $S(x)$ that the limiting distribution $P(\sigma_s, t \to \infty)$ is $\delta(\sigma_s - \sum_{i=1}^3 \lambda_i)$. This reproduces Eq. (10): We have

$$\lim_{t\to\infty} \frac{\ln V_s(t, \boldsymbol{x})}{t} = \gamma'(0) = \sum_{i=1}^3 \lambda_i < 0, \tag{14}$$

with probability 1. In application to real volumes with small but finite size, the limit above can be used only as long as the largest linear size of V_s is smaller than the smoothness scale of the flow (that is the scale below which velocity difference is well described by Taylor series).

We reach the conclusion that in the nondegenerate case of $\sum_{i=1}^3 \lambda_i < 0$ infinitesimal volumes decay to 0 with probability 1; cf. the discussion of Eqs. (9)–(11). This is how one can see that at large times the particles accumulate on a set with zero volume (the strange attractor) in the case of smooth dynamics. It is impressive that this conclusion is so general. It uses smoothness, finite correlation time [that underlies the exponential behavior of the moments in Eq. (11)], the assumption that $\gamma(k)$ is not identically zero, and volume conservation $\gamma(1) = 0$.

B. Self-similar flow in the supersonic inertial range

Remarkably, if the velocity is self-similar, which neglecting intermittency is the case of equal scaling of the solenoidal and potential components, then there is a counterpart of the above consideration in the supersonic inertial range. In this case, the volumes $V_l(t, \boldsymbol{x})$ of tracers which occupy at $t = 0$ a ball of radius l centered at $\boldsymbol{x}$ have in logarithmic time variable behavior similar to $V_s(t, \boldsymbol{x})$ in the smooth case. The flow's self-similarity implies power-law behavior of the volumes,

$$\left\langle V_l^k(t)\right\rangle \sim t^{\gamma_1(k)}, \tag{15}$$

where $\gamma_1(k)$ has behavior similar to $\gamma(k)$ in the smooth case. This behavior implies that volumes in the inertial range decay with probability 1,

$$\lim_{t\to\infty} \frac{\ln V_l(t, \boldsymbol{x})}{\ln t} = \gamma_1'(0) < 0, \tag{16}$$

which implies the development of the multifractal distribution. The rest of this section is devoted to developing a detailed physical picture of Eq. (15).

The self-similarity of the flow holds above a critical Mach number Ma_s, where the subscript stands for scaling. This number is defined by the condition that the scaling of the solenoidal, $\boldsymbol{v}_s(\boldsymbol{x}, t)$, and potential, $\boldsymbol{v}_p(\boldsymbol{x}, t)$, components of the velocity is approximately equal at $\mathrm{Ma} > \mathrm{Ma}_s$. Thus, for instance, for a second-order structure function of the components, we have

$$\begin{aligned} \langle(\boldsymbol{v}_s(\boldsymbol{x}) - \boldsymbol{v}_s(0))^2\rangle &\sim x^{\chi_2}, \\ \langle(\boldsymbol{v}_p(\boldsymbol{x}) - \boldsymbol{v}_p(0))^2\rangle &\sim x^{\chi_2+\Delta_2}, \end{aligned} \tag{17}$$

where $\Delta_2 \ll \chi_2$. At small Mach numbers, Δ_2 is comparable with χ_2; however, as the Mach number increases, the gap between the components' scalings closes. The scaling exponents of $\boldsymbol{v}_s$ and $\boldsymbol{v}_p$ differ by less than 10% already for Ma of order 1 [16]. Apparently, the scalings differ at all Ma (so Δ_2 is never 0); however, the difference decreases with Ma becoming negligible at $\mathrm{Ma} > \mathrm{Ma}_s$. It would be highly desirable to have numerical data for the dependence of χ_2 and Δ_2 on the Mach number and the compressibility of the forcing, at least in the range $1 \leqslant \mathrm{Ma} \leqslant 10$. Experimental measurements in molecular clouds provide the transverse structure function [56], which could be fit by a sum of two power laws for deriving χ_2 and Δ_2.

The critical number Ma_s is not defined sharply since it depends on the desired accuracy. For our purposes, the criterion is that at the considered scale L/l raised in the power of characteristic difference of scalings Δ_2 is approximately 1. If this condition holds, then the pair-correlation function of the concentration of tracers approximately obeys a power law; see below.

We consider the behavior of $V_l(t, \boldsymbol{x})$, where l is assumed to belong to the supersonic inertial range, $\eta \ll l \ll L$. We have

$$\partial_t V_l = \int_{\partial V_l(t)} \boldsymbol{v}\cdot d\boldsymbol{S} = \int_{V_l(t)} w(t, \boldsymbol{x})d\boldsymbol{x}, \tag{18}$$

where $\partial V_l(t)$ is the boundary of the volume at time t and $d\boldsymbol{S}$ is the surface element vector. We consider $\mathrm{Ma} > \mathrm{Ma}_s$, where the velocity in the supersonic inertial range obeys scaling r^σ, where $0 < \sigma < 1$. (Here we neglect intermittency.

There is no unique scaling exponent at $\mathrm{Ma} > \mathrm{Ma}_s$ besides at $\mathrm{Ma} \ll 1$ where the contribution of $\boldsymbol{v}_p$ into the scaling is negligible.) As will be discussed at length below, the flow scaling implies that at large times the moments obey Eq. (15), where $\gamma_1(k)$ are independent of l (here and below we do not write the dimensional factors that are irrelevant for the result). We find, similarly to the smooth case considered in the beginning of the section, that $\gamma_1(k)$ in Eq. (15) is a convex function that has two zeros at $k = 0$ and $k = 1$ and is negative for $0 < k < 1$ and positive otherwise. We observe that this function is nonlinear, so that the growth of the volumes is not self-similar despite the self-similarity of the transporting flow (we neglect intermittency for the moment). This reminds us of the solved case of the transport by incompressible self-similar flow (see the review [1]), where the statistics of the tracers is not self-similar despite the flow's self-similarity. We describe the origin of the breakdown of the self-similarity in our case.

Richardson's law for the inertial range growth of separation between two tracers in incompressible turbulence [1] states that $R^2(t) - R^2(0) \sim t^3$. A similar law holds for compressible turbulence. Using the consideration identical with that of Ref. [1] for incompressible turbulent flow with exponent σ, we find

$$R^{1-\sigma}(t) - R^{1-\sigma}(0) \sim t, \tag{19}$$

which reproduces Richardson's law for the Kolmogorov scaling $\sigma = 1/3$. The separation is independent of $R(0)$ at large t, where we can drop $R^{1-\sigma}(0)$ in the left-hand side. Disregarding the intermittency, the evolution of the PDF of $R(t)$ must be self-similar at those times [1].

We observe that tracers with infinitesimally small initial separation $R(0)$ separate by a finite distance in a finite time which is the so-called explosive separation. This type of separation is typical in rough flows where the velocity scaling exponent σ is smaller than 1 [57]. Due to the roughness, infinitely fine details of the shape develop in a finite time. At larger times, the shape, which can be defined by rescaling $V_l(t)$ to unit volume, is statistically stationary and multifractal, in complete similarity with the incompressible case [1]. Thus, the volume develops a complex multifractal form spread over a large range of spatial scales in a finite time. It is at these times that Eq. (15) holds.

The development of a stationary multifractal boundary in the incompressible rough turbulent flow is a property that has been known phenomenologically for some time [58]. There is nothing in the argumentation that depends strongly on the incompressibility and a similar fact must hold for compressible rough self-similar flow. The theoretical arguments can be seen from the studies of geometry of the configuration of N particles by taking $N \to \infty$ limit [1]. It is seen that the arguments for the evolution of the interparticle distances brought there for incompressible flow can be generalized to the compressible self-similar flow, similarly to the generalization of Richardson's law in Eq. (19). We will not attempt to provide here the full details since this section is phenomenological. However, the described multifractality of the shape seems inevitable in the light of the above studies.

The evolution of the volume simplifies at times when the shape is stationary. The volume at a later time is obtained by rescaling all lengths of the volume at an earlier time with a magnifying factor. The fine details of the volume change, however, are statistically stationary. The growth can be described by using the following order of magnitude estimate for the integral in Eq. (18),

$$\partial_t V_l = \int_{\partial V_l(t)} \boldsymbol{v} \cdot d\boldsymbol{S} \sim |\delta v_p(l(t))| A(l(t)), \tag{20}$$

where only velocity differences of the potential component appear since the sweeping by eddies with large scales does not change the volume. We do not distinguish between the velocity and its potential component in the scaling estimates below using the self-similarity assumption. The scale $l(t)$ is the typical linear size of the volume that could be defined as the gyration radius. After transients, that size obeys $l(t) \sim t^{1/(1-\sigma)}$; see Eq. (19) so that $|\delta v(l(t))| \sim l^{\sigma}(t) \sim t^{\sigma/(1-\sigma)}$. The growth is not self-similar because of the multifractality of the volume's shape that causes nontrivial dependence of moments of $A(l)$ on l. We can write $A(l) \sim l^{\delta}$, where δ fluctuates due to the multifractality and typically obeys $2 < \delta < 3$. We find $A(l(t)) \sim t^{\delta/(1-\sigma)}$, which use in Eq. (20) gives that

$$\frac{dV_l}{dt} \sim t^{(\sigma+\delta)/(1-\sigma)}; \;\; V_l(t) \sim t^{(1+\delta)/(1-\sigma)}. \tag{21}$$

Thus, the growth of the volume depends on both the scaling of velocity, described by the constant σ, as well as on the strength of the volume multifractality, described by the fluctuating exponent δ. The volume grows faster as the fractality or δ is higher, because stronger fractality leaves the volume with more area to grow through. Similarly, the growth is faster for rougher flow (smaller σ). Nonlinearity of $\gamma_1(k)$ results from averaging powers of $V_l(t)$ in Eq. (21) over δ. Similar considerations hold for time-reversed motion of the tracers so we can introduce the scaling functions $\gamma_i(k)$,

$$\langle V^k(t)\rangle \sim t^{\gamma_1(k)}, \;\; t > 0, \;\; \langle V^k(t)\rangle \sim |t|^{\gamma_2(k)}, \;\; t < 0; \tag{22}$$

cf. Eq. (23). The functions $\gamma_1(k)$ and $\gamma_2(k)$ differ because the flow statistics is not time reversible [1].

We consider how the flow intermittency changes the above consideration. The velocity scaling exponent σ is no longer constant. It changes in space; see, e.g., the multifractal model [41]. This implies the breakdown of self-similarity for the growth of $R(t)$. That can be described by the nontrivial scaling exponent function $\tilde{\gamma}(k)$ that describes the growth of the moments at large times,

$$\langle R^k(t)\rangle \sim t^{\tilde{\gamma}(k)}, \tag{23}$$

where at negligible intermittency (that depends on the Reynolds number) $\tilde{\gamma}(k) = k/(1-\sigma)$; see Ref. [59] and references therein for observations of nonlinearity. The intermittency causes fluctuations of σ in $V_l(t)$ in Eq. (21) and also changes the statistics of fluctuations of δ. All these fluctuations enter the final form of $\gamma_i(k)$ in Eqs. (22).

We observe that Eq. (15) is Eq. (11) in logarithmic time variable. Thus, we can simply use $\ln t$ instead of t in the expressions for smooth case for the study of the PDF. We introduce the random variable

$$x_l(t, \boldsymbol{x}) = \frac{\ln V_l(t, \boldsymbol{x})}{\ln t}, \;\; V_l(t, \boldsymbol{x}) = t^{x_l(t,\boldsymbol{x})}. \tag{24}$$

The variable x_l describes the scaling of V_l with time and its dependence on the realization. In the phenomenological approach of Eq. (21), this variable is $(1+\delta)/(1-\sigma)$, corrected by the l-dependent prefactor that is irrelevant asymptotically. The PDF $P(x_l,t)$ of $x_l(t)$ obeys

$$\langle V_l^k(t)\rangle \equiv \int P(x_l,t)t^{kx_l}dx_l \sim t^{\gamma_1(k)}; \tag{25}$$

cf. Eq. (12). This equation occurs in the theory of fractal dimensions; see Ref. [55] and below. Its solution is

$$P(x_l,t)\sim t^{-S_1(x_l)}, \tag{26}$$

where S_1 is the Legendre transform of γ_1. This formula is what we would find by using in the formulas of the smooth case $\ln t$ instead of t. Similarly to the smooth case, $S_1(x)$ has a unique maximum of zero at $x=\gamma_1'(0)$. Thus, $\gamma_1'(0)$ can be considered as the counterpart of the sum of Lyapunov exponents in the inertial range (in contrast with the sum, it is dimensionless). In the limit of $t\to\infty$ the PDF becomes $\delta(x_l-\gamma_1'(0))$. We reach the conclusion that volumes in the inertial range decay with probability one as described by Eq. (16). This conclusion is of the same level of generality as for the smooth flows and constitutes one of the central results of this section. Volumes of tracers decay at $\mathrm{Ma}>\mathrm{Ma}_s$ with probability 1 (which does not contradict conservation of $\langle V_l\rangle$ or growth of $\langle V_l^2\rangle$; cf. the similar fact for the smooth flow). The volumes' decay implies that the steady-state concentration is singular, as in the nondegenerate smooth case with $\sum_{i=1}^3\lambda_i<0$. Conversely, if $\mathrm{Ma}<\mathrm{Ma}_s$, then the scalings of the velocity components differ and the correlation functions of the concentration do not obey scaling as necessary for the multifractality. We conclude that the transition of tracers to multifractality occurs at Ma_s. This conclusion will be also obtained differently later.

We remark that the described behavior of V_l can be used as long as the relevant linear dimensions belong to the supersonic inertial range. Our consideration describes the volumes of the tracers and does not imply that the fluid volumes would also decay at $\mathrm{Ma}>\mathrm{Ma}_s$ (of course, the fluid fills the whole volume of the flow and the volumes' decay here is referred only as the asymptotic property of the inertial range). This is because of the volumes' back reaction on the transporting flow: The volumes resist compression; see the detailed discussion of the possible difference of the behavior of the tracer and fluid particles below. Should the difference hold, the transition to the multifractality would occur for the density at $\mathrm{Ma}_{\mathrm{cr}}>\mathrm{Ma}_s$. It would happen on further increase of Ma since increased compressibility brings increased effective attraction between the fluid particles that would eventually overcome the resistance.

C. Cascade picture of volume growth

Here we give a more detailed, cascade picture of growth of volumes. Similar to the traditional use of the cascade pictures in turbulence [41], we consider the volume evolution as a sequence of steps. At each step, the characteristic linear size l of the volume changes by a factor of order 1. This change is determined by turbulent eddies with size of order l. The locality of interactions [41] implies that changes at different steps are approximately independent. In contrast to the usual cascade models, this one allows an almost rigorous derivation.

We rewrite Eq. (18), which is valid at both positive and negative t, in the form

$$\frac{d\ln V_l}{dt}=\int_{V_l(t)} w(t,\boldsymbol{x})\frac{d\boldsymbol{x}}{V_l(t)}, \tag{27}$$

that demonstrates that the logarithmic rate of growth of the volume is given by the velocity divergence coarse grained over that volume. We consider the long-time asymptotic regime where the statistics of the shape of $V_l(t)$ is time independent; see the discussion after Eq. (15). The coarse-grained divergence has a nontrivial scaling in $l(t)$ with realization-dependent scaling exponent. We assume that the correlation time of variations of the coarse-grained divergence is determined uniquely by $l(t)$ and denote this time by $\tau_{l(t)}$. Assuming that the difference of the scaling exponents of the solenoidal and potential components can be neglected, we find that τ_l scales inversely proportionally to $\int w(t,\boldsymbol{x})d\boldsymbol{x}/V_l(t)$. This timescale is imposed by the convective term of the Navier-Stokes equation, $\partial_t\boldsymbol{v}\sim(\boldsymbol{v}\cdot\boldsymbol{\nabla})\boldsymbol{v}$, in the same way as the timescale $l/\delta v_l$ of eddies with scale l and characteristic velocity difference $l/\delta v_l$; see Ref. [41]. Thus, the dimensionless random variable,

$$\kappa_l=\tau_l\int_{V_l} w(\boldsymbol{x})\frac{d\boldsymbol{x}}{V_l}, \tag{28}$$

has distribution which is independent of l and V_l (and time). This key observation does not neglect intermittency because it includes the possibility of fluctuations of the scaling exponents of the flow divergence coarse grained over $V_l(t)$. The time τ_l scales in l so that characteristic linear size of the volume $l(t)$ increases within time $\tau_{l(t)}$ by an l-independent fluctuating factor $p>1$ which is of order 1. We find by integration of Eq. (27),

$$\ln\left(\frac{V_l(t)}{V_l(0)}\right)=\int_0^t dt'\int_{V_l(t')} w(t',\boldsymbol{x})\frac{d\boldsymbol{x}}{V_l(t')}\approx\sum_{i=1}^{N(t)}\kappa_i, \tag{29}$$

where $N(t)$ is determined by the condition that the product of $N(t)$ independent scale increase factors p_i at the ith step of the cascade gives $l(t)$,

$$l\left\langle\prod_{i=1}^{N(t)}p_i\right\rangle=\langle l(t)\rangle\propto t^{1/(1-\sigma)},\quad N(t)=\log_{\langle p\rangle}\frac{\langle l(t)\rangle}{l}. \tag{30}$$

Thus, $N(t)$ has logarithmic behavior in time t. We observe that since intermittency is not disregarded then the velocity scaling exponent σ is not defined uniquely. It is the law $\langle l(t)\rangle\propto t^{1/(1-\sigma)}$ that provides the unique definition in our consideration. The random variables κ_i are independent identically distributed random variables so that

$$\left\langle\frac{V_l^k(t)}{V_l^k(0)}\right\rangle\sim\langle\exp(k\kappa)\rangle^{N(t)}\sim(\langle p\rangle^{N(t)})^{\log_{\langle p\rangle}\langle\exp(k\kappa)\rangle}. \tag{31}$$

We conclude that

$$\langle V_l^k(t)\rangle\sim V_l^k(0)\left(\frac{\langle l(t)\rangle}{l}\right)^{\log_{\langle p\rangle}\langle\exp(k\kappa)\rangle}, \tag{32}$$

which yields $\gamma_1(k)$ in Eq. (22) as

$$\left\langle V_l^k(t)\right\rangle \sim V_l^k(0)t^{\gamma_1(k)}, \quad \gamma_1(k) = \frac{\log_{\langle p\rangle}\langle \exp(k\kappa)\rangle}{1-\sigma}. \tag{33}$$

This derivation provides a "microscopic" view of what forms $\gamma_1(k)$. The formula becomes transparent if we neglect fluctuations of p and κ using $\langle p\rangle$ instead of p and some characteristic constant value κ. We would have then, using that in one step of the cascade the volume increases by factor of $\exp(\kappa)$, that

$$l\langle p\rangle^{N(t)} = \langle l(t)\rangle, \quad V_l(t) \sim V_l(0)\exp[N(t)\kappa], \tag{34}$$

which is equivalent to Eq. (32).

The power law for the volume growth given by Eq. (33) is similar to the Richardson law; however, there is a significant difference. The volume is proportional to the initial volume and in the limit of zero $V_l(0)$ we find that $\langle V_l^k(t)\rangle$ also tends to zero. Thus, in contrast with the Richardson law, the volume growth is not explosive. This could seem to contradict the observations of growing volume of initial "points" (small balls with radius in the inertial range) in incompressible turbulence [1,57]. However, that growth is due to finite resolution scale: The infinitely resolved volumes are conserved by incompressibility. The proportionality of $V_l(t)$ to $V_l(0)$ seems to be necessary for consistency of formulas for concentration; see Eq. (35) and the next section.

We observe that the power-law behavior originates in the l independence of the statistics of κ_l in Eq. (28). If the scalings of the solenoidal and potential components do not agree then, since τ_l is determined by the solenoidal component of the flow, κ_l is l dependent. The volume growth does not obey then a power law. This introduces the condition $\mathrm{Ma} > \mathrm{Ma}_s$ in Eq. (15).

IV. FROM VOLUMES TO CONCENTRATION

In this section, we consider the buildup of large multifractal fluctuations of the concentration in the steady state from a smooth initial distribution modeled as a constant. This process is described in terms of the growth of the moments of the coarse-grained concentration. This type of evolution can occur, for instance, when there is an externally caused influx of dust particles into a molecular cloud which is in a regime of stationary compressible turbulence. The influx prepares an initial condition for the continuity equation. We assume diluteness so the evolution of concentration of the injected dust particles is independent of other dust that may already be present in the cloud.

We set the initial condition $n(t) = 1$ at a time $t < 0$ and study the evolution of concentration at time zero $n(\boldsymbol{x}|t)$. Thus, the second argument of $n(\boldsymbol{x}|t)$ is the time of setting the initial condition. The dependence on this time is studied when the moment of observation, taken to be zero, is fixed. The relaxation of $n(\boldsymbol{x}|t)$ at increasing $|t|$ to the stationary distribution is characterized by the growth of the moments of the coarse-grained concentration $n_l(\boldsymbol{x}|t)$ where the coarse-graining scale l belongs to the supersonic inertial range; see the definition of notations in Eq. (8). In numerical simulations, this setup can be realized by generating a stationary compressible turbulence with simulations of the Navier-Stokes equations starting from some negative time so that the steady state is reached by the time t. Then tracers are distributed uniformly over the volume of the flow at time t and their spatial distribution at time zero $n(\boldsymbol{x}|t)$ is studied. In other words, we study the time-zero concentration of tracers that are at time t distributed uniformly over a stationary turbulent flow that by itself exists from very large negative times.

The moments $\langle n_l^k(\boldsymbol{x}|t)\rangle$ grow starting from $\langle n_l^k(t=0,\boldsymbol{x})\rangle = 1$ and ending at $|t|\to\infty$ with the much larger steady-state values given by Eq. (7). We observe that the mass conservation means that the mass $4\pi l^3 n_l(\boldsymbol{x}|t)/3$ equals $V_l(t,\boldsymbol{x})$, where $V_l(t,\boldsymbol{x})$ was defined in the previous section. Indeed, the trajectories of all tracers located inside $V_l(t)$ converge inside the ball of radius l at time zero and the total mass of these tracers is $V_l(t)$ because of $n(t) = 1$. We find

$$\left\langle n_l^k(\boldsymbol{x}|t)\right\rangle = \frac{\left\langle V_l^k(t)\right\rangle}{(4\pi l^3/3)^k} \sim |t|^{\gamma_2(k)}, \tag{35}$$

where we used Eq. (22). This law holds at large $|t|$ as long as the typical linear size of $V_l(t)$ [similar to $l(t)$ in the consideration above] remains much smaller than L. This law could be more accessible for experimental tests than directly Eq. (22).

The growth of $V_l(t)$ with t stops when a relevant size of $V_l(t)$ becomes comparable with L. This size is defined by the condition that the volume extends so much beyond the spatial correlation length L of the velocity divergence that the divergence throughout the volume can be considered as uncorrelated. Then the divergence's average over $V_l(t)$ is small and no further growth of the volume occurs; see Eq. (27). We designate the (negative) time when this relevant size becomes comparable with L by t^*. The precise definition is not necessary here; we will only use that this time scales with L because the distances' evolution obeys a power law in time. At negative times smaller than t^*, the volume would not grow much more; cf. Ref. [53]. The time t^* depends on the order of the moment so we introduce $t^*(k)$ as the time beyond which the moment of order k stops growing. We find that in the steady state

$$\left\langle n_l^k(\boldsymbol{x}|t)\right\rangle \sim |t^*(k)|^{\gamma_2(k)} \sim \left(\frac{L}{l}\right)^{\tilde{\zeta}(k)}, \tag{36}$$

where $\tilde{\zeta}(k)$ includes both $\gamma_2(k)$ and the k dependence of $t^*(k)$. We introduced l for dimensional reasons as the only scale from which a dimensionless quantity can be formed with L. Similar consideration for the smooth case was performed in Ref. [53]. The consideration gives insight in the factors constituting $\tilde{\zeta}(k)$ in Eq. (7).

V. HENTSCHEL-PROCACCIA AND RÉNYI DIMENSIONS

In this section, we review the definitions of the generalized fractal dimensions and provide the multifractal formalism. This is done to fill the gap in the literature on compressible turbulence and demonstrate that many facts that hold for multifractal attractors of smooth chaotic systems can be transferred without change to multifractals formed by nondifferentiable rough flow in the inertial range. For instance, for fractals formed by a smooth flow, the local dimension

is constant almost everywhere, that is, except for points that carry zero total mass [60]. This is true also in our case. Another reason is introducing the less used Rényi dimensions as a tool for studying the density. These overcome many problems in measurement.

When density and concentration fields are considered in the supersonic inertial range (that is, when these fields are coarse grained over a scale in the range), they manifest multifractality above $\mathrm{Ma}_{\mathrm{cr}}$ and Ma_s, respectively (for the purpose of this section, the origin of these numbers and whether they are equal is irrelevant). For simpler notation, we will consider the density and concentration fields in the formal limit of $\eta \to 0$, having in mind the inertial range at the intermediate range between η and L. In other words, the behavior of ρ_r and n_r that holds for $l_s \ll r \ll L$ is continued to however small r. The limiting fields are singular with support on a multifractal set in space (in contrast, the fully resolved density is finite; see Sec. XI). This set has zero volume, so the probability of hitting it with a point is zero. The values of the density or the concentration are therefore either zero or infinite, so that the fields somewhat resemble δ functions: They vanish almost everywhere but have finite integral. However, the set on which the fields are infinite is much more complex than a point. For studying the distribution quantitatively, one must therefore consider a finite physical quantity. This is provided by the total fluid mass in a ball of radius l,

$$m_l(t,\boldsymbol{x}) = \int_{|\boldsymbol{x}'-\boldsymbol{x}|\leqslant l} \rho(t,\boldsymbol{x}')d\boldsymbol{x}' = \frac{4\pi l^3 \rho_l(t,\boldsymbol{x})}{3}, \qquad (37)$$

which is considered as a function of center' position $\boldsymbol{x}$ and defines the coarse-grained density over scale l, $\rho_l(t,\boldsymbol{x})$. Our considerations here are formulated in terms of the fluid density ρ but apply equally well to the tracers' concentration n. For smooth distributions, the knowledge of the limiting behavior of $m_l(\boldsymbol{x})$ at small l is equivalent to the density. However, for nonsmooth distributions, there is no well-defined density (the limit is either zero or infinite) and we operate directly with $m_l(\boldsymbol{x})$. The multifractality property is the statement of the existence of the limits,

$$\lim_{l\to 0}\lim_{\eta\to 0}\frac{\ln m_l(t,\boldsymbol{x})}{\ln(l/L)} = d(t,\boldsymbol{x}), \quad m_l(t,\boldsymbol{x}) \sim \left(\frac{l}{L}\right)^{d(t,\boldsymbol{x})}, \qquad (38)$$

for $\boldsymbol{x}$ belonging to the multifractal; see, e.g., Refs. [60,61]. Here, for transparency, we write explicitly the limit of zero η. This limit is taken before the limit of zero l and the order of limits is significant. If we took first l to zero and then η to zero, we would find $d(t,\boldsymbol{x}) = 3$ for all spatial points $\boldsymbol{x}$ because the density is a smooth field at finite η. For $\boldsymbol{x}$ outside the multifractal, the mass $m_l(t,\boldsymbol{x})$ is zero in the limit of $l \to 0$ taken after $\eta \to 0$. (There are points of the multifractal for which the limit in Eq. (38) does not exist; however, these points give zero contribution to the relevant moments of mass. See Ref. [60] and below.) The counterpart of $d(t,\boldsymbol{x})$ and the multifractal support of the concentration may be different but the line of consideration here and below is identical with the density.

We observe that for a one-dimensional curve, two-dimensional surface, and three-dimensional continuum, m_l has linear, quadratic, and cubic dependencies on l, respectively. Thus, $d(t,\boldsymbol{x})$ defines a local dimension of the multifractal. The field of dimensions $d(t,\boldsymbol{x})$ is statistically stationary. For homogeneous fractals, this field is constant on the fractal but not for multifractals. However, it is true that $d(\boldsymbol{x})$ is "almost" constant [60]. We transfer the proof from smooth systems for demonstrating this. The fluctuations of $d(\boldsymbol{x})$ in space are studied by considering $d_l(\boldsymbol{x}) = \ln m_l(\boldsymbol{x})/\ln(l/L)$ at arbitrarily small but finite l/L. The single-point probability density function (PDF) $P(d_l)$ of $d_l(\boldsymbol{x})$ is defined by

$$P(d_l) = \int \delta\left(\frac{\ln m_l(\boldsymbol{x})}{\ln(l/L)} - d_l\right)\rho(\boldsymbol{x})d\boldsymbol{x}. \qquad (39)$$

The presence of $\rho(\boldsymbol{x})$ in the averaging guarantees that only points $\boldsymbol{x}$ in the multifractal count so that $m_l(\boldsymbol{x}) \neq 0$. The PDF obeys

$$\int m_l^k(\boldsymbol{x})\rho(\boldsymbol{x})d\boldsymbol{x} = \int \left(\frac{l}{L}\right)^{kd} P(d_l)dd_l \sim \left(\frac{l}{L}\right)^{\xi(k)}, \qquad (40)$$

where $\xi(k)$ is the scaling exponent of the kth moment. The Hölder's inequality $\langle m_l^{(1-\alpha)x+\alpha y}\rho\rangle \leqslant \langle m_l^x\rho\rangle^{1-\alpha}\langle m_l^y\rho\rangle^{\alpha}$ (recall that the angular brackets stand for spatial averaging) implies that $\xi(k)$ considered as a function of k is a concave function. The scaling of the moments given by Eq. (40) implies that $P(d_l)$ obeys the asymptotic form [49,55,60,62],

$$P(d_l) \sim \left(\frac{L}{l}\right)^{S(d_l)}, \qquad (41)$$

where $S(d_l)$ is the rate function. This function is similar to that introduced in the time domain in the previous sections, and it is considered similarly. Carrying out now the integral in Eq. (40) by the saddle-point method, we obtain that $\xi(k) = \min_{d_l}[kd_l - S(d_l)]$. We find that $S(d_l)$ is concave and nonpositive and has a unique maximum of zero. We denote the value for which that maximum is attained by $D(1)$. The PDF $P(d_l)$ becomes $\delta(d_l - D(1))$ in the limit $l \to 0$. We conclude that $d(t,\boldsymbol{x}) = D(1)$ for all the points $\boldsymbol{x}$ on the multifractal except those that do not contribute to $P(d_l)$ in Eq. (39) at $l \to 0$ and thus have zero total mass. The points $\boldsymbol{x}$ for which $d(t,\boldsymbol{x}) \neq D(1)$ are thus very "dilute" in space. They form zero mass set inside the zero volume multifractal. Still, they are not negligible because they are dense in the multifractal. Thus, however small the ball of radius l is considered, we still cannot set $m_l(\boldsymbol{x}) \sim l^{D(1)}$ for $\boldsymbol{x}$ obeying $d(t,\boldsymbol{x}) = D(1)$. This is because the ball contains points with $d(t,\boldsymbol{x}) \neq D(1)$ due to which $m_l(\boldsymbol{x}) \sim l^{D(1)}$ fails; see Ref. [60] and below.

We stress that Eq. (41) relies on the scaling of the moments only. Thus, though it is derived originally for smooth chaotic systems [49,55,60,62], it holds in our case of rough velocity as well. It proves that the property that $d(\boldsymbol{x}) = D(1)$ holds for all $\boldsymbol{x}$ but those which have zero mass also characterizes the considered rough velocity case. The function $S(d)$ represents the rate of decrease with l of the fraction of the multifractal on which $d_l(\boldsymbol{x}) \neq D(1)$.

The multifractal nature of the distribution can be described by using the Hentschel-Procaccia (HP) [60,63] spectrum of dimensions defined as

$$D(k) = \lim_{l\to 0}\frac{\ln\int m_l^{k-1}(\boldsymbol{x})\rho(\boldsymbol{x})d\boldsymbol{x}}{(k-1)\ln(l/L)} = \frac{\xi(k-1)}{k-1}. \qquad (42)$$

The dimension $D(1)$ is ill defined and the limit of $D(q)$ at $q \to 1$ in nongeneric cases may depend on whether it is taken from the right or left. In our case, the limits agree and the limiting value is found by L'Hospital's rule,

$$D(1) = \lim_{l\to 0} \frac{\int \ln m_l(\boldsymbol{x})\rho(\boldsymbol{x})d\boldsymbol{x}}{\ln(l/L)}. \tag{43}$$

The $D(1)$ dimension is called information or entropy dimension since it measures information in the scatter of the multifractal in space; see below. The dimension is unique in that the logarithm of the mass is taken before the integration while it is the other way around in the definition of the $D(k)$ for $k \neq 1$ in Eq. (42). Interchanging the order of the limit and the integral and observing that points with zero mass do not contribute to the density-weighted integral, we see that $D(1)$ is that unique fractal dimension that holds for almost all the points of the multifractal, as is inferred from Eq. (38) and from the discussion that follows it.

Using Jensen's inequality, it is seen that $D(k)$ is a nonincreasing function of k. The value of $D(k)$ at zero is the box-counting dimension of the multifractal [63–65]. The limiting value of $D(k)$ at $k = \infty$ in our case of random flow must be zero because of the existence of optimal fluctuation; see Refs. [49,53] and below and cf. Ref. [63]. We observe that $D(k)$ can be written as

$$D(k) = 3 - \lim_{l\to 0} \frac{\ln\left\langle \rho_l^{k-1}\rho\right\rangle}{(k-1)\ln(L/l)}. \tag{44}$$

This gives explicitly the dimension deficit which is the difference between the space dimension 3 and $D(k)$.

We comment on the relevance of points $\boldsymbol{x}$ for which $d(t,\boldsymbol{x}) \neq D(1)$ in the calculation of $D(k)$ in Eq. (42). These points have zero mass and thus can be taken out of the domain of integration. However, as told previously, this does not mean that these points are irrelevant and we can put $m_l(\boldsymbol{x}) \sim l^{D(1)}$ in the integral. This is because $m_l(\boldsymbol{x})$ can be much larger or smaller than $l^{D(1)}$ however small l is. This is due to persistent presence of points with $d(t,\boldsymbol{x}) \neq D(1)$ inside the ball of radius l. This phenomenon comprises the strong intermittency of multifractal statistics.

A. Difficulty in experimental studies of dimensions and the Rényi dimensions

Finding the moments of mass in Eq. (40) from numerical simulations or experiments is not straightforward. The usual procedure [63] starts from a large number N of points with coordinates $\boldsymbol{x}_i$ on the multifractal. One has using discrete approximation $\rho(\boldsymbol{x}) = \sum_{i=1}^{N} \delta(\boldsymbol{x}-\boldsymbol{x}_i)/N$ that

$$\int m_l^k(\boldsymbol{x})\rho(\boldsymbol{x})d\boldsymbol{x} \approx \frac{\sum_{i=1}^{N} m_l^k(\boldsymbol{x}_i)}{N}, \tag{45}$$

which becomes exact in the continuum limit of $N \to \infty$. However, getting particles on the multifractal support of the fluid density can be nontrivial. The procedure of seeding the flow with a large number of tracer particles and studying their distribution is valid only provided that $n = \rho$ holds in the steady state, which demands a separate proof.

Thus, in order to facilitate the calculations of the fractal dimensions independent of $n = \rho$ from numerical or experimental data, we introduce a different set of dimensions [66] which seems to be more suitable for working with the density, the continuous Rényi dimensions $\tilde{D}(k)$,

$$\tilde{D}(k) = \lim_{l\to 0} \frac{\ln \int m_l^{k-1}(\boldsymbol{x})\rho_l(\boldsymbol{x})d\boldsymbol{x}}{(k-1)\ln(l/L)} = \lim_{l\to 0} \frac{\ln \int m_l^{k}(\boldsymbol{x})d\boldsymbol{x}}{(k-1)\ln(l/L)} - \frac{3}{k-1}. \tag{46}$$

The difference between this definition and Eq. (42) is that it uses for averaging of $m_l^{k-1}(\boldsymbol{x})$ the coarse-grained density $\rho_l(\boldsymbol{x})$ rather than the fine density $\rho(\boldsymbol{x})$ (our definition uses balls rather than cubes which could make a difference [64,66] but in our case seems irrelevant). In contrast with the HP dimensions, the Rényi dimensions are ill defined for $k < 0$ since any hole with finite volume gives nonintegrable m_l^k for small l. However, for $k > 0$, the dimensions are well defined and coincide with the HP dimensions, as we demonstrate below. Thus, $\tilde{D}(k)$ give a way of finding $D(k)$, circumventing the study of whether the density and the concentration coincide in the steady state; see the discussion in later sections.

We observe that $\int m_l^k(\boldsymbol{x})d\boldsymbol{x}$ considered at fixed l and $k \to 0$ is roughly the volume of points $\boldsymbol{x}$ for which $m_l \neq 0$. Correspondingly, $\int m_l^{k-1}(\boldsymbol{x})\rho_l(\boldsymbol{x})d\boldsymbol{x}$ is that volume divided by $4\pi l^3/3$ which determines the box counting dimension $\dim_{\text{box}}(\text{supp }\rho)$ of the support of ρ. Indeed, although the interchange of the limits of zero l and k is not valid, it will be seen below that

$$\lim_{k\to 0^+} \tilde{D}(k) = \dim_{\text{box}}(\text{supp }\rho) \tag{47}$$

(it is recalled that ρ in this equation is the multifractal singular distribution obtained in the limit of zero η).

Assuming it exists, the dimension $\tilde{D}(1)$ yields the limiting value of the Gibbs entropy $-\langle \rho_l \ln \rho_l\rangle$ derived from the coarse-grained density ρ_l,

$$\tilde{D}(1) = \lim_{l\to 0} \frac{\int \ln m_l(\boldsymbol{x})\rho_l(\boldsymbol{x})d\boldsymbol{x}}{\ln(l/L)} = 3 - \lim_{l\to 0} \frac{\langle \rho_l \ln \rho_l\rangle}{\ln(L/l)}. \tag{48}$$

Thus, $D(1)$, which equals $\tilde{D}(1)$ (see below) derives from the entropy, which is why it is called the information dimension.

To gain further insight into the nature of the fractal dimensions, we notice that

$$\int m_l^k(\boldsymbol{x})\rho_l(\boldsymbol{x})d\boldsymbol{x} \sim \left(\frac{l}{L}\right)^{k\tilde{D}(k+1)}. \tag{49}$$

The Rényi dimensions may therefore be written as

$$\tilde{D}(k) = 3 - \lim_{l\to 0} \frac{\ln\left\langle \rho_l^k\right\rangle}{(k-1)\ln(L/l)}, \tag{50}$$

so that $\tilde{D}(k)$ describes the spatial statistics of the coarse-grained density, rather than the statistics obtained by density-weighted averaging as in Eq. (44). The last term in Eq. (50) is minus the dimension deficit. For smooth distributions, ρ_l is independent of l at small l and $\tilde{D}(k) = 3$. We also observe that [cf. Eq. (7)]

$$\left\langle \rho_l^k\right\rangle = c_l\left(\frac{L}{l}\right)^{\zeta(k)}, \quad \tilde{D}(k) = 3 - \frac{\zeta(k)}{k-1}, \tag{51}$$

where c_l are constants of order 1. When these formulas are applied to the concentration, they provide a way for finding fractal dimensions from the cascade model; cf. Eq. (36) and see below.

The Rényi dimensions $\tilde{D}(k)$ lend themselves to easier calculations from numerical or experimental data. We demonstrate that in the range of their definition, $k > 0$, they equal the HP dimensions, $D(k) = \tilde{D}(k)$. The equality is readily demonstrated for positive integer k greater than 1. Indeed, in that case $D(k)$ describes the correlations of the positions of k particles [63]. Writing $m_l^k(\boldsymbol{x}) = \int_{|\boldsymbol{x}_i - \boldsymbol{x}|<l} \prod_{i=1}^k \rho(\boldsymbol{x}_i) d\boldsymbol{x}_i$, we have

$$\int m_l^k(\boldsymbol{x})\rho(\boldsymbol{x})d\boldsymbol{x} = \int_{r_i<l} \langle \rho(0)\rho(\boldsymbol{r}_1)\dots\rho(\boldsymbol{r}_k)\rangle \prod_{i=1}^k d\boldsymbol{r}_i, \quad (52)$$

where the correlation function $\langle \rho(0)\rho(\boldsymbol{r}_1)\dots\rho(\boldsymbol{r}_k)\rangle$ describes the probability of simultaneously finding k particles at distances $\boldsymbol{r}_i$ from the origin given that there is a particle at the origin (here particle is the fluid particle). Similarly,

$$\int m_l^k(\boldsymbol{x})\rho_l(\boldsymbol{x})d\boldsymbol{x} = \frac{3}{4\pi l^3}\int_{r_i<l} \langle \rho(0)\rho(\boldsymbol{r}_2-\boldsymbol{r}_1)\dots\rho(\boldsymbol{r}_{k+1}-\boldsymbol{r}_1)\rangle \prod_{i=1}^{k+1} d\boldsymbol{r}_i. \quad (53)$$

These representations demonstrate therefore the identical scaling of $\langle m_l^k \rho\rangle$ and $\langle m_l^k \rho_l\rangle$ in l. Thus, for all integers larger than 1, we have $D(k) = \tilde{D}(k)$. Furthermore, it was proved in Ref. [66] that $D(1) = \tilde{D}(1)$. This equality is often taken for granted without proof [63]. We conclude that $D(k) = \tilde{D}(k)$ holds for all positive integers. It was proved in Ref. [66] that the equality can be continued for all $k > 0$. Heuristic proof is obtained by observing that since the scale of spatial variations of $m_l(\boldsymbol{x})$ is of order l then at $l_0 \ll l$ we have approximate equality

$$\int m_l^k(\boldsymbol{x})\rho(\boldsymbol{x})d\boldsymbol{x} \approx \int m_l^k(\boldsymbol{x})\rho_{l_0}(\boldsymbol{x})d\boldsymbol{x}. \quad (54)$$

As there is no pathology [64], we can continue this equality asymptotically to $l_0 \sim l$, finding $D(k) = \tilde{D}(k)$.

Another advantage of the use of the Rényi dimensions is that these are directly addressed by the more intuitive Frisch-Parisi multifractal formalism [41,67], which could be the starting point of the study of multifractality; cf. Ref. [68]. The multifractal is considered as a union of fractals formed by the level sets of $d(t,\boldsymbol{x})$. We assign to the set of points with $d(t,\boldsymbol{x}) = d$ the Hausdorff dimension $S(d) + d$, where $S(d)$, for consistency with $D(k) = \tilde{D}(k)$, must be the same function that appears in Eq. (41); see Refs. [55,60] and below. The probability that a ball with radius l randomly placed in the domain of the flow intersects a fractal set with dimension $S(d) + d$ behaves as $l^{3-d-S(d)}$. This gives [41,67]

$$\int m_l^{k+1}(\boldsymbol{x})d\boldsymbol{x} \sim \int_{d_{\min}}^{d_{\max}} l^{kd+3-S(d)} dd \sim l^{3+\min_d[kd-S(d)]}, \quad (55)$$

where $(d_{\min}, d_{\max})$ is the domain of variation of $d(t,\boldsymbol{x})$. Comparing this with $\int m_l^{k+1}(\boldsymbol{x})d\boldsymbol{x} \sim l^{3+k\tilde{D}(k+1)}$ [see Eq. (49)], we find that $k\tilde{D}(k+1)$ and $S(d)$ form a Legendre transform pair. Since $kD(k+1)$ and $S(d)$ also form a Legendre transform pair [see Eqs. (40)–(42)], then we have $D(k) = \tilde{D}(k)$, confirming the self-consistency of the consideration. The multifractal formalism described above lies at the origin of the multifractal model of turbulence [41,67]. In fact, our singularities of mass in the inertial range are more similar to the singularities of turbulent velocity difference than to singularities of mass of attractors of smooth systems.

We comment that the scaling of mass and its moments is only approximate. This is due to finite difference of scalings of solenoidal and potential components of velocity discussed previously. When the above definitions are used for concentration of tracers, the simplest way of measuring the dimensions is by working with a large number of discrete particles obeying Eq. (6). It must then be ensured that the number of particles in the considered small volumes is large. Otherwise, discreteness of the particles causes deviations from the continuum behavior which we consider here. The impact of discreteness was obtained at small compressibility in Ref. [69].

VI. FRACTAL DIMENSIONS OF ISOTHERMAL TURBULENCE

In this section, we use the definitions of the previous section for providing the fractal dimensions of the isothermal turbulence. Numerical simulations performed at zero dissipative coefficients demonstrated that the single-point spatial statistics of the density is log normal; see, e.g., Refs. [16,28]. The single-point density in these simulations is asymptotically the density in the inertial range coarse grained over the resolution scale l_0 that is ρ_{l_0} (the viscous scale and viscosity are set to zero). We take it as observed fact that ρ_l in isothermal turbulence is log normal at $l > \eta$ and derive from this the fractal dimensions.

The log normality holds at intermediate Mach numbers and deviations from it were observed at higher Mach numbers [28]. In fact, deviations from log normality must hold at any Ma for the tail of the distribution of ρ_l for avoiding contradictory results concerning the fractal dimensions. These deviations are the consequence of the fact that the maximal value of ρ_l cannot exceed the total mass of the system divided by $4\pi l^3/3$. Despite the triviality of this observation, it has far-reaching consequences. The PDF of ρ_l, in contrast with the single-point PDF of the density ρ, has compact support given by the interval $[0, 3/(4\pi l^3)]$. Thus, the tail of the PDF is not log normal. This corresponds to very special behavior of $D(k)$ at large k: We have $\langle m_l^k\rangle \sim l^{\delta_0}$, where δ_0 is a k-independent constant. This type of behavior is caused by the optimal fluctuation where the maximal possible mass of order 1 is compressed in the ball of radius l; see Refs. [49,53,70]. It must be clarified that $D(k)$ derive from the behavior of m_l (see the previous section) and for them log normality cannot hold for all k; see below. In contrast, the single-point PDF of the density can be log normal with no contradiction. Finally, the PDF of finitely resolved density is considered at the PDF of ρ_l with l equal to the scale of spatial resolution.

We demonstrate that for log-normal statistics all the fractal dimensions $\tilde{D}(k)$ depend only on one parameter: the density

spectrum decay exponent δ. For that purpose, we first notice that the inverse Fourier transform of the spectrum $E(k) \propto k^{\delta-1}$ results in the following pair-correlation function at separation in the inertial range,

$$\langle \rho(0)\rho(\boldsymbol{r})\rangle = \int \exp(i\boldsymbol{k}\cdot\boldsymbol{r})E(k)\frac{d\boldsymbol{k}}{4\pi k^2} \approx c\left(\frac{L}{r}\right)^{\delta}, \quad (56)$$

where c is a constant of order 1. We therefore find from Eqs. (52) and (53) for $k = 1$ that $D(2) = \tilde{D}(2) = 3 - \delta$. Since $D(2)$ is derived from pair correlations, then it is called correlation dimension. Next, log normality of ρ_l is Gaussianity of $s_l \equiv \ln \rho_l$ so that the probability density function (PDF) $P_l(s)$ of s_l obeys

$$P_l(s) = \langle \delta(s_l - s)\rangle = \frac{1}{\sqrt{2\pi\sigma_l^2}} \exp\left[-\frac{(s - \langle s_l\rangle)^2}{2\sigma_l^2}\right], \quad (57)$$

where we designated the dispersion of s_l by σ_l^2. We have

$$\left\langle \rho_l^k \right\rangle = \langle \exp(ks_l)\rangle = \exp\left[k\langle s_l\rangle + \frac{k^2\sigma_l^2}{2}\right], \quad (58)$$

where we used the Gaussian averaging formula for the average of the exponent of the Gaussian variable ks_l. Since $\langle \rho_l\rangle = 1$ and then setting in the above formula $k = 1$, we find the identity $\langle s_l\rangle + \sigma_l^2/2 = 0$, which in turn yields

$$\left\langle \rho_l^k \right\rangle = \exp\left[\frac{k(k-1)\sigma_l^2}{2}\right]. \quad (59)$$

Employing now the last relationship in Eq. (50) results in the following expression for the Rényi dimensions for lognormal statistics:

$$\tilde{D}(k) = 3 - \lim_{l\to 0}\frac{k\sigma_l^2}{2\ln(L/l)}. \quad (60)$$

Thus, in the log-normal case, the spectrum of codimensions $3 - \tilde{D}(k)$ is a linear function of k; see a similar observation for inertial particles below the viscous scale in Ref. [54]. Setting finally $k = 2$, we find

$$\delta = 3 - \tilde{D}(2) = \lim_{l\to 0}\frac{\sigma_l^2}{\ln(L/l)}, \quad \sigma_l^2 \sim \delta \ln\left(\frac{L}{l}\right). \quad (61)$$

This implies

$$\left\langle \rho_l^k \right\rangle = \left(\frac{L}{l}\right)^{k(k-1)\delta/2}. \quad (62)$$

We conclude that fractality, which implies that the correlation dimension $D(2)$ is strictly smaller than 3 (recall that $D(2)$ is not larger than the information $[D(1)]$ and box counting $[D(0)]$ dimensions by Jensen's inequality), then $\delta = 3 - D(2)$ must be a positive number when the distribution is multifractal.

It is of interest to note the logarithmic dependence of the dispersion σ_l^2 on the coarse-graining scale. That dispersion has been intensively studied in terms of the single-point density which asymptotically gives rise to $\sigma_{l_0}^2$; see, e.g., Refs. [16,28]. However, these studies did not consider the dependence of the dispersion on the resolution's scale, with exception of Ref. [28]. Indeed, the logarithmic dependence of $\sigma_{l_0}^2$ on l_0 is quite slow and it was not detected. In the passage from 256^3 grid to 1024^3 considered in Ref. [28], the dispersion changes only by about 20%, which is the probable reason for why the dependence was not observed previously. We stress that these properties of $\sigma_{l_0}^2$ apply only in the case where the density is multifractal, which is the regime of supercritical Mach numbers larger than $\mathrm{Ma}_{\mathrm{cr}} \sim 7$; see below. Thus, there is no contradiction with previous studies that examined $\sigma_{l_0}^2$ at smaller Ma.

Returning now to Eqs. (59)–(61), the fractal dimensions may be conveniently expressed in the following way:

$$D(k) = \tilde{D}(k) = 3 - \frac{k\delta}{2}, \quad k > 0. \quad (63)$$

We consider the implication of the above relationship on the HP and the Rényi dimensions. We observe that log normality of ρ_l with respect to the spatial averaging implies also log normality with respect to the mass-weighted averaging weighted by the coarse-grained density ρ_l. Indeed, using Eq. (57), we find [71]

$$\tilde{P}_l(s) \equiv \int \delta(\ln \rho_l(\boldsymbol{x}) - s)\rho_l(\boldsymbol{x})d\boldsymbol{x} = \exp(s)P_l(s) = \frac{1}{\sqrt{2\pi\sigma_l^2}} \exp\left[-\frac{(s + \langle s_l\rangle)^2}{2\sigma_l^2}\right], \quad (64)$$

where we used $\langle s_l\rangle = -\sigma_l^2/2$. Using the definition of $D(k)$ in Eq. (44), we have from Eq. (63)

$$\left\langle \rho_l^{k-1}\rho \right\rangle \sim \left(\frac{L}{l}\right)^{k(k-1)\delta/2}. \quad (65)$$

This implies that

$$\int \delta(\ln \rho_l(\boldsymbol{x}) - s)\rho(\boldsymbol{x})d\boldsymbol{x} \sim \frac{1}{\sqrt{2\pi\sigma_l^2}} \exp\left[-\frac{(s+\langle s_l\rangle)^2}{2\sigma_l^2}\right]. \quad (66)$$

Thus, in accordance with Eq. (54), at $l_0 = l$ we find that $D(k) = \tilde{D}(k)$ implies that

$$\int \delta(\ln \rho_l(\boldsymbol{x}) - s)\rho(\boldsymbol{x})d\boldsymbol{x} \sim \int \delta(\ln \rho_l(\boldsymbol{x}) - s)\rho_l(\boldsymbol{x})d\boldsymbol{x}.$$

This consideration raises the question of whether the asymptotic equality in Eq. (66) can be replaced by approximate equality, that is, if ρ_l is log normal not only with respect to the spatial average with weight $d\boldsymbol{x}$ but also with respect to the mass-weighted average with weight $\rho(\boldsymbol{x})d\boldsymbol{x}$. This question is relevant because log normality in the cascade model would hold for mass-weighted and not space-weighted average. This question is left for future work.

A. Correcting phenomenology of compressible turbulence

A main problem of the currently existing phenomenology of the supersonic turbulence is that the scaling of the density is described with only one scaling exponent; see the introduction. Thus, the density is assumed to be fractal and not multifractal. This causes problems in the agreement with the data, as inspection of Ref. [16] reveals. The authors considered the fit of the phenomenology with the observed scalings of the first- and second-order structure functions. They saw that the density scaling exponent, that must be constant in the

phenomenological theory, differs for these orders by 40% . If we consider also the data brought for the third-order structure function, we find the variation of already about 100%. Thus, the correction of the phenomenology for multifractality seems necessary. Here, we demonstrate difficulties in this correction.

We use consideration similar to Ref. [16]. It was assumed in accordance with the observations that $\rho^{1/3}\boldsymbol{v}$ has behavior similar to the velocity of incompressible turbulence,

$$\langle|\rho^{1/3}(\boldsymbol{r})\boldsymbol{u}(\boldsymbol{r})-\rho^{1/3}(0)\boldsymbol{u}(0)|^p\rangle\sim r^{p/3}, \tag{67}$$

where the intermittency corrections are assumed to be small. The issue is how, given the above formula and the scaling of the density described by Eq. (62), we can infer the scaling exponents of the velocity. The straightforward approach of considering

$$\langle|\boldsymbol{u}(\boldsymbol{r}+\boldsymbol{l})-\boldsymbol{u}(\boldsymbol{r})|^p\rangle\sim\frac{\langle|\rho^{1/3}(\boldsymbol{r})\boldsymbol{u}(\boldsymbol{r})-\rho^{1/3}(0)\boldsymbol{u}(0)|^p\rangle}{\langle\rho_l^{p/3}\rangle} \tag{68}$$

is invalid. Indeed, this would produce Kolmogorov scaling of the third-order structure function on setting $p=3$. That scaling is at significant variance with the observations [16]. We leave the question of how the phenomenology must be corrected for future work.

B. Breakdown of log-normal approximation

The linear dependence of the fractal dimensions on the order, given by Eq. (63), gives a wrong prediction of negative $D(k)$ at large k. The contradiction with the demand that $D(k)\geqslant 0$ is caused by the use of the log-normal distribution beyond the domain of its applicability. High-order moments of the mass are determined by the tail of the mass distribution $P(m_l)$, which decays quickly beyond the maximal compressed mass. That mass is determined by an optimal fluctuation where the flow produces as large of a mass m_l in a ball of radius l as possible; see Refs. [49,53,70]. This mass is given by the total mass $L^3\langle n\rangle$ of the largest spatial region available for the compression which is the region whose size is the correlation length of the flow divergence L (if L is comparable with the total system size, then $L^3\langle n\rangle\sim 1$ since the total mass of the system is 1). The behavior of high-order moments can be seen by considering which spatial regions determine the space average of $\langle m_l^k\rangle$ at k as large as we wish. There are rare regions of space where $m_l\sim L^3\langle n\rangle$ and the density ρ_l is increased by factor of $(L/l)^3$ in comparison with the average. When we consider larger k, the contribution of these regions in $\langle m_l^k\rangle$ becomes more pronounced until these regions become the regions that define the moment. A straightforward way to see this is to write

$$\langle m_l^k\rangle\sim\int_0^{L^3\langle n\rangle} m_l^k P(m_l)dm_l, \tag{69}$$

where $P(m_l)$ is the PDF of m_l and we stress that m_l has a limited domain of variation. This way of writing makes it obvious that as k increases the integral becomes determined by the upper limit of integration [assuming log-normal $P(m_l)$ at much smaller m_l]. This breaks the log-normality assumption; cf. the simpler case of concentration of tracers transported by smooth weakly compressible flow [49,70]. The inconsistency of log-normal approximation to multifractality for high-order moments was pointed out by Mandelbrot [72]; see also Ref. [67].

Another consequence of Eq. (63) is the equality of the box-counting dimension $D(0)$ to the full spatial dimension 3. The equality of spatial and box-counting dimensions was observed previously [11,54,70,73]. It is plausible that $D(0)=3$ holds also for other nonisothermal types of compressible turbulence; see Ref. [70].

We conclude that $D(k)$ at large k are determined by the non-log-normal right tail of the PDF of $s_l=\ln\rho_l$, respectively. The actual range of k where Eq. (63) is valid must be determined numerically. It is plausible that this range includes $k=1$ and $k=2$. Indeed, $D(1)$ is determined by typical events (see the previous section) that determine the peak of the log-normal distribution. The mass moment that determines $D(2)$ is determined by the right portion of the distribution of s_l, which is well described by log-normal distribution at relevant Mach numbers [16]. We conclude that the information dimension obeys $D(1)=3-\delta/2$.

We remark that the last formula must be taken with reservation. It is found that due to intermittency the value of k, starting from which $\langle m_l^k\rangle$ and $D(k)$ are determined by the optimal fluctuation, does not need to be large. Thus, for a two-dimensional smooth system (which does not differ in the considered aspect much from our rough case) presented in Ref. [49], the correlation dimension $D(2)$ can be determined by the optimal fluctuation. Then, the log-normal approximation for $D(k)$ given by Eq. (63) cannot be used for connecting $D(1)$ and $D(2)$ and $D(1)=3-\delta/2$ does not hold. In contrast, for a similar system in three dimensions, $D(2)$ is never determined by the optimal fluctuation [70]. It is thus highly relevant for the future (numerical) studies to be able to address the k dependence of $D(k)$ and test Eq. (63).

C. Consistency with literature

Our derivation in this section provides a rigorous connection between the spectrum of the density and multifractality. We compare this result with literature in the field.

The density spectrum $E(k)$ in the supersonic inertial range of wave numbers obeys a power law $k^{\delta-1}$ which is cut off at η^{-1}. The exponent δ is an increasing function of Ma [17,28]. It crosses zero from below [16,28] at a critical Mach number $\mathrm{Ma}_{\mathrm{cr}}\sim 6$–$8$. The crossing produces a qualitative change of behavior of the average squared density $\int_0^\infty E(k)dk$. At $\mathrm{Ma}<\mathrm{Ma}_{\mathrm{cr}}$ the integral $\int_0^\infty E(k)dk$ is determined by wave numbers of the order of L^{-1} staying finite in the limit $\eta\to 0$. In contrast, at $\mathrm{Ma}>\mathrm{Ma}_{\mathrm{cr}}$ the integral is determined by wave numbers of order $\eta^{-1}\gg L^{-1}$ and the average squared density is infinite at $\eta\to 0$. This gives a description of the transition to multifractality. The density at $\mathrm{Ma}<\mathrm{Ma}_{\mathrm{cr}}$ is a large-scale nonfractal field whose pair correlation function is constant in the inertial range. The second moment of density difference at points separated by a distance r in the inertial range scales as $r^{|\delta|}$. In contrast, density at $\mathrm{Ma}>\mathrm{Ma}_{\mathrm{cr}}$ is a small-scale field whose the pair-correlation function, proportional to $r^{-\delta}$, grows at decreasing r until the cutoff at η. Density dispersion is determined by spatial fluctuations with scale η and diverges in the limit $\eta\to 0$. The statistics is multifractal in the inertial range above η with $3-\delta$ called the correlation dimension.

The current description of this transition to multifractality in the literature is misleading.

It was observed in Ref. [16] that the information dimension $D(1)$ is smaller than 3 at $\delta < 0$. Since the correlation dimension must be smaller than the information dimension (see [63] and Sec. V), then this observation implies $D(2) < 3$ at $\delta < 0$. This is in contradiction with the paragraph above that gives $D(2) = \min[3, 3 - \delta]$. This contradiction and the paragraph above hold irrespective of the validity of log normality. However, since log normality is obeyed in the considered simulations, then there is also contradiction with the formula $D(1) = 3 - \delta/2$. One reason for the discrepancy could be the incomplete resolution of δ: It was found to be resolution dependent where the sign of δ depends on the resolution. The other reason seems to be the consequence of nonrigorous procedure used in determining $D(1)$ that employed the following definition:

$$D(1) = \tilde{D}(1) = \lim_{l\to 0} \frac{\int \ln m_l(\boldsymbol{x})\rho_{l_0}(\boldsymbol{x})d\boldsymbol{x}}{\ln(l/L)}, \tag{70}$$

where l_0 is the resolution scale. The procedure for calculating the integral in the above definition used only points $\boldsymbol{x}$ where the density $\rho_{l_0}(\boldsymbol{x})$ is higher or equal to half the maximal density in the considered snapshot (with further time averaging). These points were identified as belonging to the multifractal. The rationale for this procedure is not obvious.

It was proposed in Ref. [28] that transition to fractality occurs when δ crosses -1 and not 0. However, the k^{-2} spectrum corresponding to $\delta = -1$ describes linear scaling of the squared density difference with separation. This can be the case of a passive scalar in incompressible flow [1] or Burgers turbulence [52], both of which are not fractal. However, as we stressed, for $0 > \delta > -1$ the average squared density $\int E(k)dk$ is finite at $\eta \to 0$, and this cannot be so for a singular fractal distribution. Moreover, this reference proposed that the fractal dimension, which is probably the information dimension, is $5/2 - \delta/2$, which differs from Eq. (63). The proposed heuristic derivation does not consider the fluctuations of the scaling exponents of the mass m_l with l in space. Consequently, there are differences in the prediction for the limiting information dimension at $\mathrm{Ma} = \infty$. In that limit, $E(k)$ becomes a constant, corresponding to $\delta = 1$. The prediction for the limiting dimension from Eq. (63) would be $5/2$ and not 2 as proposed in Ref. [28]. However, our prediction for the limiting dimension must be taken with a reservation. It is probable from the indication of log-normality breakdown at higher Ma in Ref. [28] that at $\mathrm{Ma} \to \infty$ log normality breaks down and a reconsideration of Eq. (63) is needed.

The considerations described above apply only in the case where the density is multifractal, which is the regime of supercritical Mach numbers larger than $\mathrm{Ma}_{\mathrm{cr}} \sim 7$; see below. We see that all $D(k)$ describable by Eq. (63) are uniformly smaller than 3 at $\delta > 0$. This is not necessarily so: In fact, moments of mass of different orders may transit to multifractal behavior at different critical Mach numbers. This could be the case of $D(k)$ with large k that are not describable by the log-normal distribution. For instance, dimensions of moderate orders could still be 3 when the high k moments of the mass are already determined by the optimal fluctuation producing $D(k) < 3$. Thus, the critical Mach number for which $D(k)$ becomes smaller than 3 could depend on k. The study of these questions is beyond our scope here.

VII. CASCADE AND TRANSITION TO MULTIFRACTALITY

In this section, we apply the cascade model developed previously to the steady-state statistics. The study of the statistics can be done using the representation of the steady-state concentration $n(\boldsymbol{x}) = \lim_{t\to-\infty} n(\boldsymbol{x}|t)$ introduced in Sec. IV. This can be written as

$$n(\boldsymbol{x}) = \lim_{T\to\infty} \exp\left[-\int_{-T}^{0} w(t, \boldsymbol{q}(t, \boldsymbol{x}))dt\right], \tag{71}$$

where we used the solution of the continuity equation given by Eq. (5). The limit may produce a singular distribution (see the discussion in Sec. XII); however, it can be defined for various quantities that remain finite at $T \to \infty$. Thus, we have the representation of the pair correlation function of concentration $f(\boldsymbol{r}) = \langle n(0)n(\boldsymbol{r})\rangle$,

$$f(\boldsymbol{r}) = \left\langle \exp\left\{-\int_{-\infty}^{0} [w(t, \boldsymbol{q}(t, \boldsymbol{r})) + w(t, \boldsymbol{q}(t, 0))]dt\right\}\right\rangle, \tag{72}$$

which for $r \neq 0$ always gives a finite quantity; see Ref. [54], below, and also Ref. [9]. We demonstrate here using this and similar representations for the higher order correlations that the steady-state concentration can be understood in detail.

A. Cascade model for correlation functions

We consider the representation of the pair-correlation function given by Eq. (72). We demonstrate that for $f(r)$ to obey a power law, which is the case of the multifractal phase of the concentration, the scalings of the compressible and solenoidal components of velocity must coincide. This is in accordance with our previous considerations.

We designate the turnover time of eddies of size r by t_r. This time is defined as the ratio of r and the characteristic value of the velocity difference at distance r (this refinement is necessary since timescales introduced by the solenoidal and potential components might differ). We have from the standard phenomenology of turbulence [41] that the trajectories $\boldsymbol{q}(t, \boldsymbol{r}))$ and $\boldsymbol{q}(t, 0)$ in Eq. (72) diverge backward in time by the distance L in characteristic time t_L. Beyond this time, $w(t, \boldsymbol{q}(t, \boldsymbol{r}))$ and $w(t, \boldsymbol{q}(t, 0))$ become decorrelated so the contribution of times $t < -t_L$ is negligible. As a result, the lower limit of integration in Eq. (72) may be replaced by $-t_L$. Then we represent the exponent as sum of contributions of time intervals during which the scale depletes by a factor of e (any other factor of order 1 could be used [41]),

$$f(\boldsymbol{r}) \approx \left\langle \exp\left\{-\sum_{i=1}^{N+1} \int_{t_{i-1}}^{t_i} [w(t, \boldsymbol{q}(t, \boldsymbol{r})) + w(t, \boldsymbol{q}(t, 0))]dt\right\}\right\rangle,$$

where $N = \ln(L/r)$ and $t_i = -t_{L/e^i}$. We set $t_{N+1} = 0$. The contribution of the ith interval is determined by eddies of size $Le^{-(i-1)}$ and can be considered independent of the other intervals because of the approximate independence of eddies

with very different size (locality of interactions) [41]. We find

$$f(\boldsymbol{r}) \sim \prod_{i=1}^{N+1} \left\langle \exp\left\{ -\int_{t_{i-1}}^{t_i} [w(t,\boldsymbol{q}(t,\boldsymbol{r})) + w(t,\boldsymbol{q}(t,0))]dt \right\} \right\rangle.$$

This formula manifests the cascade-like formation of pair correlations [41]. It is readily seen now that we need to assume that all the terms in the exponents are i independent in order to obtain a scaling law for the pair correlation. This independence occurs only if the scalings of the compressible and solenoidal components are the same because only then will the divergence's dependence on the scale coincide with $\delta v_r/r = t_r^{-1}$. Designating therefore the positive average of the ith term by $\exp(\beta)$, where β is r independent, we find $(N+1 \approx N)$

$$f(r) \sim \exp(N\beta) = \left(\frac{L}{r}\right)^{\beta}. \tag{73}$$

Thus, the correlation dimension of the concentration, namely, $3-\beta$, obeys $\beta = \ln\langle \exp(2\kappa)\rangle$, where the random variable $\tilde{\kappa}$ is the product of t_r and the fluctuating divergence w_r at scale r which is assumed to have r-independent PDF. This variable is equivalent of κ_l in Eq. (28).

Finding $f(r=l)$ is equivalent to the knowledge of the dispersion of the coarse-grained concentration n_l; see Eq. (53) at $k=1$. Thus, the above consideration establishes the cascade model representation of $\langle n_l^2\rangle$. Similar considerations hold for the moments of n_r with higher integer order. The moment of order k is found by integration of the k-point correlation function $f_k = \langle n(\boldsymbol{r}_1)n(\boldsymbol{r}_2)\ldots n(\boldsymbol{r}_k)\rangle$ that obeys

$$f_k = \left\langle \exp\left[-\sum_{i=1}^{k} \int_{-\infty}^{0} w(t,\boldsymbol{q}(t,\boldsymbol{r}_i))dt \right] \right\rangle,$$

generalizing Eq. (72). We find that similarly to $f(\boldsymbol{r})$ we can asymptotically cut the integrals at the time $-t_L^k$ at which the distances $|\boldsymbol{q}(t,\boldsymbol{r}_i) - \boldsymbol{q}(t,\boldsymbol{r}_l)|$ become equal to L. This brings the corresponding cascade representation of the kth moment of n_l. We do not provide the details, making instead a direct study of n_l.

B. Cascade model of steady-state concentration

We construct the cascade model representation for $n_l(\boldsymbol{x})$, which contains more information than only the integer moments considered above. Our starting point is the representation $n_l \sim V_l(t^*)/(4\pi l^3/3)$ introduced at the end of Sec. IV. Here, the asymptotic equality must be understood in the sense that the scaling of both sides of the equation in l is identical. This representation assumes that the growth of the volume $V_l(t)$ backward in time can be characterized by a single length scale $l(t)$, giving the overall size of the volume. It is assumed that the backward in time growth effectively stops when $l(t)$ is of order L so there is no secondary growth after $l(t)$ exceeds L. This reasonable assumption agrees with the consideration of the integer moments of $n_l(\boldsymbol{x})$ above and can be further argued for by using the Green's function representation of $n(t,\boldsymbol{x})$. Then, the cascade model for creation of fluctuations of $n_l(\boldsymbol{x})$ is obtained from the cascade model of the volume growth introduced at the end of Sec. IV. We find using Eq. (29)

$$q_l = \ln n_l \sim \ln \frac{V_l(-t_*)}{4\pi l^3/3} = \sum_{i=1}^{N_l} \kappa_i, \tag{74}$$

where the number of cascade steps N_l is determined by setting $l(t) = L$ in Eq. (30). In accord with the discussion at the end of Sec. IV, we can disregard the fluctuations of p, which gives $l\langle p\rangle^{N_l} = L$. Thus, q_l is a sum of a large number $N_l = \log_{\langle p\rangle}(L/l)$ of identically distributed independent random variables. We stress [41] that this does not necessarily imply log normality but only a large deviations form, namely, $P_l(q) \sim \exp[-N_l H(q)]$ of the probability density function (PDF) $P_l(q)$ of q_l. The non-negative convex large deviations function $H(q)$, similar to the entropy of statistical physics, has a unique minimum of zero at $q = \langle q_l\rangle$. Since $N_l \gg 1$, then $P_l(q)$ is sharply peaked at $q = \langle q_l\rangle$. The moments of q_l of not high order are determined by the region near the peak and can be obtained by using quadratic expansion of $H(q)$ near the minimum [41]. This reproduces the central limit theorem. In contrast, the high-order moments are determined by the tail of the distribution and cannot be described by the Gaussian peak. Correspondingly, the moments of the coarse-grained concentration $n_l = \exp(q_l)$ are not determined by the minimum because of exponentiation that includes the high-order moments. Thus, $n_l = \exp(q_l)$ cannot be described by log-normal distribution [41]. We rather have from Eq. (74)

$$\langle n_l^k\rangle = \langle \exp(k\kappa)\rangle^{\log_{\langle p\rangle}(L/l)} = \left(\frac{L}{l}\right)^{\log_{\langle p\rangle}\langle \exp(k\kappa)\rangle}. \tag{75}$$

The scaling exponents of $\langle n_l^k\rangle$ depend on k nonlinearly, which is the benchmark of the multifractal behavior. The exponent $\log_{\langle p\rangle}\langle \exp(k\kappa)\rangle$ divided by $k-1$ gives the dimension deficit $3 - D(k)$; see Eq. (50). The cascade model tells that multifractality arises because of fluctuations of concentration increase factor in one step $\exp(\kappa)$.

Construction of the cascade model above used evolution of trajectories backwards in time since it is this evolution that determines the concentration [53]. The more traditional forward in time form is obtained by time reversal of the previous consideration. Fluctuations of the concentration at scale l are formed by compression of a blob of tracers whose initial size is of the order of the integral scale L of the turbulence. Initial concentration inside the blob is roughly the average concentration $\langle n\rangle$. Transport of the particles leads to the fragmentation of the blob by a sequence of steps each of which decreases the characteristic length by a factor of $p > 1$. Different steps are determined by eddies with significantly different scales and can be considered independent. The continuity equation implies that the increase factor of concentration in one step is $\exp(\tau_l w_l) = \exp(\kappa_l)$, where w_l is the coarse-grained divergence. The rest of the consideration is straightforward.

The above conclusions rely on the assumption that the concentration's reaction on the flow is negligible. That assumption, of course, does not hold for the fluid density, which back reacts on the fluid velocity in a significant manner. Still, the cascade model developed here for the passive concentration can be to some extent transferrable to the active fluid density in the isothermal case. The reason that this is possible despite

the density's back reaction on the transporting velocity is that the force per unit mass exerted by the fluid pressure is proportional to the gradient of the density logarithm, which is independent of the magnitude of the density; cf. Refs. [42,43]. We observe that this view of formation of inhomogeneities is quite different from the model of superposition of many shocks used for the density [42,43,45]. This demands further studies. Though the consideration of the last two sections is quite qualitative, it provides a more consistent derivation of the cascade representation than used usually in turbulence [41]. In what follows, these considerations are confirmed quantitatively.

VIII. MULTIFRACTALITY OF TRACERS: MARKOV PROPERTY AND ZERO MODES

Unless the equality of density and concentration, if true, is proved, we have more knowledge of the statistics of active fluid density than of passive concentration in the multifractal phase. The density in isothermal turbulence is log normal and no fact of similar simplicity holds for the concentration. The log normality of the statistics of the concentration corresponds to neglecting higher than quadratic terms in the cumulant expansion of N-point correlation function, see [54] and Eq. (148) below, which would not hold usually. In this section, we study pair correlations of tracers and present theoretical reasons for the breakdown of log normality.

A. Pair correlations

We study the pair correlation function $f(\boldsymbol{r}) = \langle n(0)n(\boldsymbol{r})\rangle$ that gives the concentration spectrum $E_c(k)$,

$$E_c(k) = 4\pi k^2 \int \exp\left(-i\boldsymbol{k}\cdot\boldsymbol{r}\right) f(\boldsymbol{r}) d\boldsymbol{r}. \tag{76}$$

If anisotropy is relevant, then averaging over directions of $\boldsymbol{k}$ must be introduced in the right-hand side. The pair-correlation function $f(\boldsymbol{r})$ equals $\langle n\rangle^2$ times the radial distribution function (RDF) $g(\boldsymbol{r})$; see Appendix B. The RDF gives the probability of having two tracer particles separated by $\boldsymbol{r}$ in the steady state,

$$g(\boldsymbol{r}) = \lim_{t\to\infty} P(\boldsymbol{r}, \boldsymbol{r}', t). \tag{77}$$

Here, $P(\boldsymbol{r}, \boldsymbol{r}', t)$ is the PDF of the distance between two tracers transported by turbulence given that the initial distance is $\boldsymbol{r}'$,

$$P(\boldsymbol{r}, \boldsymbol{r}', t) = \langle \delta(\boldsymbol{q}(t, \boldsymbol{x}_1 + \boldsymbol{r}') - \boldsymbol{q}(t, \boldsymbol{x}_1) - \boldsymbol{r})\rangle, \tag{78}$$

where the average is independent of $\boldsymbol{x}_1$ by spatial homogeneity. Here and below, the angular brackets stand for averaging over the statistics of the flow and at $t = 0$:

$$P(\boldsymbol{r}, \boldsymbol{r}', 0) = \delta(\boldsymbol{r}' - \boldsymbol{r}). \tag{79}$$

The equivalence of time averaging and averaging over realizations of the flow is demonstrated in Appendix B, where further details on definitions of $f(\boldsymbol{r})$ and $g(\boldsymbol{r})$ can be found. Below, we do not distinguish $g(\boldsymbol{r})$ and $f(\boldsymbol{r})$ working in units with $\langle n\rangle = 1$.

We consider the time evolution of the distance between two tracers in Eq. (78). Typically, the particles initially separate by distance of order of the size of the vessel, which can be L or larger. Then, the particles perform occasional rare excursions to distances in the inertial range. The accumulation of statistics of these excursions forms $f(\boldsymbol{r})$. This way of obtaining the RDF is inconvenient for the study because besides the transport in the inertial range it also involves the transport on the scale of the whole vessel. Below we describe how the properties of $f(\boldsymbol{r})$ can by studied using only the inertial range statistics.

We derive local stationarity condition on $f(r)$ in the supersonic inertial range $r \ll L$. We observe that the Chapman-Kolmogorov equation is approximately true,

$$P(\boldsymbol{r}, \boldsymbol{r}', t_1 + t) \approx \int P(\boldsymbol{r}, \boldsymbol{r}'', t) P(\boldsymbol{r}'', \boldsymbol{r}', t_1) d\boldsymbol{r}'',$$
$$t_r \ll t \lesssim t_L, \quad t_1 \to \infty, \tag{80}$$

where t_r is the turnover time of eddies with size r. To prove this, we write

$$P(\boldsymbol{r}, \boldsymbol{r}', t_1 + t) = \langle \delta(\boldsymbol{q}(t_1 + t, \boldsymbol{x}_1 + \boldsymbol{r}') - \boldsymbol{q}(t_1 + t, \boldsymbol{x}_1) - \boldsymbol{r})\rangle$$
$$= \int \langle \delta(\boldsymbol{q}(t_1 + t, \boldsymbol{x}_1 + \boldsymbol{r}') - \boldsymbol{q}(t_1 + t, \boldsymbol{x}_1) - \boldsymbol{r})$$
$$\times \delta(\boldsymbol{q}(t_1, \boldsymbol{x}_1 + \boldsymbol{r}') - \boldsymbol{q}(t_1, \boldsymbol{x}_1) - \boldsymbol{r}'')\rangle d\boldsymbol{r}''. \tag{81}$$

We consider increasing t at fixed large t_1 (we will take $t_1 \to \infty$ eventually). For flow fluctuations that created $\boldsymbol{r}(t_1 + t) = \boldsymbol{r}$, the value of $r(t_1)$ increases with t. Indeed, the particles are most of the time separated by the distance of order 1 (size of the vessel) and we consider events where at some time before $t_1 + t$ the particles started to approach each other for reaching the distance $r \ll L$ at the moment of observation. The decrease of distance from $\sim L$ to r occurs by a cascade of (on average) contraction events. Qualitatively, the distance decreases from L to $L/2$ due to transport by eddy of size L, then from $L/2$ to $L/4$ by transport by eddy of size $L/2$, and then this process continues until $r \ll L$ is reached. The eddies at the different steps of the cascade are independent because of locality of interactions. Thus, if we take t much larger than the eddy turnover time of eddies of scale r, then we can assume approximate independence of the degrees of freedom of the flow that form $\boldsymbol{r}(t_1 + t)$ and $\boldsymbol{r}(t)$: The dependence comes only through eddies of size of order $r(t)$ that are correlated with $r(t)$ and determine the first step of the cascade process. Thus, $\boldsymbol{r}(t)$ on large timescales is approximately Markovian, and we find Eq. (80) by performing independent averaging of the δ functions on the right-hand side of Eq. (81). We find the stationarity condition,

$$f(\boldsymbol{r}) \approx \int P(\boldsymbol{r}, \boldsymbol{r}', t) f(\boldsymbol{r}') d\boldsymbol{r}', \quad t_r \ll t \ll t_L, \tag{82}$$

where we used Eq. (77). This condition was found previously in Ref. [57] for the white-noise model (considered below) where the Markov property holds exactly due to zero correlation time. This condition holds also in the smooth chaotic systems for r in the smoothness (viscous) range of the flow [49,74].

Keeping in mind the condition given by Eq. (79), the stationarity condition given by Eq. (82) has a power-law solution $f(r) \propto r^{-\beta}$,

$$\int P(\boldsymbol{r}, \boldsymbol{r}', t) r'^{-\beta} d\boldsymbol{r}' = r^{-\beta}, \tag{83}$$

that holds at not too large times so that the characteristic value of r' that determines the integral belongs to the inertial range; see Eq. (82). For incompressible flow, the PDF $P(\boldsymbol{r},\boldsymbol{r}',t)$ is normalized not only with respect to $\boldsymbol{r}$ but also with respect to $\boldsymbol{r}'$ (the operator is Hermitian) so that uniform distribution with $\beta=0$ is a solution. For compressible flow, $\int P(\boldsymbol{r},\boldsymbol{r}',t)d\boldsymbol{r}'$ differs from 1 and $\beta\neq 0$. Assuming now isotropy of small-scale turbulence that holds when the inertial range is appropriately large, averaging of Eq. (82) over the directions of $\boldsymbol{r}$ yields

$$f(r)\approx 4\pi\int_0^\infty \tilde{P}(r,r',t)f(r')r'^2dr', \tag{84}$$

where we denoted the angle-averaged $P(\boldsymbol{r},\boldsymbol{r}',t)$ by $\tilde{P}(r,r',t)$, using the fact that it is independent of the direction of $\boldsymbol{r}'$ due to isotropy [57]. This condition is compatible with the power-law solution $f(r)\propto r^{-\beta}$ provided that $\tilde{P}(r,r',t)$ has a proper scaling dependence on its arguments. This scaling dependence holds only when the scalings of the compressible and solenoidal components of the flow coincide; see the previous section and study of the model below, which is for $\mathrm{Ma}>\mathrm{Ma}_s$. We thus have

$$r^{-\beta}\approx 4\pi\int_0^\infty \tilde{P}(r,r',t)r'^{2-\beta}dr'. \tag{85}$$

This generalizes the condition on the scaling exponent of the pair-correlation function for smooth chaotic systems [74] to our case of nonsmooth rough velocity in the inertial range. We briefly sketch the derivation of the condition in the smooth case.

We start with Eq. (84) that holds also in the smooth case. In this case, smoothness implies that $\boldsymbol{r}(t)=W(t)\boldsymbol{r}'$, where $W(t)$ is the Jacobi matrix [1]. We find that $\tilde{P}=\tilde{P}(r,r',t)$ obeys

$$\tilde{P}=\int\frac{d\hat{r}}{4\pi}\langle\delta(r\hat{r}-W(t)\boldsymbol{r}')\rangle=\left\langle\frac{\delta(r|W(t)\hat{r}'|^{-1}-r')}{4\pi r'^2|W(t)\hat{r}'|^3}\right\rangle.$$

We find that $f(r)\sim r^{-\beta}$ solves Eq. (84) provided the $\beta-3$th moment of the distance between the particles $\langle r^{\beta-3}(t)\rangle$ is conserved. This condition was derived in Ref. [74], and the simplicity of finding the correlation dimension $3-\beta$ in comparison with other fractal dimensions was stressed in Ref. [75]. In the inertial range, we cannot make similar angle averaging that would allow rewriting Eq. (83) in terms of conserved moment of $r(t)$. In fact, we demonstrate that in our case $\langle r^{\beta-3}(t)\rangle$ is not conserved—it is rather divergent. We observe that the characteristic time of reaching r from initial distance $r'\gg r$ is independent of r. This is because of acceleration of the cascade: The total duration of the cascade process is of order of duration of the first step when the distance changes from r' to $r'/2$ that is the turnover time of eddies with size r'. Hence, r' determining the integral in Eq. (84) is independent of r: It is determined by the condition $t_{r'}\sim t$. Taking $t\sim t_L$, we find

$$f(r)\sim P(r,L,t_L)L^3, \tag{86}$$

where we used that concentration at scale L decorrelates so that $f(L)$ is of order of squared mean concentration, which is 1 in our normalization. For self-similar flow with identical (in reality close) scaling of compressible and solenoidal components, $\tilde{P}(r,r',t)$ has power-law behavior $\tilde{P}(r,r',t)\sim r^{-\beta}$ at small r; see concrete calculation for the model below. We find from Eq. (86) that

$$f(r)=\left(\frac{\tilde{L}}{r}\right)^\beta,\quad r\ll L, \tag{87}$$

where $\tilde{L}\sim L$ so that the matching condition at $r\sim L$ holds. In contrast, if the flow is not self-similar, then there is no power-law behavior and thus no multifractality. This supports that the transition to multifractality happens at the critical Mach number Ma_s where the difference of scalings of the velocity components becomes negligible. The value of Ma_s defined in this way depends on the needed resolution of the exponents and the resulting power law of $f(r)$.

We conclude that the correlation codimension $3-\beta$ can be obtained as small first argument asymptotic behavior of $\tilde{P}(r,r',t)$,

$$f(r)\propto r^{-\beta},\ \tilde{P}(r,r',t)\propto r^{-\beta};\quad r,r'\ll L,\ t\ll t_L. \tag{88}$$

This behavior is independent of r' and holds also in the limit $r'\to 0$; see the concrete calculation for the white-noise model in the next section. The limit $r'\to 0$ is finite due to the explosive separation of trajectories in the inertial range; see below and Ref. [57]. Thus, $\tilde{P}(r,t)=\tilde{P}(r,0,t)$ is the minimal object from which we can infer β. For self-similar velocities, $\tilde{P}(r,t)$ has self-similar evolution with scaling variable determined by the counterpart of the Richardson law for compressible turbulence.

It must be stressed that the nontriviality of Eq. (88) is that we use here the asymptotic PDF in the inertial range that depends on time t. The equation itself is also true for long-time limit $P(\boldsymbol{r},\boldsymbol{r}',t\to\infty)$; however, it is trivial there [see Eq. (77)]. We observe also that since $\tilde{P}(r,r',t)\sim r^{-\beta}$ at small r then $\langle r^{\beta-3}\rangle$ is the moment with largest order that diverges: Moments of order larger that $\beta-3$ are finite and moments with smaller order diverge at zero argument. Very similar statement holds for correlation dimension of attractors of smooth systems [60]. The same moment determines the correlation codimension in smooth chaotic flow where $\langle r^{\beta-3}(t)\rangle=r^{\beta-3}(t=0)$ is the unique nontrivial conserved moment of the interparticle distance [74].

B. Anomalous scaling of higher order correlations

We observe from Eq. (82) that the pair correlation function is invariant under the action of operator with kernel $P(\boldsymbol{r},\boldsymbol{r}',t)$. Thus, it is similar to the so-called zero mode [57]. Zero modes are statistically conserved functions of the evolving spatial configuration of n particles. They can have nontrivial scaling exponents, the fact that provided the key to the understanding of anomalous scaling of the passive scalar in incompressible turbulence; see Refs. [76–79] and the review [1]. In the case of compressible turbulence, the zero modes are the reason for strong breakdown of log normality in the multifractal regime; cf. Ref. [49]. Log-normality property $\langle n(\boldsymbol{r}_1)n(\boldsymbol{r}_2)\dots n(\boldsymbol{r}_n)\rangle=\prod_{i>k}\langle n(\boldsymbol{r}_i)n(\boldsymbol{r}_k)\rangle$ entails the normal scaling of the nth-order correlation function given by $n/2$ times the scaling exponent of $\langle n(0)n(\boldsymbol{r})\rangle$. We say that the log normality is broken weakly if the equality $\langle n(\boldsymbol{r}_1)n(\boldsymbol{r}_2)\dots n(\boldsymbol{r}_n)\rangle=\prod_{i>k}\langle n(\boldsymbol{r}_i)n(\boldsymbol{r}_k)\rangle$ breaks down but the normal scaling of the nth-order correlation function still

holds. Strong breakdown occurs when the scalings do not agree, the case referred to in Ref. [1] as anomalous scaling.

The study of anomalous scaling involves considering the stationarity condition on the higher order correlation function $f(\boldsymbol{r}_1,\dots,\boldsymbol{r}_n)=\langle n(0)n(\boldsymbol{r}_1)\dots n(\boldsymbol{r}_n)\rangle$. The derivation proceeds similarly to the pair correlation. We find that the $(n+1)$-point correlation function is determined by the joint PDF of the distances between $n+1$ particles, that is the transition probability $P(\boldsymbol{R},\boldsymbol{R}',t)$. Here, we introduced $(\boldsymbol{R})=(\boldsymbol{r}_1,\boldsymbol{r}_2,\dots,\boldsymbol{r}_n)$, where $\boldsymbol{r}_i$ is the distance from ith particle to "zeroth" particle; cf. Ref. [57]. We find

$$f(\boldsymbol{R})\approx\int P(\boldsymbol{R},\boldsymbol{R}'',t)f(\boldsymbol{R}'')d\boldsymbol{R}'',\quad t_r\ll t\ll t_L, \tag{89}$$

which is direct generalization of Eq. (82). Thus, $\langle n(0)n(\boldsymbol{r}_1)\dots n(\boldsymbol{r}_n)\rangle$ is the zero mode of the operator of Lagrangian evolution of distances between the particles $P(\boldsymbol{R},\boldsymbol{R}'',t)$; cf. Ref. [57]. Inspection of the zero-mode mechanism of anomalous scaling of passive scalar in incompressible turbulence [1] reveals that normal scaling is highly implausible. The problem of actual computation of the exponents is formulated for a model in the next section.

IX. USING THE MARKOV PROPERTY: THE KRAICHNAN MODEL

In this section, we introduce the Kraichnan model of the statistics of the flow velocity relying on the Markov property derived in the previous section. The purpose of this model is to facilitate the investigation of the dependence of the concentration statistics on the Mach number, both as determined by the ratio of the magnitude of the compressible and solenoidal components and by the difference of the scaling exponents of the components. Moreover, the model can be used for the consistent study of anomalous scaling.

We observe that the Chapman-Kolmogorov equation given by Eq. (80) can also be written for finite t_1 since all the used considerations apply. This time must be large so that the decoupling in the product holds. However, we pick it not so large that $P(\boldsymbol{r}'',\boldsymbol{r}',t_1)$ in Eq. (80) can still be considered as the inertial range quantity. The general solution of the Chapman-Kolmogorov equation is

$$P(\boldsymbol{r},\boldsymbol{r}',t)=\exp(t\hat{L})(\boldsymbol{r},\boldsymbol{r}'),\quad \partial_t P=\hat{L}P,\quad t\gg t_{r'}, \tag{90}$$

where $\hat{L}$ is a time-independent linear operator. This operator describes long-time transport of pairs of particles and it depends on the properties of turbulence nonlocally both in space and time. The direct study of $\hat{L}$ is hardly possible. For approximations, we can consider this operator as a series in derivative operators. By the Pawula theorem, for not developing negative transition probabilities $P(\boldsymbol{r},\boldsymbol{r}',t)$, approximations of this series must either stop at the second derivative terms or contain an infinite number of terms [80]. We will consider the most general second-order approximation consistent with the spatial homogeneity and isotropy. It will be demonstrated in the next subsection that this approximation is a rigorous way of introducing eddy diffusivity. The approximation is provided by the famous Kraichnan model that helped the breakthrough in the understanding of transport by incompressible turbulence; see Ref. [1] and references therein. We use the formulation of Ref. [53]. The flow $\boldsymbol{u}$ is assumed to be a Gaussian random field with zero mean and pair-correlation function,

$$\langle u_i(t_1,\boldsymbol{x}_1)u_k(t_2,\boldsymbol{x}_2)\rangle=\delta(t_2-t_1)[V_0\delta_{ik}-K_{ik}(\boldsymbol{r})], \tag{91}$$

where $\boldsymbol{r}=\boldsymbol{x}_2-\boldsymbol{x}_1$. The most general form of K_{ik} [obeying $K_{ik}(r=0)=0$] which is consistent with isotropy is

$$2K_{ik}=\left[\frac{(r^4u)'}{r^3}-c\right]r^2\delta_{ik}-\left[\frac{(r^2u)'}{r}-c\right]r_ir_k, \tag{92}$$

where u and v are certain scalar functions of r. Here, the used white noise in time structure of the statistics is fixed uniquely by the Markov property. The Gaussianity is not a necessary assumption as long as the study is confined to the pair correlations. Indeed, the increments of white noise over small but finite time intervals are Gaussian by the central limit theorem; cf. with the Gaussianity of Langevin forces in the theory of Brownian motion and see the Kramers-Moyal coefficients in Ref. [80]. The only assumption that is introduced by the model is that in this model $\hat{L}(\boldsymbol{r},\boldsymbol{r}')=\nabla_i\nabla_k K_{ik}(\boldsymbol{r})\delta(\boldsymbol{r}-\boldsymbol{r}')$, where the operators act to the right; see Ref. [53]. Thus, the operator $\hat{L}$ is the most general differential operator of the second order which is consistent with conservation of probability and isotropy (there could be also another term of $\nabla_i\tilde{u}_i(\boldsymbol{r})\delta(\boldsymbol{r}-\boldsymbol{r}')$; however, this term would correspond to a mean flow).

The tensor $K_{ik}(\boldsymbol{r})$ or equivalently the functions $u(r)$ and $c(r)$ must be picked for best fitting of the data. For instance, the arguments of the previous section demonstrate that at small r the NS turbulence corresponding to the multifractal phase of the tracers gives

$$P(\boldsymbol{r},0,t)\sim\frac{\text{const}}{r^\beta},\quad r\to 0. \tag{93}$$

This behavior is reproduced by the model described by Eq. (91) with certain values of the constant in the numerator and the exponent β in the denominator derived from $u(r)$ and $c(r)$; see below. These values must be gauged so that the above behavior is reproduced. More information on how the functions $u(r)$ and $c(r)$ are fixed can be found in Appendix C, where the model is introduced in detail. It is demonstrated there that $u(r)$ is a linear combination of the inverse Fourier transforms $f(r)$ and $h(r)$ of effective solenoidal and potential spectral functions. The functions $f(k)$ and $h(k)$ are not the spectra of the solenoidal and potential components of turbulence and their scalings differ from those of these spectra. They are similar to spectrum in the frequency–wavenumber domain evaluated at zero frequency; see details in Appendix C. On long timescales, the model reproduces the pair dispersion in the NS flow at least qualitatively. Finally, the function $c(r)$ is nonzero if and only if the flow has finite compressibility. The correlation function of the velocity divergence may therefore be calculated in terms of the $c(r)$ and is given by

$$\langle w(t,\boldsymbol{x})w(t',\boldsymbol{x}')\rangle=\delta(t'-t)(3c(r)+rc'(r)), \tag{94}$$

In this section, the model is used only in the inertial range; for the discussion of the use in the viscous range, see Sec. XI.

A. Yaglom-type relation and eddy diffusivity assumption

The Kraichnan model provides a consistent way for resolving the ambiguity in the eddy diffusivity approximation that occurs due to compressibility. We start from deriving an exact relation for the tracers concentration in a Navier-Stokes (NS) turbulence. This is the counterpart of Yaglom's relation for scalar turbulence [1,81]. Starting with the stationarity condition $\partial_t \langle n(\boldsymbol{x}_1) n(\boldsymbol{x}_2)\rangle = 0$, after moving the time derivative under the average and using Eq. (1) we find

$$\boldsymbol{\nabla} \cdot \langle (\boldsymbol{v}(\boldsymbol{r}) - \boldsymbol{v}(0)) n(0) n(\boldsymbol{r})\rangle = 0, \tag{95}$$

where $\boldsymbol{r} = \boldsymbol{x}_2 - \boldsymbol{x}_1$ and we used the statistics homogeneity. Using isotropy and regularity at zero, we find

$$\langle (\boldsymbol{v}(\boldsymbol{r}) - \boldsymbol{v}(0)) n(0) n(\boldsymbol{r})\rangle = 0. \tag{96}$$

For Yaglom's relation, the right-hand side in Eq. (96) is a finite constant and the scaling of the scalar in the inertial range is found from that of the velocity by power counting. In our case, however, the scaling of $\langle n(0)n(\boldsymbol{r})\rangle$ is determined not by the absolute scaling of the velocity but rather by the relative scalings and magnitudes of the compressible and solenoidal components; see below.

We cannot decouple the velocity and the concentration in Eq. (96); however, it is plausible that similarly to the passive scalar case [81] we can use the eddy diffusivity approximation, at least qualitatively,

$$\langle (\boldsymbol{v}(\boldsymbol{r}) - \boldsymbol{v}(0)) n(0) n(\boldsymbol{r})\rangle = -\boldsymbol{\nabla}_k (K_{ik}(\boldsymbol{r}) \langle n(0) n(\boldsymbol{r})\rangle), \tag{97}$$

where $K_{ik}(\boldsymbol{r})$ is the eddy diffusivity tensor that is taken for fitting the data. In the Kraichnan model, Eq. (97) is exact with K_{ik} given by Eqs. (91) and (92) as can be seen from the equation on the pair correlation function [53]. We thus have from Eqs. (96) and (97) that

$$K_{ik} \boldsymbol{\nabla}_k \ln \langle n(0) n(\boldsymbol{r})\rangle = -\boldsymbol{\nabla}_k K_{ik}. \tag{98}$$

This equation becomes a first-order ordinary differential equation for $\langle n(0)n(\boldsymbol{r})\rangle$ upon the use of isotropy. Its solution is given by

$$\langle n(0) n(\boldsymbol{r})\rangle = \exp\left[\int_r^\infty \frac{c(r')dr'}{r' u(r')}\right]. \tag{99}$$

This solution was presented in Ref. [53], where the case with power-law decay of $c(r)/u(r)$ beyond the viscous range and smooth behavior inside the viscous range were considered. This is the case of multifractality in the viscous range, not considered here.

The behavior of $\langle n(0)n(\boldsymbol{r})\rangle$ in the inertial range depends on the magnitudes of scaling exponents of the compressible component $c(r)$ and solenoidal component $u(r)$. For $\mathrm{Ma} < \mathrm{Ma}_s$, the scaling exponent of $c(r)$ in the inertial range is smaller than that of the solenoidal component as in Ref. [53]. For instance, in the pseudosound regime at small Mach numbers, the spectrum of the compressible component is proportional to k^{-3}, which decays much more quickly than the almost Kolmogorov spectrum of the solenoidal component [82]. In this case and also below the sonic scale at $\mathrm{Ma} > \mathrm{Ma}_s$, we find from Eq. (99) that $\langle n(0)n(\boldsymbol{r})\rangle$ is smoothly dependent on r. There is no divergent power-law dependence that characterizes multifractal distributions. In contrast, above the sonic scale at $\mathrm{Ma} > \mathrm{Ma}_s$ the scalings of $c(r)$ and $u(r)$ can be approximated as identical. Then, the ratio $c(r)/u(r)$ is given by the constant β in the inertial range where the notation is used for consistency with the results of the previous sections. We therefore find

$$\langle n(0) n(\boldsymbol{r})\rangle = \left(\frac{\tilde{L}}{r}\right)^\beta, \quad \frac{c(r)}{u(r)} \approx \beta, \quad \eta \ll r \ll L, \tag{100}$$

where $\tilde{L}$ is a cutoff scale of the order of the integral scale L. Equation (87) is thus recovered. It is remarkable that the common scaling exponent of $c(r)$ and $u(r)$ drops from $\langle n(0)n(\boldsymbol{r})\rangle$. In contrast, the relative magnitude β of the compressible and solenoidal components determines the scaling. Qualitative reasons for this are provided by the cascade model presented in Sec. VII.

B. Supercritical transport in Kraichnan model

We formulate the Kraichnan model of transport in the supersonic inertial range at $\mathrm{Ma} > \mathrm{Ma}_s$. In that regime, the solenoidal and potential components of the velocity are characterized by the same scaling exponent. We therefore introduce in the inertial range $u(r) = c_0' r^{\xi-2}$ and $c(r) = c_0 r^{\xi-2}$, where ξ, c_0', and c_0 are constants [57],

$$2K_{ik} = [c_0'(2+\xi) - c_0] r^\xi \delta_{ik} + \left[\frac{c_0}{\xi} - c_0'\right] \xi r^{\xi-2} r_i r_k. \tag{101}$$

The scaling exponent ξ is chosen so that the condition of modeling the NS turbulence given by Eq. (C3) in Appendix C holds. Thus, if the scaling exponent of the NS velocity is α (so that the spectrum decays as $k^{-1-2\alpha}$) then $\xi = 1 + \alpha$; see the consideration after Eq. (C6). The Kolmogorov value $\alpha = 1/3$ corresponds therefore to $\xi = 4/3$ and not $\xi = 2/3$; see Ref. [1]. Besides ξ, the model is characterized by another dimensionless parameter, $\beta = c_0/c_0'$; see Eq. (100). Here, the overall magnitude of K determines a dimensionless timescale $\tau = c_0' t$ that has no qualitative relevance and drops from the steady-state averages. Therefore, without loss of generality, we set below $c_0' = 1$. Instead of β, we can use the compressibility degree $\mathcal{P}$ that is defined as the ratio of $\langle (\boldsymbol{\nabla} \cdot \boldsymbol{u})^2\rangle$ and $\langle (\boldsymbol{\nabla u})^2\rangle$ and is given by Ref. [57],

$$\mathcal{P} = \frac{\beta}{\xi[3 + \xi - \beta]}, \quad 0 \leqslant \mathcal{P} \leqslant 1. \tag{102}$$

Thus, the model is determined by $\mathcal{P}$ and ξ, both of which can be modeled as monotonously growing functions of Ma. The compressibility $\mathcal{P}$ grows from a certain finite value at Ma_s to 1 at infinite Mach number. The exponent ξ grows from some value larger than 4/3 at Ma_s up to a value ξ_∞ at $\mathrm{Ma} = \infty$. The value of $\xi_\infty = 3/2$ that corresponds to k^{-2} spectrum of the Burgers equation is a reasonable and widely accepted conjecture [83].

C. Clumping transition

The clumping transition has been invoked in Ref. [57] as an important mechanism for the transition to multifractality. Within that scenario, increasing the Mach number leads to a transition from a finite number of encounters between a pair of particles to particles sticking to each other with probability 1.

Here, we briefly consider that transition and demonstrate that it is not likely to occur in NS compressible turbulence. In order to do that, we revert to Eq. (102) that yields

$$\beta = \frac{\mathcal{P}\xi[3+\xi]}{1+\mathcal{P}\xi}. \tag{103}$$

As β represents the difference between the space dimension and the correlation dimension, it is necessarily a growing function of Ma. That difference between the space and the correlation dimensions, called dimension deficit, grows linearly with the compressibility degree $\mathcal{P}$ at small compressibility. (This range is purely theoretical since there are no cases of weakly compressible flows with identical scalings of solenoidal and potential components known to us. This situation would be highly interesting; see Appendix D.) For $\mathcal{P} > 3/\xi^2$, the value of β becomes larger than 3, which corresponds to negative correlation dimension. For such values of β, namely bigger than 3, the integral of the correlation function given by Eq. (100) diverges at zero, thus yielding an (unphysical) infinite mass in an arbitrarily small ball. Thus, the expression for the correlation function breaks down for $\mathcal{P}$ above $3/\xi^2$. This signifies the clumping transition as two tracers glue to each other at large times with probability 1. The PDF $P(\boldsymbol{r}, \boldsymbol{r}_0, t)$ in this case is a sum of a regular term and a $\delta(\boldsymbol{r})$ term whose amplitude grows from zero at $t = 0$ to one at $t = \infty$; see Ref. [57]. Correspondingly, the steady-state correlation function is $\delta(\boldsymbol{r})$ in this case.

We saw previously that for compressible turbulence the value of ξ is bounded from above by 3/2. The resulting value of $3/\xi^2$ is larger than 1 so that the range $\mathcal{P} > 3/\xi^2$ is unphysical. Thus, assuming that the Kraichnan model provides a realistic description of the NS compressible turbulence leads to the conclusion that no clumping transition occurs in that turbulence. We hypothesize that this conclusion is true; however, complete settling of this issue requires further studies. We finally remark that in contrast to the clumping transition, the infinite recurrence transition that is discussed in the next two subsections may occur in NS turbulence.

D. PDF of the distance and pair correlations

We confirm Eq. (88) by direct calculation. In the Kraichnan model, $P(\boldsymbol{r}, \boldsymbol{r}', t)$ obeys the Fokker-Planck equation [1,57],

$$\partial_{|\tau|} P = \nabla_i \nabla_l (K_{il}(\boldsymbol{r}) P), \quad P(\tau = 0) = \delta(\boldsymbol{r} - \boldsymbol{r}'), \tag{104}$$

where the evolution can be considered both for positive and negative dimensionless time τ. This equation necessarily has the same form as the evolution equation of $\langle n(0) n(\boldsymbol{r})\rangle$ provided in Ref. [53]; cf. Eq. (82). The turbulent diffusion operator $\nabla_i \nabla_l K_{il}$ describes a power-law growth of $r(|\tau|)$ in the inertial range,

$$\frac{d\langle r^k(|\tau|)\rangle}{d|\tau|} = \frac{d}{d|\tau|}\int r^k P(\boldsymbol{r}, \boldsymbol{r}', |\tau|) d\boldsymbol{r} = \int r^k d\boldsymbol{r} \nabla_i \nabla_l (K_{il}(\boldsymbol{r}) P)$$
$$= k(k+1+\xi-\beta)\langle r^{k+\xi-2}\rangle, \tag{105}$$

where we integrated by parts and employed Eqs. (79) and (80) as well as the relationship

$$K_{il} \nabla_i \nabla_l r^k = k r^{k+\xi-2}(k+1+\xi-\beta) \tag{106}$$

that holds in the inertial range and is obtained by direct calculation using Eq. (101). We find, by setting $k = 2 - \xi$,

$$\langle r^{2-\xi}(\tau)\rangle = r^{2-\xi}(0) + (2-\xi)(3-\beta)|\tau|, \tag{107}$$

which is the form that the Richardson law, given by Eq. (19), takes in the Kraichnan model. As discussed after Eq. (19), the separation $r(\tau)$ is independent of the initial condition at times larger than $r^{2-\xi}(0)$. There, the power-law growth holds: $\langle r^{2-\xi}(\tau)\rangle \approx (2-\xi)(3-\beta)|\tau|$. Such a type of separation of trajectories that remains finite in the limit of zero $r(0)$ is called explosive [57] in order to distinguish them from the more usual chaotic separation, where $r(t) = 0$ at $r(0) = 0$. The explosive separation is a characteristic property of the inertial range separation by nondifferentiable rough velocity where roughness causes nonuniqueness of the trajectories.

Returning to Eq. (104), it has a self-similar solution,

$$f_s(\boldsymbol{r}, \tau) = \frac{|\tau|^{b_0-1}(2-\xi)^{2b_0-1}}{4\pi r^\beta \Gamma(1-b_0)} \exp\left[-\frac{r^{2-\xi}}{(2-\xi)^2|\tau|}\right], \tag{108}$$

where $b_0 = (\beta - \xi - 1)/(2-\xi)$, and we normalized the solution so that $\int f(\boldsymbol{r}) d\boldsymbol{r} = 1$. This solution coincides with the finite limit $P(\boldsymbol{r}, r' \to 0, \tau)$; see Ref. [57] and Appendix D. The solution is quite similar in properties to the fundamental solution of the ordinary diffusion equation. In fact, considering the dependence of the model on ξ as a parameter that varies in the maximal allowed [1] range $0 \leqslant 0 < 2$, we have that at $\xi = 0$ and $\beta = 0$ turbulent diffusion reduces to the ordinary diffusion. The above formula reduces then to the Green's function of diffusion equation. At finite ξ and β, as in ordinary diffusion, $f_s(r, \tau)$ describes the long-time asymptotic form of $P(\boldsymbol{r}, \boldsymbol{r}', \tau)$. Thus, at large times the evolution of separation is self-similar, giving $\langle r^n(|t|)\rangle \propto |t|^{n/(2-\xi)}$. The counterpart of the Richardson law is then $\langle r^2(|t|)\rangle \propto |t|^{2/(2-\xi)}$.

We see from Eq. (108) that the scaling exponent of the pair-correlation function of the concentration determines the scaling of $P(r, r' \to 0, \tau)$ at small r in accord with Eq. (88). The confirmation in the case of $r' \neq 0$ is more complex. It is provided in Appendix D along with the formula for the moments of the distance between two tracers.

E. Infinite recurrence transition

We observe that at small compressibility $\mathcal{P}$ the parameter b is negative and the integral of $P(r, r_0 \to 0, t)$ over t converges at large times. Thus, the particles collide, reaching $r(t) = 0$ at most a finite number of times; cf. similar considerations for usual diffusion. However, as the compressibility increases, a transition occurs at $\beta = 1 + \xi$ or $\mathcal{P} = (1+\xi)/(2\xi)$ and b becomes positive for larger compressibilities. The time integral diverges at large times so that particles will collide an infinite number of times with probability 1. This trapping effect of compressibility discovered in Ref. [57] makes the behavior of pairs of tracers qualitatively different from that in the incompressible flow.

In contrast with the clumping transition, for the infinite recurrence transition the Kraichnan model indicates that this transition can occur in the NS turbulence. Indeed, for $4/3 \leqslant \xi \leqslant 3/2$, the value of $\mathcal{P} = (1+\xi)/(2\xi)$ is below 1. Deciding whether the transition does occur requires numerical studies.

F. Anomalous scaling and zero modes

Finally, we comment on the scaling of higher order correlation functions of the concentration that determine the fractal dimensions of positive integer order. These functions obey in the Kraichnan model a closed PDE: They are zero modes of the operator $\sum_{nl} \nabla_{r_n^i} \nabla_{r_l^k} K_{ik}(\boldsymbol{r}_n - \boldsymbol{r}_l)$, where $\boldsymbol{r}_n$ are the points in the correlation function [1,49]. Zero modes provide a known way of producing anomalous scaling exponents, in our case nontrivial dependence of $D(k)$ on k; cf. the previous section.

We examine the validity of this consideration outside the Kraichnan model. We observe that similar to our study of the pair correlations we find that $P(\boldsymbol{R}, \boldsymbol{R}', t)$ in Eq. (89) is given by $\exp(t\hat{L}_n)(\boldsymbol{R}, \boldsymbol{R}')$ with certain linear operator $\hat{L}_n$. In the Kraichnan model, $\hat{L}_n$ reduces to a linear combination of the pair-dispersion operators $\hat{L}$. This reduction would not hold for propagators $P(\boldsymbol{R}, \boldsymbol{R}', t)$ of the NS flow. However, the reduction introduced by the Kraichnan model is similar to neglecting the intermittency of the flow and it is valid qualitatively. The reason is that the intermittency of the statistics of the transported quantity, tracers' concentration in our case, is much stronger than the intermittency of the transporting velocity. For instance, the difference of the scaling exponent of the fourth-order correlation function of the concentration and twice the scaling exponent of the pair correlation is finite even when the transporting velocity is self-similar: The concentration is intermittent even when the flow is not. This was found in the case of a passive scalar transported by incompressible turbulence where the scalar is not self-similar even though the transporting flow is a self-similar Gaussian flow with little structure [1]. The reason for this phenomenon, called anomalous scaling, is the zero modes described in the previous section. These modes define the correlation functions and have intrinsically anomalous scaling independent of whether the velocity scaling is anomalous. The situation seems similar in our case also though the detailed calculations are outside the scope of this paper. It must be kept in mind though that for other questions the neglect of intermittency could be not valid. For instance, pair dispersion in the Kraichnan model is self-similar; however, intermittency of turbulence would cause breakdown of this self-similarity.

G. Transition to multifractality in NS turbulence

We consider Eq. (99) at any Ma, not necessarily in the multifractal phase. We find using the formula for c/ru derived in Appendix C,

$$\ln\langle n(0)n(\boldsymbol{r})\rangle = \int_{r/\tilde{L}}^{1} \frac{(b+1)(b+7)(a+7)\Gamma' r'^{\Delta-1} dr'}{8(b+7)+2(b+3)(a+7)\Gamma' r'^{\Delta}}, \quad (109)$$

where $\Delta = (b-a)/2$ is half the difference of decay exponents b and a of the spectra of potential and solenoidal components of velocity, respectively, and Γ' is the ratio of the magnitudes of potential and solenoidal components; see details in Appendix C. The integration variable here is the ratio of the scale and the upper cutoff scale $\tilde{L}$, which is determined by the breakdown of scaling of c and u and is of order of the integral scale L. This scale is $\tilde{L}$ in Eq. (100).

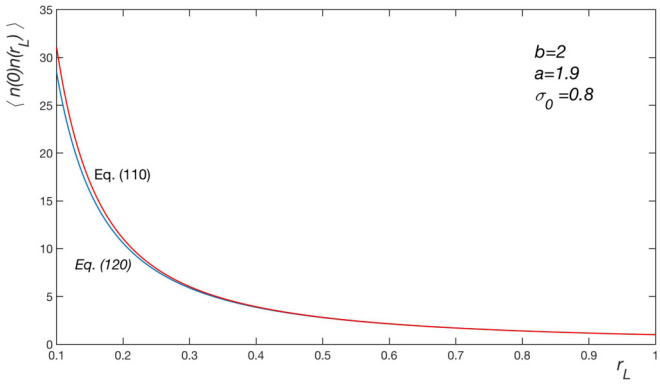

FIG. 1. The tracers' pair correlation function in the high-Mach-number regime. $r_L = r/\tilde{L}$.

Integration of Eq. (109) gives

$$\langle n(0)n(\boldsymbol{r})\rangle = \left[\frac{\sigma_0+1}{\sigma_0+(r/\tilde{L})^{\Delta}}\right]^{(b+1)(b+7)/(2(b+3)\Delta)}. \quad (110)$$

We introduced the dimensionless quantity $\sigma_0 = 4(b+7)/[(b+3)(a+7)\Gamma']$. We have $\sigma_0 \sim 1/\Gamma'$ for physically relevant values of a and b, so σ_0 characterizes the ratio of the magnitudes of solenoidal and potential components.

The above equation is a concise prediction of the model that holds at any Ma. In the limit of small Mach numbers, we have $\sigma_0 \gg 1$ and the pair-correlation function is nearly constant at $r \ll L$. At Ma and Δ of order 1, where $\sigma_0 \sim 1$, the pair-correlation function has some changes in the inertial range. The power law becomes valid as the Mach number increases and Δ becomes much smaller than 1. For the study of this limit, it is useful to rewrite the pair correlation function as

$$\ln\langle n(0)n(\boldsymbol{r})\rangle = \frac{(b+1)(b+7)}{2(b+3)\Delta} \times \ln\left(\frac{2(b+3)(a+7)\Gamma'(r/\tilde{L})^{\Delta}\left((\tilde{L}/r)^{\Delta}-1\right)}{8(b+7)+2(b+3)(a+7)\Gamma'(r/\tilde{L})^{\Delta}}+1\right), \quad (111)$$

This can be approximated for $\Delta \ll 1$ as

$$\langle n(0)n(\boldsymbol{r})\rangle \approx \exp\left\{\frac{\beta}{\Delta}\left[\left(\frac{\tilde{L}}{r}\right)^{\Delta}-1\right]\right\}, \quad (112)$$

with

$$\beta = \frac{(a+7)(b+1)(b+7)\Gamma'}{8(b+7)+2(b+3)(a+7)\Gamma'}. \quad (113)$$

We see that Eq. (100) is a good approximation under the condition $\Delta \ln(\tilde{L}/r) \ll 1$. These formulas can be used for fitting the parameters of the model with the help of future numerical data. Figure 1 depicts the tracers' pair correlation function as obtained from the Kraichnan model, i.e., Eq. (110) (blue line) as compared to the approximating power low given by Eq. (100) (red line). It should be mentioned that Fig. 1 represents a valid picture only down to the sonic length. As commented above, below that scale the pair correlation function flattens significantly. The pair correlation function

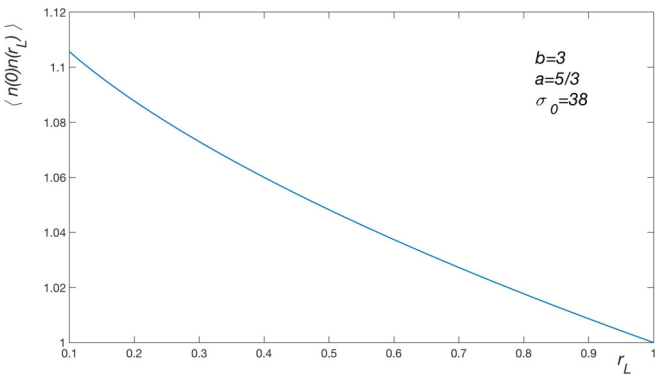

FIG. 2. The tracers' pair correlation function in the low-Mach-number regime as predicted by Eq. (110). $r_L = r/\tilde{L}$.

according to Eq. (110) in the small-Mach-number regime is shown in Fig. 2. As expected, in that regime the concentration fluctuations are small and close to a constant value over the inertial range.

Thus, we confirmed again that multifractality is approximate. This is because the density fluctuations are created by the potential component of the velocity but particles' separation is determined by the complete velocity. Strictly speaking, the multifractality holds only when the scalings of the velocity components are identical.

X. ACCELERATION OF FORMATION OF PLANETESIMALS

Transition to multifractality implies a strong increase of the pair correlation function of concentration at small distances. The flow transport brings the tracers close much more often than below the transition. This implies a strong increase in the collision rate of particles above the transition, as we demonstrate in this section. The rate increases by a large parameter over a short interval of Mach numbers where the pair correlation transitions from the stretched exponential to the power-law form; see Eq. (99). The physical system that we use for consideration is formation of planetesimals.

We consider a model where formation of planetesimals occurs due to coalescence of particles of dust. The particles are transported by the compressible turbulent flow of a gas that is characterized by large Mach and Reynolds numbers. The particles are assumed to have negligible inertia and move as tracers.

The solution is assumed to be dilute. Thus, we can neglect the particles' back reaction on the flow and consider only binary collisions. Two dust particles of radii a_1 and a_2 collide when their centers are at a distance $a_1 + a_2$ from each other. Thus, $a_1 + a_2$ is the effective interaction radius of the particles. We assume that the collision leads to coalescence with probability P_{12} that depends on a_i. This probability characterizes short-range interactions and is the counterpart of the collision efficiency in the similar problem of coalescence of droplets in rain formation [84]. The rate of coalescence per unit volume γ_{12} of dust particles of radii a_1 and a_2 is given by Refs. [84,85],

$$\gamma_{12} = -P_{12}\int_{w_r<0, r=a_1+a_2} dS\langle n_2(0)n_1(\boldsymbol{r})w_r(\boldsymbol{r})\rangle, \quad (114)$$

where n_i is the concentration of the particles with radius a_i and $w_r(\boldsymbol{r}) = v_r(\boldsymbol{r}) - v_r(0)$ is the radial component of the velocity difference of the colliding particles. The integral above is over that part of the surface of the ball of radius $a_1 + a_2$ on which $w_r < 0$. This condition ensures that the particles approach and not separate. The angular brackets stand for the spatial averaging. We can simplify Eq. (114) by employing the continuity equation,

$$\partial_t n_i + \boldsymbol{\nabla}\cdot(n_i\boldsymbol{v}) = 0, \quad (115)$$

where $i = 1, 2$. Using the same steps taken for deriving Eq. (95), we find

$$\boldsymbol{\nabla}\cdot\langle n_2(0)n_1(\boldsymbol{r})[\boldsymbol{v}_1(\boldsymbol{r}) - \boldsymbol{v}_2(0)]\rangle = 0. \quad (116)$$

Finally, we find by integrating over the volume of the ball with radius $a_1 + a_2$ and using the divergence theorem, the following constraint:

$$\int \langle n_2(0)n_1(\boldsymbol{r})w_r\rangle dS = 0. \quad (117)$$

Thus, we can write Eq. (114) in the form

$$\gamma = \frac{P_{12}}{2}\int_{r=a_1+a_2} dS\langle n_2(0)n_1(\boldsymbol{r})|w_r|\rangle, \quad (118)$$

The derivation of similar identity in the incompressible isotropic case was done in Ref. [85]. This way of rewriting γ_{12} is useful because averaging conditioned on sign of w_r is more difficult.

We observe from the cascade picture of the formation of fluctuations of the concentration that for r in the inertial range $\langle n_2(0)n_1(\boldsymbol{r})\rangle$ is determined by many steps of the cascade and only the last step is correlated with w_r. Thus, neglecting one step in comparison with many, we can perform independent averaging, $\langle n_2(0)n_1(\boldsymbol{r})|w_r|\rangle = S(r)\langle n_2(0)n_1(\boldsymbol{r})\rangle$, where $S(r) = \langle|w_r(r)|\rangle$. Invoking isotropy, we find

$$\gamma_{12} = 2\pi P_{12}(a_1 + a_2)^2 S(a_1 + a_2)\langle n_2(0)n_1(a_1 + a_2)\rangle. \quad (119)$$

The structure function $S(r)$ changes smoothly at the transition to multifractality [at the transition the scaling exponents of solenoidal and potential components of the velocity become similar, which does not bring a strong change of $S(r)$]. Thus, we can concentrate on the change of γ_{12} due to $\langle n_2(0)n_1(a_1 + a_2)\rangle$. In the multifractal phase, this is given simply by

$$\langle n_2(0)n_1(a_1 + a_2)\rangle = \langle n_1\rangle\langle n_2\rangle\left(\frac{L}{a_1 + a_2}\right)^{3-D_t(2)}, \quad (120)$$

where $D_t(2)$ is the correlation dimension of the multifractal formed by the tracers. We remark that particles with different a_i are identically moving tracers so the probability of finding another particle at fixed distance r from a given particle is independent of the particle radii a_i. The above formula assumes that $a_1 + a_2$ belongs in the supersonic inertial range that is larger than the sonic scale l_s but smaller than L. In this case, at the transition γ_{12} is increased by the factor of $(L/(a_1 + a_2))^{3-D_t(2)}$.

A. Pair correlations and collisions below the sonic scale

It is probable that in many applications the case of colliding particles with $a_1 + a_2 < l_s$ would be relevant. The description of the collision rate in this case requires the knowledge of the pair-correlation function of the concentration below η. Turbulence below η is either dissipative or it has a small Mach number. In both cases, the fluctuations of the density stop increasing below η, resulting in the flattening of the correlation functions at $r < \eta$,

$$\langle n(0)n(r)\rangle \sim \langle n\rangle^2\left(\frac{L}{\eta}\right)^{3-D_t(2)}, \quad \langle \rho(0)\rho(r)\rangle \sim \left(\frac{L}{\eta}\right)^{3-D(2)}. \tag{121}$$

This can be confirmed for the Kraichnan model using Eq. (99). Correspondingly, we find for the correlation function in the rate of collisions,

$$\langle n_2(0)n_1(a_1+a_2)\rangle \sim \langle n_1\rangle\langle n_2\rangle\left(\frac{L}{\eta}\right)^{3-D_t(2)}. \tag{122}$$

Thus, as the interaction radius of the colliding particles decreases, the collision kernel increases up to $a_1 + a_2 = \eta$. The increase factor for smaller $a_1 + a_2$ is size independent.

Finally, we remark that the total collision rate is given by summing over the rates of collisions of particles with all radii combinations a_1 and a_2.

XI. INTERNAL ENERGY, ITS EVOLUTION, AND ZERO SUM OF LYAPUNOV EXPONENTS

The considerations of the previous sections belonged to the supersonic inertial range. There the density in the multifractal phase is singular. Thus, if the density behavior, understood as behavior of the coarse-grained density ρ_r, could be continued to infinitely small r then the resulting field would be singular and supported on a constantly evolving multifractal set. However, this type of distribution would have infinite internal energy. For instance, in the case of the isothermal flow, the internal energy is proportional to the Gibbs entropy, which is infinite for multifractal distributions as seen from Eq. (4); cf. Ref. [9]. Thus, the fully resolved density field cannot be multifractal unless we are willing to drop the framework of dissipative Navier-Stokes equations. In this section, we demonstrate rigorously that finiteness of the internal energy demands that the sum of Lyapunov exponents is zero.

Our main assumption is that there is a dissipation scale l_d below which the flow is smooth. This assumption is the counterpart of the similar assumption in incompressible turbulence below the viscous scale [41]. The regularization at small scales that smooths both the flow and the density is caused by the finite value of the dissipation coefficients (for density, finite speed of sound forming l_s is also relevant; see below). Thus, shock solutions have a finite density and a finite width which are determined by the values of the dissipation coefficients; cf. the introduction. We assume finiteness of velocity divergence w in the calculation. The proof of vanishing of the sum of the Lyapunov exponent would be immediate on somewhat stronger assumption that the density is finite (in fact, it was considered in Ref. [1] as needing no proof). This proof is considered at the end of the section. The juxtaposition of this result with simulations of Ref. [5] is done in the next section.

A. Finite internal energy and zero sum of Lyapunov exponents of time-reversed flow

Here, we demonstrate that the sum of Lyapunov exponents of time reversal of a compressible flow must be zero. This conclusion holds for any compressible flow in a finite volume, not necessarily turbulent. We set the initial condition for the density in the past $\rho(t, \boldsymbol{x}) = 1$, where t is a negative time. Then, after some finite relaxation time τ_0, the flow is stationary. This way of reaching steady state was used in Ref. [31]. Thus, $\rho(0, \boldsymbol{x})$ is the steady-state density at $|t| \gg \tau_0$. We have, using Eq. (5),

$$\lim_{t\to-\infty}\frac{\ln\rho(0,\boldsymbol{x})}{|t|} = \lim_{t\to-\infty}\int_0^t w(t', \boldsymbol{q}(t', \boldsymbol{x}))\frac{dt'}{|t|} = \sum_{i=1}^{3}\lambda_i^-(\boldsymbol{x}), \tag{123}$$

where the sum of Lyapunov exponents of time-reversed flow $\sum_{i=1}^{3}\lambda_i^-(\boldsymbol{x})$ is defined as

$$\sum_{i=1}^{3}\lambda_i^-(\boldsymbol{x}) \equiv \lim_{t\to-\infty}\frac{1}{|t|}\ln\det\frac{\partial \boldsymbol{q}(t,\boldsymbol{x})}{\partial x}. \tag{124}$$

Thus, the sum gives the logarithmic rate of growth of infinitesimal volumes in time-reversed flow; cf. Eq. (10). We observe that the integral in Eq. (123) involves a finite interval of order τ_0, where $w(t, \boldsymbol{q}(t, \boldsymbol{x}))$ is nonstationary. This interval can be neglected due to $t \to \infty$ limit so the stationary $w(t, \boldsymbol{q}(t, \boldsymbol{x}))$ can be employed in the equation.

By the ergodic theorem [11], the limiting function $\sum_{i=1}^{3}\lambda_i^-(\boldsymbol{x})$ is independent of $\boldsymbol{x}$ with exception of a nonempty set Ω of $\boldsymbol{x}$ with zero total volume. The value of the almost constant limit for the sum is nonpositive [9,10]. If $\sum_{i=1}^{3}\lambda_i^-$ were negative, then $\rho(0, \boldsymbol{x})$ would be supported on a set with zero spatial volume; see Eq. (123). However, then the singularities of the density, that must provide for finite mass after integration over Ω, would be so strong that the internal energy given by Eq. (4) would be infinite. We conclude that it is necessary that

$$\sum_{i=1}^{3}\lambda_i^-(\boldsymbol{x}) = 0 \tag{125}$$

holds with possible exception of a set of zero total volume. Using the formula for the sum from Ref. [86], that generalizes the formula of Ref. [10] for $\sum_{i=1}^{3}\lambda_i$, we find

$$\sum_{i=1}^{3}\lambda_i^- = -\int_{-\infty}^{0}\langle w(0)w(t)\rangle dt = 0,$$
$$\langle w(0)w(t)\rangle = \int w(0,\boldsymbol{x})w[t,\boldsymbol{q}(t,\boldsymbol{x})]d\boldsymbol{x}. \tag{126}$$

Thus, $w(t)$ is an anticorrelated process. A similar proof can be constructed for the sum of Lyapunov exponents of the flow itself.

B. Finite internal energy and zero sum of Lyapunov exponents

We prove that $\sum_{i=1}^{3}\lambda_i$, defined in Eq. (10), is zero. We observe that mass conservation $\rho(0,\boldsymbol{x}) = \rho[t,\boldsymbol{q}(t,\boldsymbol{x})]\det\nabla\boldsymbol{q}(t,\boldsymbol{x})$ implies that the Gibbs entropy defined in Eq. (4) obeys

$$S(t) = -\int \rho(0,\boldsymbol{x})\ln\rho[t,\boldsymbol{q}(t,\boldsymbol{x})]d\boldsymbol{x} = S(0) + \int_0^t dt' d\boldsymbol{x}\rho(0,\boldsymbol{x})w[t',\boldsymbol{q}(t',\boldsymbol{x})], \quad (127)$$

where we used Eq. (5). This formula for the increment of internal energy, proportional to S, holds for any initial condition. We consider it in the steady state. We have

$$\lim_{t\to\infty}\frac{S(t)-S(0)}{t} = \int\sum_{i=1}^{3}\lambda_i(\boldsymbol{x})\rho(0,\boldsymbol{x})d\boldsymbol{x}, \quad (128)$$

where we introduced the $\boldsymbol{x}$ dependence in the limit in Eq. (10). By the ergodic theorem, $\sum_{i=1}^{3}\lambda_i(\boldsymbol{x})$ must be constant with possible exception of a set Ω' of zero volume. We observe that $\sum_{i=1}^{3}\lambda_i(\boldsymbol{x})$ is finite on that set. The integral of $\sum_{i=1}^{3}\lambda_i(\boldsymbol{x})\rho(0,\boldsymbol{x})$ over Ω' must be zero since a nonzero value would demand strong singularities of the density that would produce infinite internal energy. We conclude that Ω' can be neglected in the integral in Eq. (128), giving

$$\lim_{t\to\infty}\frac{S(t)-S(0)}{t} = \sum_{i=1}^{3}\lambda_i = 0, \quad (129)$$

where we used that the left-hand side is zero by finiteness of the internal energy. This finishes the proof described in the introduction.

The Gibbs entropy, considered as functional of the density field, attains maximum at the constant density which provides the state of the maximal disorder. This was used in Ref. [10] for demonstrating that in general $\sum_{i=1}^{3}\lambda_i \leqslant 0$; cf. Ref. [9]. An unrestricted smooth compressible vector field would produce a negative sum. Thus, the compressible turbulent flow below the viscous scale is nongeneric, realizing the equality $\sum_{i=1}^{3}\lambda_i = 0$. Some insight into this nongeneric behavior can be obtained using the formula for the sum [10],

$$\int_0^\infty \langle w(0)w(t)\rangle dt = -\sum_{i=1}^{3}\lambda_i = 0; \quad (130)$$

cf. with Eq. (126). (Here, $\langle w(0)w(t)\rangle$ is generally not even function of t since spatial averaging does not correspond to the average over the steady-state density.) Thus, $w(t)$ is anticorrelated with its own initial condition so that the integral of $\langle w(0)w(t)\rangle$ over positive or negative times is zero. The physical interpretation of this result is as follows [53]: The divergence in the fluid particle's frame, $w[t,\boldsymbol{q}(t,\boldsymbol{x})]$, is not stationary since $\boldsymbol{q}(t,\boldsymbol{x})$, that is distributed uniformly at $t=0$, accumulates with time in compression regions that are characterized by negative w. Thus, at $t=0$, we have $\langle w(0)\rangle = \langle\nabla\cdot\boldsymbol{v}(\boldsymbol{x})\rangle = 0$, while at small times Eq. (A1) implies that $\langle w[t,\boldsymbol{q}(t,\boldsymbol{x})]\rangle = -t\langle w^2\rangle < 0$. This accumulation, however, is transient and occurs at times of the order of the correlation time of $w(t)$. At times larger than the correlation time, the back reaction of the density on the flow through $-\nabla p$ causes the compression to turn into rarefaction so that the time integral of $\langle w(0)w(t)\rangle$ is zero; cf. Refs. [53,87]. Thus, if initially $\boldsymbol{x}$ is in a compression region, then after time of order of the correlation time of $w(t)$ the trajectory will be typically found in a rarefaction region and vice versa. Stronger consequences for anticorrelations hold if the density can be assumed to be finite; see below and Appendix A.

Finally, we provide the form of anticorrelations in space rather than in time. We observe that using the identity $\int w(t,\boldsymbol{q}(t,\boldsymbol{x}))\rho(0,\boldsymbol{x})d\boldsymbol{x} = \int\rho(t,\boldsymbol{q})w(t,\boldsymbol{q})d\boldsymbol{q}$ we have from Eq. (127) that

$$\lim_{t\to\infty}\frac{1}{t}\int_0^t\langle\rho w\rangle = \lim_{t\to\infty}\frac{S(t)-S(0)}{t} = 0. \quad (131)$$

We find that in the steady state

$$\langle\rho w\rangle = 0, \quad \langle\boldsymbol{v}\cdot\nabla\rho\rangle = 0. \quad (132)$$

Thus, on the average the density is constant along the instantaneous streamlines of the flow. Correspondingly, the density is on the average constant along a closed streamline and is locally axially symmetric around vortex filaments.

C. Finiteness of density and its gradients

Here, we will consider the consequences of the assumption that the density and its gradients are finite below the scale l_d determined by the dissipation coefficients. This assumption originates in the structure of the shocks and parallels the assumption of finite gradients below the Kolmogorov scale of the incompressible turbulence [41]; cf. with the previous assumption on the flow differentiability. Similarly to incompressible turbulence, this assumption might not be fully true; however, it is certainly a good assumption in the light of the presently available knowledge (see the discussion in Ref. [41]). Infinite density or its gradients would produce infinities in dissipative Navier-Stokes equations of compressible flow whose existence seems not plausible. We remark that though multifractal-type singularities of the density are impossible, the weaker singularities providing for a finite internal energy could occur in principle.

We start from considering the consequences of the finiteness of the density. Since the density is finite, then taking the logarithm of Eq. (5) yields

$$\lim_{t\to\pm\infty}\frac{1}{t}\ln\left[\frac{\rho(0,\boldsymbol{x})}{\rho(t,\boldsymbol{q}(t,\boldsymbol{x}))}\right] \propto \lim_{t\to\pm\infty}\int_0^t w[t',\boldsymbol{q}(t',\boldsymbol{x})]\frac{dt'}{t} = 0,$$

that holds for all $\boldsymbol{x}$. The last limit for ∞ and $-\infty$ represents sums of Lyapunov exponents of the flow and its time reversal, considered previously in this section. Thus, the previous results are recovered effortlessly [1].

Finiteness of the density gradients implies fine-tuning between the advection and the compression. Indeed, advection creates sharp contrasts of the passively transported field, thus developing infinite gradients. This includes the dissipation range where the flow is smooth [1]. For instance, random shocks with smooth density below l_d would still create infinite gradients of the concentration. In turn, compression tends to develop infinite densities as is well known from the theory of dissipative dynamical systems; see, e.g., Refs. [1,9,11,75].

How the fine-tuning provided for a finite density gradient is realized can be described in detail at small Ma; see the next sections. We remark already here that although the above discussion shows that n develops infinite gradients in contrast with ρ, this does not show that n and ρ differ as densities. We demonstrate in the next section that at small Ma coarse graining over arbitrarily small scale makes n coincide with ρ so that n and ρ are identical physically, describing the same mass distribution.

We stress that the observations of these relations, however, require flow resolution below the dissipation scale. For instance, the anticorrelation property of $w[t, \boldsymbol{q}(t, \boldsymbol{x})]$ holds separately along each of the fluid trajectories along which w must be sign alternating; see above. Thus, it can be missed in numerical simulations if $\boldsymbol{q}(t, \boldsymbol{x})$ is not well resolved below η during the correlation time of w. This could provide a different reason, besides that n and ρ differ, for why nonzero sums of Lyapunov exponents were reported in simulations [5]. There the Kolmogorov scale was half the grid size and the observations of Lyapunov exponents could be contaminated by the inertial range.

Finally, we remark that for nonbarotropic fluids there are more possibilities for the singular behavior. For ideal gas, the density can become infinite without violating the finiteness of the internal energy density and the pressure if the temperature drops to zero. This seemingly would not happen in the ordinary conservative fluid mechanics but can happen in the presence of cooling terms violating the local conservation of energy. These terms describe local dissipative processes such as radiation and do appear in applications. Finite-time blowup of density is possible in this case by keeping the pressure and its gradients finite; see, e.g., Refs. [88,89] for ideal hydrodynamics in one and three dimensions, respectively, and Ref. [90] for the nonideal case. In this work, we will not consider these cases, confining ourselves to the ordinary fluid mechanics.

D. Zero sum of Lyapunov exponents and the Kraichnan model

It is seen by combining Eqs. (126) and (130) that

$$\int_{-\infty}^{\infty} \langle w(0)w(t)\rangle dt = 0. \tag{133}$$

We consider here the implications of this equality for the Kraichnan model.

The assumption of the flow differentiability in the dissipation range $r < l_d$ is modeled by requiring that the functions c and u in Eq. (92) have regular Taylor expansion at $r \ll l_d$. The sum of the Lyapunov exponents is given by $\sum_{i=1}^{3} \lambda_i = -(1/2)\int \langle w(0)w(t)\rangle dt = -3c(0)/2$; see Ref. [53] for details. Thus, we must set $c(0) = 0$. However, this would produce zero single-point fluctuations of $w(t, \boldsymbol{x})$; see Eq. (94). The reason is that δ-function correlation cannot describe the zero-correlation time limit in the dissipation range: The vanishing of $\int_{-\infty}^{0} \langle w(0)w(t)\rangle dt$ and nonvanishing of $\int_{-\infty}^{0} \langle w(0)w(t)\rangle t dt$ considered at the end of Appendix A imply that $\langle w(0)w(t)\rangle$ has the behavior of $\delta'(t)$, not of $\delta(t)$. Nevertheless, as long as the model is used in the inertial range only, it produces physically reasonable results. For r in the inertial range, the $\delta(t)$ behavior is reasonable because $\int \langle w_r(0)w_r(t)\rangle dt$ is nonzero where w_r is coarse grained over scale r. There are anticorrelations of w_r in the inertial range also; however, they are not that restrictive.

If we do consider the pair-correlation function of the Kraichnan model in the dissipation range, the results crucially depend on whether $c(0) = 0$. If $c(0) = 0$, then $\langle n^2\rangle$ is finite [since $u(0) \neq 0$], so the distribution is smooth in the dissipation range. In contrast, $c(0) \neq 0$ produces power-law divergence of $\langle n(0)n(\boldsymbol{r})\rangle$. This describes multifractal distribution in the dissipation range; see Ref. [53]. Whether it could be that for tracers $\sum_{i=1}^{3} \lambda_i \neq 0$ and multifractality holds also at small scales, as claimed in Ref. [5], demands further studies. Some light on this question is shed in the next section.

XII. MUST DENSITY AND CONCENTRATION COINCIDE IN THE STEADY STATE?

It might seem self-evident that all initial conditions for the continuity equation relax at large times to the same solution. Indeed, the difference of two different solutions is also a solution whose spatial integral vanishes. Positive and negative regions of an initial condition with zero spatial integral would be mixed by turbulence. Thus, at large times, coarse graining over an infinitesimal scale would wash out the field contrasts, producing zero. This is quite similar to mixing by incompressible turbulence [1], where the only difference is that in our case the trajectories' mixing is confined to the nontrivial support of the steady-state density instead of the whole volume. Thus, any two solutions of the continuity equation would agree at large times after coarse graining.

If the above consideration using the assumption of the mixing is true, then any initial (normalized) distribution of tracers relaxes after some time to a universal limiting distribution independent of the initial condition. Moreover, this distribution equals the steady-state fluid density. This conclusion would have far-reaching theoretical and experimental consequences. Theoretically, it would allow us to study the fluid density using well-developed techniques for the study of passively transported concentrations [1]. Experimentally, it would provide the simplest way of observing the multifractal structure of the density. One could spread in space a large number of tracer particles that obey Eq. (6) and study the stationary distribution on which they settle after transients [5]. The study of multifractals via large number of points distributed on them is standard [63].

In this section, we undertake critical examination of the assumption that concentration and density coincide in the steady state. The reasons for questioning the equality that usually is taken for granted (see, e.g., Ref. [5]) were sketched in the introduction and are detailed here. The simplest argument for the equality would be uniqueness of the steady-state solution that often holds due to dissipation. However, the continuity equation is not dissipative and the steady-state solutions are not unique. This is well known for incompressible nonrandom flows: A measure concentrated on a periodic orbit would solve the continuity equation and be different from a constant solution $n = 1$; see, e.g., Ref. [91]. Similarly, for random flows a measure supported on any level set of pointwise first Lyapunov exponent is stationary [60]. Thus, uniqueness cannot be used for proving the equality of the density and the

concentration in the steady state. Mixing also cannot be taken for granted. The density could not mix with the tracers by creating a nonmixing set on which it would be supported due to interaction with the transporting flow; cf. the introduction. We remark that the steady-state solution $n = \rho$ of course exists as it is most obvious from,

$$\partial_t \frac{n}{\rho} + (\boldsymbol{v}\cdot\nabla)\frac{n}{\rho} = 0, \tag{134}$$

implied by Eqs. (1). However, it can become unstable if fluid particles form a configuration that preserves itself thanks to the interaction with the transporting flow. Small deviation of tracers from this configuration could grow; cf. the introduction (in the case of continuum fields, configuration is a field configuration).

We start by providing an example that helps show how the difference between passive and active scalars can arise.

A. The continuity equation is conservative

The main difficulty in proving that in the steady state $n = \rho$ is that the continuity equation is conservative. One can introduce a conserved distance between two smooth solutions of the continuity equation (the steady state can be considered by studying the long-time evolution of smooth solutions). This distance is similar to the H function of Boltzmann or entropy $-H$; see its use for the relaxation of solutions of the more general Fokker-Planck equation in Ref. [80]. We define H function for two smooth positive solutions of the continuity equation $n_1(t,\boldsymbol{x})$ and $n_2(t,\boldsymbol{x})$ obeying $\int n_i(t,\boldsymbol{x})d\boldsymbol{x} = 1$ as

$$H(t) = \int n_1 \ln\frac{n_1}{n_2} d\boldsymbol{x}. \tag{135}$$

We observe that $H(t)$ is a non-negative function. Using $\int n_i(\boldsymbol{x},t)d\boldsymbol{x} = 1$, we may rewrite H as

$$\begin{aligned} H &= \int \left[n_1 \ln\frac{n_1}{n_2} - n_1 + n_2\right] d\boldsymbol{x} \\ &= \int n_2[R\ln R - R + 1]d\boldsymbol{x}, \end{aligned} \tag{136}$$

where we introduced $R \equiv n_1/n_2$. The last term in the above equation is always not positive as it follows from

$$R\ln R - R + 1 = \int_1^R \ln x dx \geqslant 0, \tag{137}$$

that holds for any $R \geqslant 0$. We see that $H = 0$ only at $n_1(t,\boldsymbol{x}) = n_2(t,\boldsymbol{x})$. Thus, $H(t)$ is non-negative and it vanishes only if the solutions agree pointwise, providing a good definition of the distance between n_i. By changing the integration variable in Eq. (135) from $\boldsymbol{x}$ to $\boldsymbol{q}(t,\boldsymbol{y})$, it is found that $H(t) = H(0)$. This is the consequence of mass conservation $n(t=0,\boldsymbol{y})d\boldsymbol{y} = n(t,\boldsymbol{x})d\boldsymbol{x}$ and conservation of n_1/n_2 on $\boldsymbol{q}(t,\boldsymbol{y})$ that follows from applying Eq. (134) to n_1/n_2. Thus, the distance between the solutions is conserved and pointwise relaxation to $n_1 = n_2$ is not possible.

The way out of the above difficulty is demonstrating that the pointwise concentration does not have a physical meaning. The measurable quantity is the mass distribution, which is described by the coarse-grained field n_ϵ. However small ϵ is, the creation of finite contrasts of concentration over an infinitesimally small scale in the limit of infinite evolution time allows for relaxation of n_ϵ to the same distribution despite the pointwise difference. This can be illustrated by considering the case of small Mach number that is of its own interest.

B. Relaxation of concentration to density at Ma $\ll 1$

It is instructive to consider the case of Ma $\ll 1$, where there is a solution for the density in terms of the flow. The solution is not unique and depends on interaction with heat [92]; see also Refs. [93–96]. In the case of isothermal flow, we have $\rho(t,\boldsymbol{x}) = 1 + c\mathrm{Ma}^2 p(t,\boldsymbol{x})$, where c is a constant and p is the pressure as obtained from the incompressible Navier-Stokes equations. The pressure obeys the Poisson equation $\nabla^2 p = -\nabla_k u_i^0 \nabla_i u_k^0$, where $\boldsymbol{u}^0$ is the incompressible turbulent flow (divergence of the forcing is assumed to be zero here) and its smallest scale of variations in space [41] is the Kolmogorov scale η. Since the pressure is defined up to a constant, it is assumed with no loss of generality that $\langle p\rangle = 0$. The solution makes it explicit that the density field has a finite scale of spatial variations due to the interaction with the flow. Proportionality of the density and pressure spectra in the inertial range was confirmed for the considered regime by recent numerical simulations [28,82] for Ma < 0.3. The spectrum ($\sim k^{-7/3}$ where k is the wave number) indicates that the density is a large-scale nonfractal field with positive scaling exponents in the inertial range. The nonfractal nature of the density fluctuations at low Mach numbers is supported also by other scenarios that hold for Ma $\ll 1$, having $k^{-5/3}$ spectrum [92,97]; see also Refs. [51,98,99].

It is readily seen that the assumption that $n/\rho = \text{const}$ pointwise is self-contradictory. Passive concentration transported by low-Mach-number flow must approximately obey transport by incompressible turbulence. However, that creates finite contrasts over infinitesimal scales associated with indefinite growth of ∇n. This is in contradiction with finite $\nabla\rho$ above.

We demonstrate that despite the pointwise difference, the concentration $n_\epsilon(t,\boldsymbol{x})$ coarse-grained over scale ϵ relaxes to $\rho(t,\boldsymbol{x})$ at large t for any finite ϵ. We assume that the fluid flow is in the steady state and consider the evolution of concentration of tracers injected at some $t < 0$ with initial distribution $n(t,\boldsymbol{x}) = 1$ (different initial conditions for concentration are demonstrated to converge to the same solution in the next subsection). We study the limit of infinite evolution time by considering the concentration at time zero $n(\boldsymbol{x})$ at $t \to -\infty$ as in Sec. IV. We have from Eq. (134)

$$n(\boldsymbol{x}) = \frac{\rho(\boldsymbol{x})}{\rho(t,\boldsymbol{q}(t,\boldsymbol{x}))}. \tag{138}$$

Coarse graining over a scale $\epsilon \ll \eta$ gives

$$\frac{n_\epsilon(\boldsymbol{x})}{\rho(\boldsymbol{x})} = \int_{|\boldsymbol{x}'-\boldsymbol{x}|<\epsilon} \frac{d\boldsymbol{x}'}{(4\pi\epsilon^3/3)\rho(t,\boldsymbol{q}(t,\boldsymbol{x}'))}. \tag{139}$$

Relaxation of $n_\epsilon(\boldsymbol{x})$ to $\rho(\boldsymbol{x})$ means that the right-hand side of Eq. (139) relaxes to 1. We find, using the form of the density at Ma $\ll 1$,

$$\int_{|\boldsymbol{x}'-\boldsymbol{x}|<\epsilon} \frac{d\boldsymbol{x}'}{\rho(t,\boldsymbol{q}(t,\boldsymbol{x}'))} \approx \int_{|\boldsymbol{x}'-\boldsymbol{x}|<\epsilon} [1 - c\mathrm{Ma}^2 p(t,\boldsymbol{q}(t,\boldsymbol{x}'))]d\boldsymbol{x}'.$$

We observe that we can use in the integral in the considered order in Ma the trajectories of incompressible flow. The mixing property of (time-reversed) incompressible flow shows that a ball of radius ϵ is smeared at large times over the whole volume of the flow so that at large times $3\int_{|\boldsymbol{x}'-\boldsymbol{x}|<\epsilon} p(t,\boldsymbol{q}(t,\boldsymbol{x}'))d\boldsymbol{x}'/(4\pi\epsilon^3) = \langle p\rangle$. However, $\langle p\rangle = 0$ by the made assumption. Therefore, we find $n_\epsilon(\boldsymbol{x}) = \rho(\boldsymbol{x})$.

We remark that relaxation after coarse graining is equivalent to the relaxation in the sense of measures or distributions, that is,

$$\lim_{t\to\infty}\frac{\int f(\boldsymbol{x})n(t,\boldsymbol{x})d\boldsymbol{x}}{\int f(\boldsymbol{x})\rho(t,\boldsymbol{x})d\boldsymbol{x}} = 1 \tag{140}$$

for any smooth function f. Here, smoothness of f allows us to change $n(t,\boldsymbol{x})$ in the numerator by n coarse grained over a scale much smaller than the scale of smoothness of f.

The extension of the above proof that, as distributions, n equals ρ to the case of finite Mach number is nonevident and requires another approach. The simplest is to prove the relaxation for tracers.

C. Natural measure for the tracers

We consider relaxation of different initial conditions for the tracers' concentration to the same limiting distribution that was taken for granted in the previous sections. We start with a physical approach that observes that the dust particles, as compared with idealized tracers, perform Brownian motion with a certain diffusion coefficient κ. Thus, the full continuity equation for their concentration is $\partial_t n + \nabla\cdot(n\boldsymbol{v}) = \kappa\nabla^2 n$. The presence of a finite κ destroys the nondissipative nature of the continuity equation [100]. It is readily seen that with the diffusion term the time derivative of H introduced in Subsec. XII A is [80]

$$\dot{H} = -\kappa\int n_1(\nabla\ln(n_1/n_2))^2 d\boldsymbol{x} \leqslant 0, \tag{141}$$

where the equality holds for $n_1 = n_2$ only. This equation implies relaxation to $n_1 = n_2$ since $H \geqslant 0$. Diffusion makes the equation dissipative and all initial conditions relax in the limit of large evolution times to the same smooth (due to $\kappa > 0$) stationary solution $n^\kappa(t,\boldsymbol{x})$, where we stress the dependence on κ. We can define the so-called [11–13] natural measure n^s by

$$n^s_\epsilon(\boldsymbol{x}) = \lim_{\kappa\to 0} n^\kappa_\epsilon(\boldsymbol{x}). \tag{142}$$

Here, we use the standard assumption that small finite κ is only relevant below a certain diffusive scale so that coarse graining over a much larger (yet macroscopically small) scale ϵ is independent of κ; see Ref. [1] and references therein. Since Eq. (142) defines $n^s_\epsilon(\boldsymbol{x})$ for any $\epsilon > 0$, it defines n_s completely. The definition can be given an explicitly ϵ-independent form by the demand that for any smooth function $f(\boldsymbol{x})$ we have

$$\int f(\boldsymbol{x})n^s(\boldsymbol{x})d\boldsymbol{x} = \lim_{\kappa\to 0}\int f(\boldsymbol{x})n^\kappa(\boldsymbol{x})d\boldsymbol{x}. \tag{143}$$

The equivalence holds because on scales larger than the diffusive scale n^κ coincides with n^s. We observe that diffusion introduces white noise in the equation of motion of the tracer. Thus, $n^\kappa(\boldsymbol{x})$ can be considered as the probability density function (PDF) of the tracer position. The PDF's limit of $\kappa\to 0$ is not necessarily smooth so it might not be definable as an ordinary function; however, the limiting averages of arbitrary function of the position $f(\boldsymbol{x})$ are well defined by Eq. (143). Moreover, the different point correlation functions also have a well-defined $\kappa\to 0$ limit. For instance, the generalization of Eq. (99) to the case with finite κ is [53]

$$\langle n(0)n(\boldsymbol{r})\rangle = \exp\left[\int_r^\infty \frac{r'c(r')dr'}{r'^2u(r')+2\kappa}\right]. \tag{144}$$

The $\kappa\to 0$ limit is regular and reproduces Eq. (99).

Thus, we demonstrated that n^s is the universal limiting distribution of tracers at scales that are not too small for diffusion to become relevant. The universality is due to the physical assumption that distribution of tracers with slightly different small diffusion coefficients looks identical at a finite scale. The formal proof is standard [12,13] and relies on the mixing assumption that is provided below. It must be stressed that this proof shows that a generic initial condition for the continuity equation relaxes as a measure (see above) to n^s but, however, does not exclude the existence of measure zero initial conditions for which the relaxation would fail; see Subsec. XII F. The natural measure n^s solves the ordinary continuity equation without the diffusion term (it is a weak solution). This way of constructing the natural measure n_s as the zero-noise limit of the PDF of a stochastic process constitutes a rigorous mathematical approach [101] that in our case is dictated by the physics of the problem.

It is often possible to write n^s explicitly. For this, it is useful to construct n^κ by setting the initial condition at $t = -T$ and considering $n(\boldsymbol{x}) \equiv n(0,\boldsymbol{x})$ in the infinite evolution time limit $T\to\infty$. We take with no loss of generality a uniform initial condition $n(-T,\boldsymbol{x}) = 1$. We have, from Eq. (142),

$$n^s_\epsilon(\boldsymbol{x}) = \lim_{\kappa\to 0}\lim_{T\to\infty} n_\epsilon(\boldsymbol{x}) = \lim_{T\to\infty}\lim_{\kappa\to 0} n_\epsilon(\boldsymbol{x}). \tag{145}$$

We assume here that the order of the limits can be changed, which is a form of a mixing assumption. Observing that $n(\boldsymbol{x})$ at $\kappa\to 0$ becomes the solution of the continuity equation given by Eq. (5), we find [54]

$$n_\epsilon(\boldsymbol{x}) = \lim_{T\to\infty}\left(\exp\left[-\int_{-T}^0 w(t,\boldsymbol{q}(t,\boldsymbol{x}))dt\right]\right)_\epsilon. \tag{146}$$

For other approach to this representation, see Ref. [9]. The statistics of the natural measure can be studied using in Eq. (146) the stationary statistics of the velocity. The rule of the thumb is that the change of the order of limits (which is the only nonrigorous assumption made in the derivation) is valid as long as the answers obtained from Eq. (146) are finite. For instance, the pair correlation function of concentration $f(\boldsymbol{r}) = \langle n(0)n(\boldsymbol{r})\rangle$ is

$$f(\boldsymbol{r}) = \left\langle\exp\left(-\int_{-\infty}^0 [w(t,\boldsymbol{q}(t,\boldsymbol{r})) + w(t,\boldsymbol{q}(t,0))]dt\right)\right\rangle, \tag{147}$$

where the coarse graining can be dropped at finite $|\boldsymbol{r}|$. Application of the cumulant expansion theorem to $\langle n(0)n(\boldsymbol{r})\rangle/\langle n(0)\rangle\langle n(\boldsymbol{r})\rangle$ with average concentrations

represented via Eq. (146) gives [54,102]

$$\ln f(\boldsymbol{r}) = g(\boldsymbol{r}) + \cdots, \tag{148}$$

where the dots stand for higher order mixed [involving both $w(t,\boldsymbol{q}(t,\boldsymbol{r}))$ and $w(t,\boldsymbol{q}(t,0))$] cumulants and [54]

$$g(\boldsymbol{r}) = \int_{-\infty}^{0} dt dt' \langle\langle w(t,\boldsymbol{q}(t,0)) w(t',\boldsymbol{q}(t',\boldsymbol{r}))\rangle\rangle, \tag{149}$$

where double angular brackets stand for dispersion. The representation given by Eq. (148) is useful often.

D. Impact of effective diffusion on the density

We saw above that the question of relaxation to a universal distribution that is independent of the initial condition is easy in the presence of dissipation. If we could introduce some diffusion to the continuity equation for the density, it would solve the problem of relaxation. However, there is no reason to introduce this term. If it is introduced in a numerical scheme artificially, then this demands a validity check. However, smoothness of the density field, if it can be assumed, does imply the regularity of the limit of zero diffusion at finite times, that is,

$$\rho(t,\boldsymbol{x}) \approx \rho^{\kappa}(t,\boldsymbol{x}), \quad \partial_t \rho^{\kappa} + \nabla\cdot(\rho^{\kappa}\boldsymbol{v}) = \kappa\nabla^2\rho^{\kappa}. \tag{150}$$

Unfortunately, this could not be used for proving the relaxation since the diffusive term brings dissipation and its accumulation over time can bring a finite effect in the steady-state limit of infinite evolution time. The way of proving the relaxation without introducing diffusion is the mixing assumption.

E. Mixing

The property that is needed for proving relaxation of concentration to density, staying in the frame of nondissipative continuity equation, is mixing [12,13]. The assumption of mixing shows that different time correlation functions defined with the help of ρ in the limit of large times reduce to the product of averages (the same assumption can be used for proving the relaxation of distributions of tracers to unique limiting distribution using that distribution instead of ρ below). In our case, the averaging measure is time dependent, being stationary only statistically, which demands a slight modification in the form of the mixing assumption. We assume that for any smooth functions $f(\boldsymbol{x})$ and $g(\boldsymbol{x})$,

$$\lim_{t\to\infty} \frac{\int f(\boldsymbol{q}(t,\boldsymbol{x}))g(\boldsymbol{x})\rho(\boldsymbol{x})d\boldsymbol{x}}{\int f(\boldsymbol{x})\rho(t,\boldsymbol{x})d\boldsymbol{x}\int g(\boldsymbol{x})\rho(\boldsymbol{x})d\boldsymbol{x}} = 1, \tag{151}$$

where the integral in the numerator of the left-hand side defines the correlation function $\langle f(t)g(0)\rangle$. For time-independent flows, this reduces to the usual form [12,13] on using $\rho(t,\boldsymbol{x}) = \rho(\boldsymbol{x})$. Our Eq. (151) incorporates that in the decomposition $\langle f(t)g(0)\rangle \approx \langle f(t)\rangle\langle g(0)\rangle$, that holds at large times, we must use $\rho(t,\boldsymbol{x})$ for averaging f and not $\rho(t=0,\boldsymbol{x})$. We observe that Eq. (151) is a bilinear relation. Its elementary form is obtained by taking for f and g the indicators $\chi_\epsilon(\boldsymbol{x}-\boldsymbol{x}_1)$ and $\chi_\epsilon(\boldsymbol{x}-\boldsymbol{x}_2)$ for some $\boldsymbol{x}_1$ and $\boldsymbol{x}_2$. Here, $\chi_\epsilon(\boldsymbol{x})$ equals 1 for $|\boldsymbol{x}|<\epsilon$ and 0 otherwise. We have from Eq. (151)

$$\lim_{t\to\infty} \frac{\int_{|\boldsymbol{x}-\boldsymbol{x}_2|<\epsilon}\chi_\epsilon(\boldsymbol{q}(t,\boldsymbol{x})-\boldsymbol{x}_1)\rho(\boldsymbol{x})d\boldsymbol{x}}{\int_{|\boldsymbol{x}-\boldsymbol{x}_1|<\epsilon}\rho(t,\boldsymbol{x})d\boldsymbol{x}\int_{|\boldsymbol{x}-\boldsymbol{x}_2|<\epsilon}\rho(\boldsymbol{x})d\boldsymbol{x}} = 1. \tag{152}$$

This becomes for ϵ much smaller than the scale of variations of the density, assumed to be finite,

$$\lim_{t\to\infty} \frac{\int_{|\boldsymbol{x}-\boldsymbol{x}_2|<\epsilon}\chi_\epsilon(\boldsymbol{q}(t,\boldsymbol{x})-\boldsymbol{x}_1)d\boldsymbol{x}}{(4\pi\epsilon^3/3)^2\rho(t,\boldsymbol{x}_1)} = 1. \tag{153}$$

We observe that

$$\frac{\int_{|\boldsymbol{x}-\boldsymbol{x}_2|<\epsilon}\chi_\epsilon(\boldsymbol{q}(t,\boldsymbol{x})-\boldsymbol{x}_1)d\boldsymbol{x}}{(4\pi\epsilon^3/3)^2} = n_\epsilon(t,\boldsymbol{x}_1), \tag{154}$$

where $n(t,\boldsymbol{x})$ is (normalized) solution of the continuity equation obeying the initial condition $n(t=0,\boldsymbol{x}) = \chi_\epsilon(\boldsymbol{x}-\boldsymbol{x}_2)/(4\pi\epsilon^3/3)$. We obtain, combining the last equations,

$$\lim_{t\to\infty} \frac{n_\epsilon(t,\boldsymbol{x}_1)}{\rho(t,\boldsymbol{x}_1)} = 1. \tag{155}$$

Finally, linearity of the continuity equation and arbitrariness of $\boldsymbol{x}_2$ and ϵ imply that coarse-grained concentration relaxes to the density in the limit of large evolution time for arbitrary initial condition.

We can get insight into the nature of the mixing assumption given by Eq. (151) by using for f and g the indicators χ_A and χ_B of some volumes A and B in space [12]. We find

$$\lim_{t\to\infty} \frac{\int_B \chi_A(\boldsymbol{q}(t,\boldsymbol{x}))\rho(\boldsymbol{x})d\boldsymbol{x}}{\int_A\rho(t,\boldsymbol{x})d\boldsymbol{x}\int_B\rho(\boldsymbol{x})d\boldsymbol{x}} = 1. \tag{156}$$

The assumption in this form shows that asymptotically at large times the mass fraction of points of B that are found inside A equals the mass fraction of A in the whole volume. In other words, the mass of B is redistributed over the volume uniformly with respect to ρ. Mixing can also be given a probabilistic interpretation: Given that the particle is initially in B, the probability of finding it in A is the probability of A. Thus, asymptotically at large times the fluid particle distributes in space independently of where it was initially; see details in Ref. [91]. This is not self-evident, though. However large the time is, there is memory of the initial condition in Eq. (5): The trajectory $\boldsymbol{q}(t,\boldsymbol{x})$ and the divergence on it and $\rho(\boldsymbol{x})$ must combine in smooth and finite field $\rho(t,\boldsymbol{x})$. For instance, in the previously considered case of $\mathrm{Ma}\ll 1$, the density evolution is nongeneric: It preserves smoothness in contrast with the concentration evolution that does not. We consider the memory effect in more detail.

F. Memory and magnetic-field-vorticity example

Here, we consider the memory effect and illustrate its possibility using the example of the difference of passive magnetic field and active vorticity considered in the introduction. We consider the evolution in the steady state,

$$\rho(\boldsymbol{x}) = \rho(-T,\boldsymbol{q}(-T,\boldsymbol{x}))\exp\left[-\int_{-T}^{0} w(t,\boldsymbol{q}(t,\boldsymbol{x}))dt\right], \tag{157}$$

that differs from Eq. (146) by the $\rho(-T,\boldsymbol{q}(-T,\boldsymbol{x}))$ prefactor. If the density forms a special configuration that preserves

itself thanks to coupling with the flow, then $\rho(-T,\boldsymbol{x})$ differs from a generic function that relaxes to the natural measure. It depends on past interactions of the density and the flow and is correlated with the instantaneous flow. Its evolution is tuned with the velocity and $\boldsymbol{q}(t,\boldsymbol{x})$ depends on $\rho(-T,\boldsymbol{x})$. Thus, Eq. (157) does not necessarily describe the relaxation to the natural measure as it would for a generic (normalized) prefactor. This possibility must be considered since concentration obeying Eq. (146) is a functional of the stationary velocity, and a similar fact for the density, that back reacts on the velocity, would be not evident.

The (possible) difference can be illustrated further by trying to apply for the fluid density the same procedure that we used for deriving the representation for the steady-state concentration given by Eq. (146). We start with unit initial condition on the density $\rho(-T)=1$. In that approach, the solution in Eq. (146) holds for $\rho(\boldsymbol{x})$; however, $\boldsymbol{w}(t,\boldsymbol{x})$ in the integrand is not stationary. Indeed, the transient period of relaxation to the steady state at times close to $-T$ is never forgotten because there is no dissipation. In this sense, the important and profound distinction between the tracers' concentration and the fluid density is that initial conditions are forgotten for the former but not necessarily for the latter, which is correlated with the flow velocity; cf. Ref. [14]. Further study of concentration relaxation to the density and the validity of the mixing assumption must probably be done numerically and experimentally.

We consider the known example where the active vorticity and passive magnetic fields obey the same first order in time evolution and yet differ. The difference is because the initial conditions for the vorticity of the incompressible Navier-Stokes flow $\boldsymbol{u}$ are nongeneric; cf. the introduction. If the magnetic resistivity coincides with the fluid viscosity ν, then passive magnetic field $\boldsymbol{B}$ obeys

$$\partial_t \boldsymbol{B}+(\boldsymbol{u}\cdot\nabla)\boldsymbol{B}=(\boldsymbol{B}\cdot\nabla)\boldsymbol{u}+\nu\nabla^2\boldsymbol{B},\quad \nabla\cdot\boldsymbol{B}=0. \tag{158}$$

The flow $\boldsymbol{u}$ is assumed to obey the usual Navier-Stokes equations of nonconducting fluid which do not contain $\boldsymbol{B}$. The vorticity $\boldsymbol{w}$ obeys the same equation as $\boldsymbol{B}$,

$$\partial_t \boldsymbol{w}+(\boldsymbol{u}\cdot\nabla)\boldsymbol{w}=(\boldsymbol{w}\cdot\nabla)\boldsymbol{u}+\nu\nabla^2\boldsymbol{w},\quad \nabla\cdot\boldsymbol{w}=0; \tag{159}$$

however, $\boldsymbol{u}$ is, of course, not independent of $\boldsymbol{w}$. We introduce the Green's function $G_{ik}(t,\boldsymbol{x};\boldsymbol{x}')$ via

$$\begin{aligned}&\partial_t G_{ik}+(\boldsymbol{u}\cdot\nabla)G_{ik}=(G_{ik}\nabla_i)\boldsymbol{u}+\nu\nabla^2 G_{ik},\\ &\nabla_i G_{ik}=0,\quad G_{ik}(t=0,\boldsymbol{x};\boldsymbol{x}')=\delta_{ik}\delta(\boldsymbol{x}-\boldsymbol{x}').\end{aligned} \tag{160}$$

We can write both the vorticity and the magnetic field as

$$\begin{aligned}B_i(t,\boldsymbol{x})&=\int G_{ik}(t,\boldsymbol{x};\boldsymbol{x}')B_k(t=0,\boldsymbol{x}')d\boldsymbol{x}',\\ w_i(t,\boldsymbol{x})&=\int G_{ik}(t,\boldsymbol{x};\boldsymbol{x}')w_k(t=0,\boldsymbol{x}')d\boldsymbol{x}'.\end{aligned} \tag{161}$$

The solution for the magnetic field produces unlimited growth of the field for generic initial conditions; see Ref. [15] and references therein. These conditions are transformed by the integral kernel $G_{ik}(t,\boldsymbol{x};\boldsymbol{x}')$ into a growing vector field. However, $\boldsymbol{w}(t,\boldsymbol{x})$, which is obtained from $\boldsymbol{w}(t=0,\boldsymbol{x})$ by the same linear integral transformation, is a stationary field which does not grow. Thus, initial conditions for the vorticity are nongeneric. Of course, $t=0$ is an arbitrary moment of time in this consideration, so the vorticity is nongeneric at any time. This is the situation that could be realized for the fluid density.

G. Instability as possible origin of the difference of active and passive scalars

We finish this section, that provides more questions than answers, with the example of difference of active and passive fields that holds due to instability, that we consider somewhat differently than in the original report [8]; cf. the introduction. It was observed by Batchelor and Kraichnan that vorticity in two-dimensional Navier-Stokes (NS) turbulence obeys the same equation as that of a passive scalar (here and below, we consider equal diffusivity coefficients of fields) [1]. Direct cascades of both quantities to smaller scales proceed similarly: Fields' blobs are stretched by the large-scale flow. However, vorticity is active and it rotates the blob, which decelerates the stretching. This results in steady-state statistics that are different from those of the passive scalar [1,103]. Still, the analogy is useful, providing the reference from which the full solution derives [103–108].

The key to the difference between active and passive fields is the difference of their behaviors under perturbations. For instance, one can consider the identical equations for the vorticity ω and the passive scalar θ in incompressible two-dimensional turbulent flow $\boldsymbol{u}$ where the forcing f and the viscosity ν coincide [8],

$$\begin{aligned}\partial_t\omega+(\boldsymbol{v}\cdot\nabla)\omega&=f+\nu\nabla^2\omega,\\ \partial_t\theta+(\boldsymbol{v}\cdot\nabla)\theta&=f+\nu\nabla^2\theta.\end{aligned} \tag{162}$$

Here, f is the curl of the force that drives $\boldsymbol{u}$. The difference $\phi=\omega-\theta$ obeys

$$\partial_t\phi+(\boldsymbol{v}\cdot\nabla)\phi=\nu\nabla^2\phi, \tag{163}$$

that has a possible steady-state solution $\phi=0$ and $\omega=\theta$. Yet, it was observed in Ref. [8] (which used a somewhat different structure of dissipative term where instead of $\nu\nabla^2$ a combination of large-scale friction and Laplacian to power 8 were used; the dissipative term, however, was linear so our consideration would apply) that there is a significant difference between the fields. The forcing that was used consisted of keeping a low wave-number component of the fields at the same constant value. However, this type of forcing in fact depends on the considered field so that f depends on the field that it forces. Thus, a difference of forces of ω and θ, that vanishes only at $\omega=\phi$, must be introduced in the right-hand side of Eq. (163). Thus, even though $\phi=0$ is a valid solution of the equations, its small perturbations result in the appearance of force in Eq. (163) that can further increase the perturbation, resulting in instability. It is this instability that was observed. In the case where f in Eqs. (162) are identical, external forces independent of the fields $\omega=\theta$ would hold.

XIII. CONCLUSIONS AND OPEN QUESTIONS

The main goal of the current work was to shed light on the complex behavior of compressible turbulent flow and in particular on the mass density of the fluid and the concentration

of passive tracer particles. As a result, the following issues and fundamental problems have been addressed and solved.

We traced the origin of the multifractality of the concentration to the increasing self-similarity of the flow at increasing Mach number, due to the approach of the scalings of the solenoidal and potential components of the flow. It was demonstrated that the concentration's transition to multifractality is smooth. Detailed description of the turbulent transport was provided with the help of the Kraichnan model of turbulence whose parameters were related to the actual properties of the NS turbulence.

We provided a formula for the fractal dimensions of the density of isothermal compressible turbulence. We demonstrated that the high-order dimensions are determined by rare events that correspond to the tails of the density distribution and are not describable by the log-normal distribution.

Multifractality is a form of clustering which appears at increasing compressibility of the flow due to the increasing tendency of the Lagrangian trajectories to cluster in regions with negative divergence. This tendency would lead to exactly multifractal distribution of tracers if the scalings of the solenoidal and potential components of the velocity were identical. However, the scalings approach a common value only asymptotically with increasing the Mach number. The difference 2Δ of the decay exponents of the spectra of potential and solenoidal components is of order 1 at $\mathrm{Ma} < 1$. It decreases as Ma increases: For instance, the difference is about 5% at $\mathrm{Ma} = 6$ in the case of Ref. [16]. We derived the pair-correlation function of concentration for the general case $\Delta \neq 0$ and demonstrated that the power-law scaling is a good approximation at scale r if $\Delta \ln(L/r) \ll 1$. Correspondingly, the mutlifractality is a good approximation in the whole of the supersonic inertial range provided that $\Delta \ln(L/l_s) \ll 1$. Since L/l_s is a power of Ma, by neglecting weak logarithmic dependence on the Mach number, we find that the concentration of tracers is multifractal under the condition $\Delta \ll 1$. This is only an order of magnitude condition so the critical Mach number Ma_s at which the transition occurs depends on the desired accuracy.

We conclude from the above that though it is not clear whether there is a sharply defined critical Mach number beyond which the scalings agree and multifractality holds exactly (probably not), in practice we can use $\Delta \ll 1$ as the transition criterion. At $\Delta \sim 1$, the influence of the potential component on the small-scale evolution of the concentration is negligible and the fluctuations of the concentration below L are small or of order 1. At $\Delta \ll 1$, the dust particles concentrate on a constantly evolving, statistically stationary, multifractal seen as clusters and filaments in space; cf. Ref. [2].

The considerations above assume that the potential and solenoidal components of the flow obey a power-law scaling. The scaling has been observed; see, e.g., [16]. However, careful investigation of the provided data demonstrates that the power law could only be an approximation to a more complex dependence. If that is the case, then our theory in terms of Δ also becomes an approximation. However, the results of the Kraichnan model for the pair-correlation function of tracers do not assume the scaling of velocity components and could be used for the study of more complex dependencies. These generalizations might be needed in the future should it be found that the power-law scaling of the flow components is not a good approximation.

We remark that the singularity of the natural measure (the steady-state concentration) of a self-similar compressible flow is a universal property independent of the details of the flow. This universality is well known for chaotic flows below the scale of smoothness (which is the case of trivial self-similarity determined by the linear scaling of the velocity difference). In that case, the singularity of the natural measure is a consequence of the exponential dependence of small particles' volumes on time. That dependence and conservation of the total volume of the flow imply that the sum of the Lyapunov exponents is non-negative. Thus, for nondegenerate flows with a strictly negative sum, the steady-state concentration, described by the sum, is singular. Similar universality holds for the natural measure of a rough self-similar flow (the flow is rough if the scaling exponent of its difference is smaller than 1 so that there is no differentiability [1]). The volumes have a power-law behavior so in logarithmic timescale we can carry over the proof for the smooth case. This proof provides us also with a generalization of the sum of the Lyapunov exponents in the inertial range.

The transition to multifractality for the density is less understood. The spectrum of the density is usually fit with a power law [16], though it is proposed that this law is only an approximation [28]. In fact, we demonstrated that the spectrum of the concentration obeys a power law only approximately. This makes it plausible that the power law of the density spectrum is also only an approximation. If we use this approximation, then the transition occurs when the spectrum decay exponent, considered as a function of Ma, passes -1 from below (which seems to be underappreciated [16,28]). At this Mach number, the concentration must also be multifractal. Indeed, the fluid density back reaction on the transporting velocity tends to arrest the formation of large densities and density gradients and, as a result, the density transition to multifractality occurs at a Mach number $\mathrm{Ma}_{\mathrm{cr}}$ larger than or equal to (if the fields coincide) Ma_s. The behavior of the density at $\mathrm{Ma} < \mathrm{Ma}_{\mathrm{cr}}$ is qualitatively similar to the small Mach number behavior where the density is proportional to the pressure of incompressible turbulence [92–96]. The gas particles form clusters and filaments at $\mathrm{Ma} > \mathrm{Ma}_{\mathrm{cr}}$.

Our current understanding of the concentration's transition to multifractality is only moderately good. We do not have a good way for estimating Ma_s because that number is determined by the details of the strongly nonlinear flow. The theory of Ma_s would demand the study of developing shocks; see the introduction. It can be estimated from simulations [16,28] as $\mathrm{Ma}_s \simeq 4$–6. It is probable that as the compressibility of the stirring force increases, the Ma_s decreases. Further numerical studies are required. In contrast, we have a good qualitative understanding of how the transition occurs. We have developed a cascade model of the formation of the fluctuations of the concentration which is more quantitative than usual in the theory of turbulence. That model describes the transition and fractal dimensions in terms of the properties of the flow.

Rigorous formulation for the fractal dimensions of the concentration is possible within the framework of the Kraichnan model. That model already proved highly useful in qualitative studies of turbulent transport and has become standard [1]. By

using this model, one can study the impact of the difference of scalings of solenoidal and potential components on the pair-correlation function in detail (in contrast, our derivation of multifractality for self-similar compressible flows does not need modeling). Our use of this model is dictated uniquely by the derived Markov property of the distance and eddy diffusivity assumption. We found that pair correlations at distance r are proportional to $(r+f)^h$ with f and h that depend on Ma reproducing the previously described behavior in all ranges of Ma. In the multifractal phase, the Kraichnan model estimates the scaling exponent of the pair-correlation function of the concentration, equivalent to the correlation dimension, as the ratio of the second-order structure functions of the potential and the solenoidal components of the velocity. The ratio is scale independent by $\mathrm{Ma} > \mathrm{Ma}_s$ and remarkably the common scaling exponent drops from the exponent. This prediction captures qualitatively the observed dependence of the scaling exponent on the compressibility of the forcing [18]. Quantitatively, our study only yields an order of magnitude estimate of the exponent which is on general grounds is bounded between 0 and 3. Thus, if our calculated exponent is small, then the observed exponent must also be small, and if our exponent is of order 1, then the observed exponent is of order 1 also. In contrast, we could make a quantitative prediction for the Navier-Stokes turbulence that the PDF of the distance between two tracers in the supersonic inertial range obeys a power law at small distances with an exponent that is equal to the exponent of the steady-state correlation function. This is the counterpart of the formula for the correlation dimension in terms of the statistics of the separation for smooth systems [49,74]. Finally, we demonstrated that the scaling of higher order correlation functions is anomalous due to the zero modes similarly to the incompressible case [1].

The transition of the density to multifractality is even less understood than that of the concentration due to the strong nonlinear interactions of the density and the velocity. We do not know what changes in turbulent velocity occur at $\mathrm{Ma}_{\mathrm{cr}}$ and if they occur at all. So far, no changes were observed. We can estimate from simulations [16,28] that $\mathrm{Ma}_{\mathrm{cr}} \simeq 7$–$8$. We propose to look for changes in the velocity at $\mathrm{Ma} = \mathrm{Ma}_{\mathrm{cr}}$ in terms of the behavior of the Lagrangian trajectories. Indeed, we demonstrated by the study of the Kraichnan model that it is probable that separation of tracers in the supersonic inertial range undergoes a qualitative change at a Mach number Ma_r larger than Ma_s. The separation at $\mathrm{Ma} < \mathrm{Ma}_r$ occurs similar to that in incompressible turbulence, obeying a modified Richardson law. A pair of tracers approach each other at most a finite number of times, after which they are permanently separated. In contrast, at $\mathrm{Ma} > \mathrm{Ma}_r$, trajectories of the two particles approach each other infinite number of times with probability 1, due to the trapping effect of the compressibility [57,109,110]. This transition does not cause a change in the behavior of the pair correlation functions of the concentration. We demonstrated that another transition discovered in Ref. [57], where the tracer particles stick to each other with probability 1, probably cannot occur in three-dimensional NS turbulence. It seems that the above recurrence transition could correspond to the density transition from a large-scale to a small-scale field. Thus, we propose to study if there is a relation or equality between Ma_r and $\mathrm{Ma}_{\mathrm{cr}}$.

More knowledge of the fractal dimensions $D(k)$ of the active fluid density may currently be extracted from numerical simulations than corresponding information concerning the passive concentration. The statistics of the density in isothermal turbulence is observed to be log normal; see, e.g., Refs. [16,28]. For this type of statistics, all fractal dimensions can be described as $D(k) = 3 - k\delta/2$, where δ determines the spectrum decay exponent $1-\delta$. This result has been derived previously in a different context [54]. We see that the formula for $D(k)$ is inconsistent at large k, giving negative dimension. The inconsistency of log-normal approximation to multifractality for $D(k)$ at large orders was observed by Mandelbrot in [72] and by Frisch and Parisi in Ref. [67]. The reason for the breakdown of the log-normal approximation at these orders is that the corresponding moments of the mass are determined by tails of the PDF of the logarithm of the density. The tails are determined by rare events for which the log-normal approximation breaks down. To avoid misunderstanding, we talk here of the PDF of finitely resolved density that determines the fractal dimensions. The single-point PDF of the density can be strictly log normal without contradictions. We remark also that log normality implies that a box-counting dimension $D(0)$ equals the space dimension 3, which makes this dimension less interesting.

We have $\delta > 0$ for $\mathrm{Ma} > \mathrm{Ma}_{\mathrm{cr}}$, where all the dimensions that are describable by a log-normal approximation are strictly less than three, $3 - D(k) = k\delta/2$. This is the reason why in defining the phase transition to multifractality with dimensions less than three there is no need to specify which of $D(k)$ determines the transition to multifractality. A similar fact holds for the concentration: If intermittency is neglected, then all $D(k)$ become less than three at Ma_s, where the flow becomes self-similar (intermittency would introduce the corresponding refinements). However, the dimensions $D(k)$ with large k, that are not describable by the log-normal approximation, could become less than three at Ma different from $\mathrm{Ma}_{\mathrm{cr}}$. Since $D(k)$ is a nonincreasing function of k, then they could become less than three at $\mathrm{Ma} < \mathrm{Ma}_{\mathrm{cr}}$. Consideration of fractal dimensions of nonisothermal turbulence where log normality does not hold [44,45,111] is beyond the scope of this work.

We raised the fundamental question of possible difference of the active fluid density and passive tracer concentration in the steady state. We demonstrated that although the fluid density and the concentration of tracers obey the same continuity equation, the proof of their equality is elusive. There is no uniqueness of the steady-state solution and mixing of the fluid density may fail due to the possibility of self-organization of the fluid density in a state that is stabilized by the interaction with the flow. The same state could be unstable for the concentration. We are reminded of other cases in the fluid mechanics where the instability causes the active and passive scalars to differ in the steady state. We demonstrate that the current numerical data, though inconclusive, seems to indicate that the fields differ. We provided a number of testable predictions that will help to resolve the question. These are rigorous and semirigorous results on the density and the concentration that are valuable independently of the fields' equality.

In order to facilitate the difference's identification in experiment, we describe the situation that would hold if the density and the concentration are revealed to differ, $\mathrm{Ma}_s < \mathrm{Ma}_{\mathrm{cr}}$. The

difference is most striking at $\mathrm{Ma}_s < \mathrm{Ma} < \mathrm{Ma}_{\mathrm{cr}}$, where the concentration is multifractal and the density is smooth. Both fields are transported along the same Lagrangian trajectories and obey the continuity equation with the same velocity. Motions of volumes of tracer and fluid particles are identical; however, their stability properties differ. The density and the concentration are different stationary distributions of the same continuity equation. The density evolves from measure zero (in functional space) initial conditions that are consistent with the velocity. These initial conditions are special: The resulting density fluctuations are finite at $\eta \to 0$ despite that the limit is infinite for typical initial conditions. For tracers, the evolution of the same initial condition would be unstable: It is the interaction with the velocity that stabilizes the evolution of the density. The steady-state concentration can be obtained by evolution of typical initial conditions. It gives the natural measure of the dynamics defined by Lagrangian evolution, which is singular at $\eta \to 0$. At $\mathrm{Ma} > \mathrm{Ma}_{\mathrm{cr}}$, both fields are multifractal; however, the fractal dimensions of the concentration are smaller than those of the density. The structures manifested by the two fields are different; cf. Ref. [2]. In fact, the smallest scale of the multifractal can be somewhat different for gas and dust because the scaling mechanisms differ; cf. Ref. [41].

If it is found that the statistics of the concentration and the density differ, then this would make the measurement of the usually used Hentschel-Procaccia (HP) fractal dimensions of the density challenging. We would not have the representation of the multifractal support of the density as the limit of large number of discrete particles spread over the multifractal that is used in the definition [63]. Indeed, if we spread particles in space, then after transients they would be located on the multifractal support of the natural measure and not the density. This and other problems, however, do not arise if the Rényi dimensions are employed. These are more suitable for working with continuum fields, and their use in numerical studies seems to be advantageous. These dimensions are derived from the usual spatial moments of the coarse-grained density and coincide with the HP dimensions where both are well defined. We provide the proof of the fundamental property that the information dimension in the supersonic inertial range describes the scaling of the mass up to points with zero total mass. This proof is needed because the flow is not smooth, as in the usually considered situations.

We compare the statistics of the density and the concentration. The fields coincide at small Mach numbers, where they are reducible in the pseudosound regime to the statistics of the pressure p of incompressible turbulence (we remark that the equality $n = 1 + c\mathrm{Ma}^2 p$ could be used for experimental measurements of pressure since observation of tracers is simple). Other regimes are possible; see, e.g., Ref. [92] for the theory and Ref. [82] for observations. The statistics in the pseudosound regime is not log normal since the pressure is not. For the positive tail, however, log normality was observed [98]. When Ma increases, the concentration and density can become different. The concentration transits to multifractality when the scaling of the solenoidal and potential components of velocity becomes approximately equal. For the density of isothermal turbulence, the increase of Ma causes transition to log-normal statistics. When the statistics is already log-normal, further increase of Ma induces transition to multifractality when the decay exponent of the density spectrum passes one from above. This transition occurs simultaneously with the concentration's transition or when the scaling of the solenoidal and potential components of velocity is already approximately equal and the concentration is multifractal.

We demonstrated that the collision kernel of the particles is significantly increased due to the transition to multifractality. The transition is thus expected to have dramatic consequences on the formation of stars and other processes with coagulation of particles in high-Re and high-Ma compressible turbulence.

Our derivation of the spectrum of the fractal dimensions of the density in terms of one parameter δ calls for the construction of a phenomenology of the turbulence that would provide us with the scaling exponents of the velocity. Indeed, it would seem that if we use the assumption that $\rho^{1/3}\boldsymbol{v}$ has scaling identical with incompressible velocity [16] then we could predict the scaling of the velocity in terms of δ. We demonstrated that this is not straightforward, if doable at all. Construction of a prediction for the velocity scaling that includes multifractality of density is one of the challenges for future work.

Particles transported by the flow have inertia that was neglected in our study; cf. Ref. [2]. The limit of zero inertia is singular in incompressible turbulence; see, e.g., Ref. [50]. We briefly consider it in the compressible case. The limit is not singular in the inertial range, as can be confirmed by using the Kraichnan model. In the viscous range, this may be different because the sum of the Lyapunov exponents is no longer zero. When inertia is small, the particle coordinate $\boldsymbol{x}(t)$ obeys [112]

$$\dot{\boldsymbol{x}} = \boldsymbol{u}(t, \boldsymbol{x}(t)), \quad \boldsymbol{u} = \boldsymbol{v} - \tau_s \boldsymbol{a}, \tag{164}$$

where τ_s is the Stokes time that appears in the law of motion $\tau_s \ddot{\boldsymbol{x}} = \boldsymbol{v}(t, \boldsymbol{x}(t)) - \dot{\boldsymbol{x}}$ and $\boldsymbol{a} = \partial_t \boldsymbol{v} + (\boldsymbol{v} \cdot \nabla)\boldsymbol{v}$ is the Lagrangian accelerations of the fluid. The assumption of linear friction holds provided the Reynolds number of the perturbation of the flow caused by the presence of the particle is small. It can be corrected [2]. In the leading order at small τ_s, we have for the sum of the Lyapunov exponents λ_i^p of the flow of the particles using the formula $\sum_{i=1}^3 \lambda_i^p = -\int_0^\infty \langle \nabla \cdot \boldsymbol{u}(0) \nabla \cdot \boldsymbol{u}(t) \rangle dt$ of [10]

$$\sum_{i=1}^{3} \lambda_i^p \approx \tau_s \int_0^\infty (\langle \nabla \cdot \boldsymbol{a}(0) w(t) \rangle + \langle w(0) \nabla \cdot \boldsymbol{a}(t) \rangle) dt - \int_0^\infty \langle w(0) [\delta \boldsymbol{x}(t) \cdot \nabla] w(t) \rangle dt, \tag{165}$$

where we used the result that the sum of the Lyapunov exponents of the fluid particles is zero. The last term describes the change in the correlation function due to the finite deviation $\delta \boldsymbol{x}(t)$ of the trajectory of the particle from the trajectory of the fluid particle; cf. Ref. [113]. Thus, $\sum_{i=1}^3 \lambda_i^p \neq 0$ and particles' distribution is multifractal up to the smallest scales (finite size of the particles). This can produce non-negligible correction in the collision kernel of dust particles that are smaller than the viscous length.

Our consideration of the statistics of the concentration was independent of the origin of the velocity. Thus, all our considerations hold also for transport of tracers by the velocity

that comes from the solution of the magnetohydrodynamic equations (MHD). The concentration will become multifractal at Ma_s, at which the scalings of solenoidal and potential components of the MHD velocity become similar. It is plausible that the fluid density is not log normal for isothermal MHD since the magnetic stress tensor breaks the invariance with respect to multiplication of the density by a multiplicative constant. This question requires numerical studies.

Finally, the account of intermittency, necessary at very large Reynolds numbers and hardly doable with the presently existing knowledge or data, probably modifies the condition for the multifractality transition of the concentration. The condition of identical scaling of the solenoidal and the potential components of the flow becomes the condition of identical scaling of structure functions of the components with a given order.

ACKNOWLEDGMENTS

I.F. thanks G. Falkovich and S. Tcheremchantsev for helpful discussions. This work was supported by Grant No. 366/15 of the Israel Science Foundation.

APPENDIX A: ANTICORRELATIONS OF VELOCITY DIVERGENCE

Here, we provide further details on anticorrelations of $w[t,\boldsymbol{q}(t,\boldsymbol{x})]$ described in Sec. XI, assuming that the density is finite. We use the identity [10,86]

$$\langle w[t,\boldsymbol{q}(t,\boldsymbol{x})]\rangle \equiv \int w[t,\boldsymbol{q}(t,\boldsymbol{x})]d\boldsymbol{x} = -\int_0^t \langle w(0)w(t')\rangle dt'. \tag{A1}$$

where $\langle w(0)w(t)\rangle = \int w(0,\boldsymbol{x})w[t,\boldsymbol{q}(t,\boldsymbol{x})]d\boldsymbol{x}$ was defined in the main text. The above relationship holds for time independent or stationary flows, but is not necessarily restricted to spatially homogeneous flows, at $t>0$ or $t<0$. We observe that vanishing of the sums of Lyapunov exponent of the flow, and its time-reversal implies that at large times (positive or negative) $w[t,\boldsymbol{q}(t,\boldsymbol{x})]$, that becomes a stationary process, has zero average (since the average is the sum of the Lyapunov exponents). We introduce the asymptotic correlation functions,

$$f_\pm(t) = \lim_{t'\to\pm\infty}\langle w[t',\boldsymbol{q}(t',\boldsymbol{x})]w[t'+t,\boldsymbol{q}(t'+t,\boldsymbol{x})]\rangle. \tag{A2}$$

Starting from Eq. (5) we obtain that [here, $\boldsymbol{q}(t)=\boldsymbol{q}(t,\boldsymbol{x})$]

$$\left\langle \ln^2\left(\frac{\rho(0)}{\rho(t,\boldsymbol{q}(t))}\right)\right\rangle = \int_0^t dt_1dt_2\langle w[t_1,\boldsymbol{q}(t_1)]w[t_2,\boldsymbol{q}(t_2)]\rangle.$$

In the limit of large t, the right-hand side becomes approximately $t\int_{-\infty}^{\infty} f_+(t')dt'$. Since the left-hand side of the last equation is finite, then we must have (we use that t above can be negative)

$$\int_{-\infty}^{\infty} f_\pm(t)dt = 0. \tag{A3}$$

Thus, correlation functions of the stationary limiting processes $w[t,\boldsymbol{q}(t,\boldsymbol{x})]$ at $t\to\pm\infty$ have zero integrals. This brings a simple representation for Lagrangian differences of the density.

1. The first moment of $\langle w(0)w(t)\rangle$ is the asymptotic logarithmic increment of the density

The difference in the fluid particle velocity at two different times (Lagrangian increments) is a much studied characteristics of turbulence; see, e.g., Ref. [114]. We consider the Lagrangian increments of the density. We observe that the random variables,

$$I = \int_{-\infty}^0 w[t,\boldsymbol{q}(t,\boldsymbol{x})]dt,\quad I_+ = \int_0^\infty w[t,\boldsymbol{q}(t,\boldsymbol{x})]dt, \tag{A4}$$

that involve infinite integration range are well defined as $\langle I^2\rangle$ and $\langle I_+^2\rangle$ are finite by Eq. (A3). Using Eq. (A1),

$$\begin{aligned}\langle I\rangle &= \lim_{T\to\infty}\int_{-T}^0 \langle w(0)w(t)\rangle(t+T)dt\\ &= \lim_{T\to\infty}\int_{-T}^0 tdt\langle w(0)w(t)\rangle - T\\ &\quad\times\int_{-\infty}^{-T}\langle w(0)w(t)\rangle dt.\end{aligned} \tag{A5}$$

Assuming that $\langle w(0)w(t)\rangle$ decays faster than $1/t^2$, the last integral vanishes at $T\to\infty$. Then, using Eq. (5), we find for the difference of $\langle\ln\rho\rangle$,

$$\begin{aligned}&\langle\ln\rho\rangle - \lim_{t\to-\infty}\langle\ln\rho(t,\boldsymbol{q}(t,\boldsymbol{x}))\rangle\\ &\quad= \int_{-\infty}^0 |t|\langle w(0)w(t)\rangle dt = -\langle I\rangle,\\ &\langle\ln\rho\rangle - \lim_{t\to\infty}\langle\ln\rho(t,\boldsymbol{q}(t,\boldsymbol{x}))\rangle\\ &\quad= \int_0^\infty t\langle w(0)w(t)\rangle dt = \langle I_+\rangle.\end{aligned} \tag{A6}$$

In the integral for $\langle I_+\rangle$, the factor t gives smaller weight to positive small time values of $\langle w(0)w(t)\rangle$ and larger weight to negative larger time values that exist due to the constraint of zero sum of Lyapunov exponents, $\int_0^\infty\langle w(0)w(t)\rangle dt = 0$, so $\langle I_+\rangle < 0$. Similarly $\langle I\rangle > 0$. Therefore, the average difference of $\langle\ln\rho\rangle$ is the first moment of $\langle w(0)w(t)\rangle$, while the zeroth moment is zero.

APPENDIX B: PAIR-CORRELATION FUNCTION AND RDF

Here, we provide in more detail the definition of the RDF and the relation between the time averaging and averaging over the statistical ensemble of velocity fields. The concentration field of N particles in the unit volume with coordinates $\boldsymbol{x}_i(t)$ is $n(t,\boldsymbol{x}) = \sum_{i=1}^N \delta(\boldsymbol{x}_i(t)-\boldsymbol{x})/N$. We introduced the normalization factor so that $\langle n\rangle = 1$ independently of N. The radial distribution function (RDF) $g(\boldsymbol{r})$ is defined as

$$g(\boldsymbol{r}) = \langle n(0)n(\boldsymbol{r})\rangle = \lim_{N\to\infty}\frac{\sum_{i,k=1}^N \delta(\boldsymbol{x}_k(t)-\boldsymbol{x}_i(t)-\boldsymbol{r})}{N^2}, \tag{B1}$$

where $N\to\infty$ is the continuum limit and the formula is readily verified using the definition $\langle n(0)n(\boldsymbol{r})\rangle = \int n(t,\boldsymbol{x})n(t,\boldsymbol{x}+\boldsymbol{r})d\boldsymbol{x}$. Thus, the RDF counts the fraction of pairs separated by given distance $\boldsymbol{r}$ and is normalized so that it tends to one at large r.

Since $f(\boldsymbol{r})$ is a two-particle quantity, it can be derived from the problem of two particles only in the flow. We perform time averaging of Eq. (B1). Ergodicity of the flow in the two-particle phase space, that is, of the flow $(\boldsymbol{v}(\boldsymbol{x}_k), \boldsymbol{v}(\boldsymbol{x}_i))$, implies equality of time averages of all pairs, giving

$$g(\boldsymbol{r}) = \langle \delta(\boldsymbol{x}_k(t) - \boldsymbol{x}_i(t) - \boldsymbol{r}) \rangle_t, \tag{B2}$$

where the subscript t stands for time averaging. We can consider time average over arbitrarily large time T as average over N results of time averaging over time intervals $t_0(i, i+1)$, where $N = T/t_0$ and i runs from zero to $N-1$. If t_0 is large, then we can consider flows at disjoint time intervals as independent. Thus, we can instead perform averaging over flows at different time intervals or equivalently we can find $g(\boldsymbol{r})$ as average over ensemble of realizations of the flow. In this formulation, we consider two particles put in the flow with some initial positions $\boldsymbol{x}_1$ and $\boldsymbol{x}_1 + \boldsymbol{r}'$. We study the evolution of the distance $\boldsymbol{r}(t) = \boldsymbol{q}(t, \boldsymbol{x}_1 + \boldsymbol{r}') - \boldsymbol{q}(t, \boldsymbol{x}_1)$ between them. Different realizations of the flow produce different evolution of $\boldsymbol{r}(t)$, defining the PDF of the distance $P(\boldsymbol{r}, \boldsymbol{r}', t)$ as given in Eq. (78) of the main text. In that equation, the angular brackets stand also for averaging over the statistics of the flow. The limiting PDF is $\boldsymbol{r}'$ independent and gives $g(\boldsymbol{r})$ in Eq. (77) of the main text. This can be readily verified by inspection of the representation of $g(\boldsymbol{r})$ as average over time averages over intervals with arbitrarily large length t_0.

APPENDIX C: KRAICHNAN MODEL

We stressed in the main text that our usage of the Kraichnan model is understood as a model that reproduces the long-time asymptotic form of the propagator at least qualitatively. We consider here how the model is gauged so that the propagators produced by the NS flow and the model are similar.

We consider the demand that the model reproduces the long-time behavior of the dispersion given by [1],

$$\langle (\boldsymbol{r}(t) - \boldsymbol{r}(0))^2 \rangle = 2 \int_0^t dt_1 \int_0^{t_1} dt_2 \langle \delta \boldsymbol{v}(t_1) \cdot \delta \boldsymbol{v}(t_2) \rangle, \tag{C1}$$

where $\delta \boldsymbol{v}(t) \equiv \boldsymbol{v}(t, \boldsymbol{q}(t, \boldsymbol{x} + \boldsymbol{r})) - \boldsymbol{v}(t, \boldsymbol{q}(t, \boldsymbol{x}))$ and we used

$$\boldsymbol{r}(t) = \boldsymbol{q}(t, \boldsymbol{x} + \boldsymbol{r}) - \boldsymbol{q}(t, \boldsymbol{x}) = \boldsymbol{r}(0) + \int_0^t \delta \boldsymbol{v}(t') dt'. \tag{C2}$$

Taking the time derivative and using that eddies of scale r have the correlation time $t_r \sim r/\delta v_r$, we have

$$\frac{d}{dt} \langle (\boldsymbol{r}(t) - \boldsymbol{r}(0))^2 \rangle \sim \int_{-\infty}^t \langle \delta \boldsymbol{v}(t) \cdot \delta \boldsymbol{v}(t') \rangle dt' \sim \delta v_r^2 t_r \sim r \delta v_r,$$

where we do not distinguish the solenoidal and potential components of the flow considering at the moment the multifractal phase where the components scale similarly. We demand that the white noise in time velocity of the Kraichnan model $\boldsymbol{u}$ produces the same long-time growth of the dispersion, as implied by the law above. We have for the dispersion in the white noise model

$$\frac{d}{dt} \langle (\boldsymbol{r}(t) - \boldsymbol{r}(0))^2 \rangle = \int_{-\infty}^t \langle \delta \boldsymbol{u}(t) \cdot \delta \boldsymbol{u}(t') \rangle dt' \sim r^\xi, \tag{C3}$$

where we used that $K_{ik}(\boldsymbol{r}) \propto r^\xi$; see Sec. IX. Thus, we fix the value of ξ by the demand that in the multifractal phase $r \delta v_r \sim r^\xi$. If the solenoidal component of the Navier-Stokes compressible turbulence has a spherically normalized spectrum proportional to k^{-a}, then the velocity scales in space as $r^{(a-1)/2}$, giving $\xi = (a+1)/2$.

The above consideration disregards the intermittency of the flow, which is not a bad assumption, as discussed in Subsec. IX F. Thus, if the growth of $r(t)$ at large times is self-similar with a good approximation (which it must be in the multifractal phase; cf. the incompressible turbulence case [1]), then the Kraichnan model, where the growth is self-similar, will reproduce the law of growth of the distance up to a multiplicative constant. This overall constant of proportionality is, however, of less interest to us since it does not enter the scaling exponent of the pair-correlation function β. This exponent is roughly the ratio of the magnitudes of the potential and solenoidal components; see the main text.

We see that the spatial scaling of $\boldsymbol{u}$ is different from the scaling of $\boldsymbol{v}$, which is so also in the incompressible case [1] and below. Since zero correlation time results in effective Gaussianity [80], then the statistics is taken Gaussian with zero mean. The statistics is completely determined by the pair-correlation function,

$$\langle u_i(t, \boldsymbol{x}) u_k(t', \boldsymbol{x}') \rangle = \delta(t - t') D_{ik}(\boldsymbol{r}), \tag{C4}$$

where $\boldsymbol{r} = \boldsymbol{x}' - \boldsymbol{x}$. It is assumed that the statistics is stationary, spatially uniform, and isotropic. Thus, the Fourier transform of $D_{ik}(\boldsymbol{r})$ has the following general form ($\hat{k} = \boldsymbol{k}/k$),

$$D_{ik}(\boldsymbol{k}) = f(k)(\delta_{ik} - \hat{k}_i \hat{k}_k) + h(k) \hat{k}_i \hat{k}_k, \tag{C5}$$

with arbitrary functions $f(k)$ and $h(k)$. In this model, the symmetries imply that the solenoidal $\boldsymbol{s}$ and potential components $\boldsymbol{p}$ of the flow, $\boldsymbol{u} = \boldsymbol{s} + \boldsymbol{p}$, are independent,

$$\begin{aligned} \langle s_i(t, \boldsymbol{k}) s_k(t', \boldsymbol{k}') \rangle &= 8\pi^3 \delta(t' - t) \delta(\boldsymbol{k} + \boldsymbol{k}') f(k) (\delta_{ik} - \hat{k}_i \hat{k}_k), \\ \langle p_i(t, \boldsymbol{k}) p_k(t', \boldsymbol{k}') \rangle &= 8\pi^3 \delta(t' - t) \delta(\boldsymbol{k} + \boldsymbol{k}') h(k) \hat{k}_i \hat{k}_k. \end{aligned} \tag{C6}$$

Thus, $f(k)$ and $h(k)$ represent the spectra (not normalized spherically) of the solenoidal and potential components, respectively. We stress that these are not the spectra of the components; these are only their representations that have scaling different from the scalings of the spectra of the components of the NS flow. We fix the scalings of $f(k)$ and $h(k)$ by extension of the procedure that we used above for fixing ξ in the multifractal phase. We demand that time integrals of the different time pair correlation functions of the solenoidal and potential components of the NS flow coincide with their counterparts for the Kraichnan model; see Ref. [1]. This condition guarantees that the model reproduces the impact of these components on pair dispersion separately, which is necessary for discussion of the concentration which is influenced by the components differently. Thus, considering as previously that the solenoidal component of the Navier-Stokes compressible turbulence has a spherically normalized spectrum proportional to k^{-a}, we find that the solenoidal component of $\boldsymbol{u}$ must scale as $r^{(a+1)/2}$, resulting in $f(k) \sim k^{-3-(a+1)/2}$. Similarly, if the spherically normalized spectrum of the potential component is proportional to k^{-b}, then $h(k) \sim k^{-3-(b+1)/2}$. These scaling relations refer to the supersonic inertial range. We observe that $f(k)$ and $h(k)$ depend on the temporal correlations of turbulence and not

only on the spectra of the components of the turbulent flow that characterize the instantaneous statistics. Therefore, the proportionality constants in $f(k) \sim k^{-3-(a+1)/2}$ and $h(k) \sim k^{-3-(b+1)/2}$ are nontrivial functionals of the spatiotemporal statistics of turbulence. The ratio of these constants, that defines β as demonstrated in the main text, is roughly the ratio of the components' spectra at zero frequency. Thus, β can be considered as a ratio of magnitudes of potential and solenoidal components; however, providing this ratio in terms of instantaneous statistics of turbulence is impossible. This is in contrast with the scaling exponents for which the temporal behavior is fixed by the robust relation $t_r \sim r/\delta v_r$ implied by the NSE.

We find in real space

$$\langle s_i(t,\boldsymbol{x}) s_k(t',\boldsymbol{x}')\rangle = \delta(t'-t)[\delta_{ik} f(r) + \nabla_i \nabla_k f_1(r)] = \delta(t'-t)\left[\frac{r_i r_k}{r}(f_1'/r)' - \delta_{ik}\frac{f_1' + r(f_1)''}{r}\right], \tag{C7}$$

where $f(r)$ is the inverse Fourier transform of $f(k)$,

$$f(r) = \int f(k)\exp(-i\boldsymbol{k}\cdot\boldsymbol{r})\frac{d\boldsymbol{k}}{8\pi^3} = \int_0^\infty \frac{f(k)\sin(kr)kdk}{2\pi^2 r}. \tag{C8}$$

We introduced the function $f_1(r)$,

$$f_1(r) \equiv \int_0^\infty \frac{f(k)dk}{2\pi^2}\frac{\sin(kr)}{kr}, \quad f(r) = -\frac{(rf_1)''}{r}. \tag{C9}$$

We introduce the function $u_0(r)$,

$$u_0 r^2 = \frac{2f_1'}{r} + v_0, \quad \frac{f_1' + r(f_1)''}{r} = -v_0 + \frac{(r^4 u_0)'}{2r}, \tag{C10}$$

where the constant v_0 is taken so that $u_0(0)$ has regular Taylor expansion at the smallest r where the viscosity smooths the flow,

$$v_0 = -2f_1''(r=0) = \frac{2f(r=0)}{3}; \tag{C11}$$

cf. Ref. [53]. The contribution of the potential component to the pair correlation function in real space is given by

$$\langle p_i(t,\boldsymbol{x}) p_k(t',\boldsymbol{x}')\rangle = -\delta(t'-t)\left[\frac{\delta_{ik}h_1'(r)}{r} + \frac{r_i r_k (h_1'/r)'}{r}\right],$$

$$h_1 = \int_0^\infty \frac{h(k)dk}{2\pi^2}\frac{\sin(kr)}{kr}, \quad h = -\frac{(rh_1)''}{r} = -h_1'' - \frac{2h_1'}{r}.$$

Adding up both contributions, we find

$$\langle u_i(t,\boldsymbol{x}) u_k(t',\boldsymbol{x}')\rangle = \delta(t'-t)\left\{\frac{[(r^2u_0)' - 2(h_1'/r)']r_i r_k}{2r} + v_0\delta_{ik} - \frac{[(r^4u_0)' + 2h_1'(r)]\delta_{ik}}{2r}\right\}. \tag{C12}$$

Finally, we introduce

$$u = u_0 + \frac{h_1''(r) - h_1''(0)}{r^2}, \quad c = -\frac{h'}{r}, \quad V_0 = v_0 - h_1''(0),$$

where $u(r)$ and $c(r)$ have regular Taylor expansion in the viscous range and $-3h_1''(0) = h(0)$. Using these functions and V_0, we reproduce the correlation function in the form that was used in Ref. [53] and is given by Eqs. (91) and (92) from the main text.

We consider in more detail the form of the functions above in the real space. We can easily see from $f(k) \propto k^{-3-(a+1)/2}$ that

$$f(0) - f(r) = \theta_1 r^{(a+1)/2}, \quad r \ll L. \tag{C13}$$

It is seen by performing an inverse Fourier transform of the first of Eqs. (C6),

$$\langle [s_i(t,\boldsymbol{r}) - s_i(t,0)][s_i(0,\boldsymbol{r}) - s_i(0,0)]\rangle = \delta(t)\int f(k)[1-\exp(i\boldsymbol{k}\cdot\boldsymbol{r})]\frac{d\boldsymbol{k}}{2\pi^3} = 4\delta(t)\big[f(0) - f(r)\big], \tag{C14}$$

that θ_1 is a positive constant characterizing the magnitude of the solenoidal component; cf. Ref. [115]. Similarly, we have from $h(k) \propto k^{-3-(b+1)/2}$ that

$$h(0) - h(r) = \theta_2 r^{(b+1)/2}, \quad r \ll L, \tag{C15}$$

where θ_2 is a positive constant characterizing the magnitude of the potential component. We assumed that both a and b change between 1 and 3. Indeed, the decay exponent of the spectrum of the solenoidal component changes between about the Kolmogorov value 5/3 at small Mach numbers to probably the Burgers equation's value 2 at large Mach numbers. Similarly, the decay exponent of the spectrum of potential component changes between about the incompressible turbulence's pressure spectrum exponent's value of 3 at $\mathrm{Ma} \ll 1$ to the same Burgers equation's value 2 at large Mach numbers.

We have from the definitions that

$$\frac{c}{ru} = -\frac{h'}{2[f_1'(r)/r - f_1''(0)] + h_1''(r) - h_1''(0)}. \tag{C16}$$

We observe from Eqs. (C9) and (C13) that

$$(rf_1)'' = r[f(0) - f(r) - f(0)] = \theta_1 r^{(a+3)/2} - rf(0).$$

We find by integrating this equation twice and demanding regularity of f_1 at small r implied by the definition in Eq. (C9) that

$$f_1 = \frac{4\theta_1 r^{(a+5)/2}}{(a+5)(a+7)} - \frac{r^2 f(0)}{6} + c_f, \tag{C17}$$

where c_f is a constant. This gives

$$\frac{f_1'}{r} - f_1''(0) = \frac{2\theta_1 r^{(a+1)/2}}{a+7}. \tag{C18}$$

Similarly, we have

$$(rh_1)'' = r[h(0) - h(r) - h(0)] = \theta_2 r^{(b+3)/2} - rh(0),$$

$$h_1 = \frac{4\theta_2 r^{(b+5)/2}}{(b+5)(b+7)} - \frac{r^2 h(0)}{6} + c_h, \tag{C19}$$

where c_h is a constant. This gives

$$h_1''(r) - h_1''(0) = \frac{(b+3)\theta_2 r^{(b+1)/2}}{b+7}. \tag{C20}$$

We find from Eq. (C16) using the formulas above that

$$\frac{c}{ru} = \frac{(b+1)(b+7)(a+7)\Gamma' r^{\Delta-1}\tilde{L}^{-\Delta}}{8(b+7)+2(b+3)(a+7)\Gamma'(r/\tilde{L})^{\Delta}},$$

where $\Delta = (b-a)/2$. We introduced dimensionless constant $\Gamma' = \theta_2\tilde{L}^{\Delta}/\theta_1$ with scale $\tilde{L}$ of order L. This scale is defined as the effective upper cutoff of the inertial range. The equation above, derived from the asymptotic power laws in the inertial range, holds below $\tilde{L}$ so that Eq. (109) from the main text is true at $r \ll L$. This constant gives the ratio of the structure functions of the potential and solenoidal component at the scale L. Since at these scales the structure functions are approximately equal to the dispersion of the respective velocity component, then Γ' is roughly the ratio of magnitudes of the potential and solenoidal components.

APPENDIX D: SUPERCRITICAL TRANSPORT

Here, we confirm the prediction that the scaling exponent of the pair-correlation function of the concentration determines the scaling of $P(r, r', \tau)$ at small r also at finite r' in accord with Eq. (88). We denote by $P(r, \boldsymbol{r}', |t|)$ the PDF $P(\boldsymbol{r}, \boldsymbol{r}', |t|)$ averaged over all directions of $\boldsymbol{r}$. Isotropy implies that $P(r, \boldsymbol{r}', |t|)$ is independent of the direction of $\boldsymbol{r}'$ so $P(r, \boldsymbol{r}', |t|) = P(r, r', |t|)$. The angle-averaged PDF obeys a closed equation whose solution can be written as [57,109]

$$P(r, r', \tau) = \frac{(rr_0)^{(\beta-\xi-1)/2}\Gamma(1-b_0)}{|\tau|^{b_0}(2-\xi)^{2b_0}} I_{-b_0}\left[\frac{2(rr')^{(2-\xi)/2}}{(2-\xi)^2|\tau|}\right] \times \exp\left[-\frac{r'^{2-\xi}}{(2-\xi)^2|\tau|}\right] f_s(r, \tau), \quad \text{(D1)}$$

where I_{-b_0} is the modified Bessel function of the first kind of index $-b_0$. It is readily seen that $P(r, r' \to 0, \tau) = f_s(r, \tau)$, as claimed previously. Quite similarly, we have

$$P(r, r', \tau) \sim \exp\left[-\frac{r'^{2-\xi}}{(2-\xi)^2|\tau|}\right] f_s(r, \tau) \quad \text{(D2)}$$

at small r. This confirms Eq. (86):

$$P(r, L, t_L)L^3 \sim f_s(r, c_0' t_L)L^3 \sim \frac{(c_0' t_L)^{b_0-1}}{r^{\beta}} L^3 \sim \left(\frac{L}{r}\right)^{\beta},$$

where we used $(2-\xi)(b_0-1) = \beta - 3$ and restored dimensional time by multiplying with c_0'.

For future reference, we bring the formula for the moments $\langle r^k(t)\rangle = 4\pi \int_0^{\infty} P(r, r_0, t) r^{2+k} dr$. Integration using Eq. (D1) gives [57]

$$\langle r^k(t)\rangle = \frac{\Gamma[k/(2-\xi)+1-b_0]}{\Gamma(1-b_0)}[(2-\xi)^2|t|c_0']^{k/(2-\xi)} \times F\left(-\frac{k}{2-\xi}, 1-b_0, -\frac{r_0^{2-\xi}}{(2-\xi)^2|t|c_0'}\right), \quad \text{(D3)}$$

where $F(a, b, z)$ is confluent hypergeometric function. This holds for all the convergent moments that obey $k > \beta - 3$, where $\beta - 3 < 0$. This formula is provided in Ref. [57] only for $k \geqslant 0$. Moments of negative order become relevant in the curious hypothetical situation of weakly compressible flow with identical scaling of the solenoidal and potential components. In that case, if inertial range is large, we could get large fluctuations of the concentration, however small the compressibility is: The factor $(L/r)^{\beta}$ can get large for small fixed β if r is suitably small.

[1] G. Falkovich, K. Gawedzki, and M. Vergassola, Particles and fields in fluid turbulence, Rev. Mod. Phys. **73**, 913 (2001).

[2] P. F. Hopkins and H. Lee, The fundamentally different dynamics of dust and gas in molecular clouds, Mon. Not. R. Astron. Soc. **456**, 4174 (2016).

[3] H. Lee, P. F. Hopkins, and J. Squire, The dynamics of charged dust in magnetized molecular clouds, Mon. Not. R. Astron. Soc. **469**, 3532 (2017).

[4] A. Celani, M. Cencini, A. Mazzino, and M. Vergassola, Active Versus Passive Scalar Turbulence, Phys. Rev. Lett. **89**, 234502 (2002).

[5] C. Schwarz, C. Beetz, J. Dreher, and R. Grauer, Lyapunov exponents and information dimension of the mass distribution in turbulent compressible flows, Phys. Lett. A **374**, 1039 (2010).

[6] D. J. Price and C. Federrath, A comparison between grid and particle methods on the statistics of driven, supersonic, isothermal turbulence, Mon. Not. R. Astron. Soc. **406**, 1659 (2010).

[7] J. J. Monaghan, Smoothed particle hydrodynamics, Ann. Rev. Astron. Astrophys. **30**, 543 (1992).

[8] A. Babiano, C. Basdevant, B. Legras, and R. Sadourny, Vorticity and passive-scalar dynamics in two-dimensional turbulence, J. Fluid Mech. **183**, 379 (1987).

[9] D. Ruelle, Smooth dynamics and new theoretical ideas in nonequilibrium statistical mechanics, J. Stat. Phys. **95**, 393 (1999).

[10] G. Falkovich and A. Fouxon, Entropy production and extraction in dynamical systems and turbulence, New J. Phys. **6**, 50 (2004).

[11] J. R. Dorfman, *An Introduction to Chaos in Nonequilibrium Statistical Mechanics*, (Cambridge University Press, Cambridge, UK, 1999).

[12] I. G. Sinai, *Introduction to Ergodic Theory* (Princeton University Press, Princeton, NJ, 1976).

[13] I. G. Sinai, *Topics in Ergodic Theory* (Princeton University Press, Princeton, NJ, 1994).

[14] P. Grassberger, Estimating the fractal dimensions and entropies of strange attractors, Chaos **1**, 291 (1986).

[15] A. Brandenburg and K. Subramanian, Astrophysical magnetic fields and nonlinear dynamo theory, Phys. Rep. **417**, 1 (2005).

[16] A. G. Kritsuk, M. L. Norman, P. Padoan, and R. Wagner, The statistics of supersonic isothermal turbulence, Astroph. J. **665**, 416 (2007).

[17] J. Kim and D. Ryu, Density power spectrum of compressible hydrodynamic turbulent flows, Astr. J. Lett. **630**, L45 (2005).

[18] C. Federrath, R. S. Klessen, and W. Schmidt, The fractal density structure in supersonic isothermal turbulence: Solenoidal versus compressive energy injection, Astr. J. **692**, 364 (2009).

[19] T. S. Tricco, D. J. Price, and G. Laibe, Is the dust-to-gas ratio constant in molecular clouds? Mon. Not. R. Astron. Soc.: Lett. **471**, L52 (2017).

[20] R. C. Fleck, Jr., Scaling relations for the turbulent, non-self-gravitating, neutral component of the interstellar medium, Astroph. J. **458**, 739 (1996).

[21] C. F. von Weizsacker, The evolution of galaxies and stars, Astroph. J. **114**, 165 (1951).

[22] M. J. Lighthill, in *IAU Symposium 2: Gas Dynamics of Cosmic Clouds* (North Holland, Amsterdam, 1955), p. 121.

[23] A. G. Kritsuk, S. D. Ustyugov, M. L. Norman, and P. Padoan, in *Numerical Modelling of Space Plasma Flows: ASTRONUM-2008*, edited by N. V. Pogorelov, E. Audit, P. Colella, and G. P. Zank, ASP Conference Series Vol. 406 (Astronomical Society of the Pacific, San Francisco, 2009), p. 15.

[24] Y. Kaneda, T. Ishihara, M. Yokokawa, K. Itakura, and A. Uno, Energy dissipation rate and energy spectrum in high resolution direct numerical simulations of turbulence in a periodic box, Phys. Fluids **15**, L21 (2003).

[25] C. Federrath, On the universality of supersonic turbulence, Mon. Not. R. Astron. Soc. **436**, 1245 (2013).

[26] P. Goldreich and S. Sridhar, Toward a theory of interstellar turbulence. 2: Strong alfvenic turbulence, Ap. J. **438**, 763 (1995).

[27] J. Cho and A. Lazarian, Compressible magnetohydrodynamic turbulence: Mode coupling, scaling relations, anisotropy, viscosity-damped regime, and astrophysical implications, Mon. Not. R. Astron. Soc. **345**, 325 (2003).

[28] L. Konstandin, W. Schmidt, P. Girichidis, T. Peters, R. Shetty, and R. S. Klessen, Mach number study of supersonic turbulence: The properties of the density field, Mon. Not. R. Astron. Soc. **460**, 4483 (2016).

[29] G. Kowal and A. Lazarian, Scaling relations of compressible MHD turbulence, Astroph. J. **666**, L69 (2007).

[30] W. Schmidt, C. Federrath, and R. Klessen, Is the Scaling of Supersonic Turbulence Universal? Phys. Rev. Lett. **101**, 194505 (2008).

[31] C. Federrath, J. Roman-Duval, R. S. Klessen, W. Schmidt, and M. M. Mac Low, Comparing the statistics of interstellar turbulence in simulations and observations: Solenoidal versus compressive turbulence forcing, Astron. Astroph. **512**, A81 (2010).

[32] G. Falkovich, I. Fouxon, and Y. Oz, New relations for correlation functions in Navier-Stokes turbulence, J. Fluid Mech. **644**, 465 (2010).

[33] H. Aluie, Compressible Turbulence: The Cascade and its Locality, Phys. Rev. Lett. **106**, 174502 (2011).

[34] S. Galtier and S. Banerjee, Exact Relation for Correlation Functions in Compressible Isothermal Turbulence, Phys. Rev. Lett. **107**, 134501 (2011).

[35] H. Aluie, S. Li, and H. Li, Conservative cascade of kinetic energy in compressible turbulence, Astro. J. Lett. **751**, L29 (2012).

[36] R. Wagner, G. Falkovich, A. G. Kritsuk, and M. L. Norman, Flux correlations in supersonic isothermal turbulence, J. Fluid Mech. **713**, 482 (2012).

[37] S. Galtier and S. Banerjee, in *Proceedings of the Annual Meeting of the French Society of Astronomy and Astrophysics*, 277 (Société Francaise d'Astronomie et d'Astrophysique, Paris, 2013).

[38] H. Aluie, Scale decomposition in compressible turbulence, Phys. D (Amsterdam, Neth.) **247**, 54 (2013).

[39] S. Banerjee and S. Galtier, Exact relation with two-point correlation functions and phenomenological approach for compressible magnetohydrodynamic turbulence, Phys. Rev. E **87**, 013019 (2013).

[40] A. G. Kritsuk, R. Wagner, and M. L. Norman, Scaling in supersonic isothermal turbulence, in *Numerical Modeling of Space Plasma Flows ASTRONUM-2014* (Astronomical Society of the Pacific, San Francisco, 2015), Vol. 498, p. 16.

[41] U. Frisch, *Turbulence: The Legacy of A. N. Kolmogorov* (Cambridge University Press, Cambridge, UK, 1995).

[42] D. Biskamp, *Magnetohydrodynamic Turbulence* (Cambridge University Press, Cambridge, UK, 2003).

[43] Å. K. Nordlund and P. Padoan, The density PDFs of supersonic random flows, in *Proceedings of the 2nd Guillermo Haro Conference, Interstellar Turbulence*, edited by J. Franco and A. Carraminana (Cambridge University Press, 1999), p. 218.

[44] E. Vazquez-Semadeni, Hierarchical structure in nearly pressureless flows as a consequence of self-similar statistics, Astrophys. J. **423**, 681 (1994).

[45] T. Passot and E. Vazquez-Semadeni, Density probability distribution in one-dimensional polytropic gas dynamics, Phys. Rev. E **58**, 4501 (1998).

[46] A. Celani, A. Lanotte, A. Mazzino, and M. Vergassola, Fronts in passive scalar turbulence, Phys. Fluids **13**, 1768 (2001).

[47] B. I. Shraiman and E. D. Siggia, Scalar turbulence, Nature (London) **405**, 639 (2000).

[48] Q. Ni and S. Chen, Effects of shock topology on temperature field in compressible turbulence, arXiv:1506.04179 (unpublished).

[49] J. Bec, K. Gawedzki, and P. Horvai, Multifractal Clustering in Compressible Flows, Phys. Rev. Lett. **92**, 224501 (2004).

[50] G. Falkovich, A. Fouxon, and M. G. Stepanov, Acceleration of rain initiation by cloud turbulence, Nature (London) **419**, 151 (2002).

[51] G. L. Eyink and T. D. Drivas, Cascades and Dissipative Anomalies in Compressible Fluid Turbulence, Phys. Rev. X **8**, 011022 (2018).

[52] E. Balkovsky and A. Fouxon, Universal long-time properties of Lagrangian statistics in the Batchelor regime and their application to the passive scalar problem, Phys. Rev. E **60**, 4164 (1999).

[53] E. Balkovsky, G. Falkovich, and A. Fouxon, Intermittent Distribution of Inertial Particles in Turbulent Flows, Phys. Rev. Lett. **86**, 2790 (2001).

[54] I. Fouxon, Distribution of Particles and Bubbles in Turbulence at a Small Stokes Number, Phys. Rev. Lett. **108**, 134502 (2012).

[55] P. Grassberger, R. Badii, and A. Politi, Scaling laws for invariant measures on hyperbolic and nonhyperbolic atractors, J. Stat. Phys. **51**, 135 (1988).
[56] L. Qian, D. Li, Y. Gao, H. Xu, and Z. Pan, Studies of turbulence dissipation in the taurus molecular cloud with core velocity dispersion, Astrophys. J. **864**, 116 (2018).
[57] K. Gawedzki and M. Vergassola, Phase transition in the passive scalar advection, Phys. D (Amsterdam, Neth.) **138**, 63 (2000).
[58] K. Sreenivasan, Fractals and multifractals in fluid turbulence, Ann. Rev. Fluid Mech. **23**, 539 (1991).
[59] L. Biferale, A. S. Lanotte, R. Scatamacchia, and F. Toschi, Intermittency in the relative separations of tracers and of heavy particles in turbulent flows, J. Fluid Mech. **757**, 550 (2014).
[60] Ya. Pesin, *Dimension Theory in Dynamical Systems* (University of Chicago Press, Chicago, 1997).
[61] D. Harte, *Multifractals: Theory and Applications* (CRC Press, Boca Raton, FL, 2001).
[62] T. C. Halsey, M. H. Jensen, L. P. Kadanoff, I. Procaccia, and B. I. Shraiman, Fractal measures and their singularities: The characterization of strange sets, Phys. Rev. A **33**, 1141 (1986).
[63] H. G. E. Hentschel and I. Procaccia, The infinite number of generalized dimensions of fractals and strange attractors, Phys. D (Amsterdam, Neth.) **8**, 435 (1983).
[64] F. Germinet and S. Tcheremchantsev, Generalized fractal dimensions on the negative axis for compactly supported measures, Math. Nach. **279**, 543 (2006).
[65] S. Tcheremchantsev, Mixed lower bounds for quantum transport, J. Funct. Anal. **197**, 247 (2003).
[66] J.-M. Barbaroux, F. Germinet, and S. Tcheremchantsev, Generalized fractal dimensions: Equivalences and basic properties, J. Math. Pures Appl. **80**, 977 (2001).
[67] U. Frisch and G. Parisi, On the singularity structure of fully developed turbulence, in *Turbulence and Predictability in Geophysical Fluid Dynamics and Climate Dynamics*, edited by M. Gil, R. Benzi, and G. Parisi (Amsterdam, New York, North-Holland, 1985).
[68] B. B. Mandelbrot, Multifractal measures, especially for the geophysicist, Pure Appl. Geophys. **131**, 5 (1989).
[69] L. Schmidt, I. Fouxon, and M. Holzner, Inertial particles distribute in turbulence as Poissonian points with random intensity inducing clustering and supervoiding, Phys. Rev. Fluids **2**, 074302 (2017).
[70] I. Fouxon and X. Zhou, Kaplan-Yorke type conjecture for generalized dimensions of strange attractors (unpublished).
[71] P. F. Hopkins, A model for (non-lognormal) density distributions in isothermal turbulence, Mon. Not. R. Astron. Soc. **430**, 1880 (2013).
[72] B. B. Mandelbrot, Intermittent turbulence in self-similar cascades: Divergence of high moments and dimension of the carrier, J. Fluid Mech. **62**, 331 (1974).
[73] S. Tasaki, T. Gilbert, and J. R. Dorfman, An analytical construction of the SRB measures for Baker-type maps, Chaos: Int. J. Nonlinear Sci. **8**, 424 (1998).
[74] P. H. Baxendale, Statistical equilibrium and two-point motion for a stochastic flow of diffeomorphisms, in *Spatial Stochastic Processes* (Birkhäuser, Boston, 1991).
[75] P. Grassberger and I. Procaccia, Characterization of Strange Attractors, Phys. Rev. Lett. **50**, 346 (1983).
[76] B. I. Shraiman and E. D. Siggia, Anomalous scaling of a passive scalar in turbulent flow, Compt. R. Acad. Sci. **321**, 279 (1995).
[77] M. Chertkov, G. Falkovich, I. Kolokolov, and V. Lebedev, Normal and anomalous scaling of the fourth-order correlation function of a randomly advected passive scalar, Phys. Rev. E **52**, 4924 (1995).
[78] K. Gawedzki and A. Kupiainen, Anomalous Scaling of the Passive Scalar, Phys. Rev. Lett. **75**, 3834 (1995).
[79] K. Gawedzki and A. Kupiainen, in *Low-Dimensional Models in Statistical Physics and Quantum Field Theory*, edited by H. Grosse and L. Pittner (Springer, Berlin, 1996).
[80] H. Risken, *The Fokker-Planck Equation*, (Springer, Berlin, 1996).
[81] A. S. Monin and A. M. Yaglom, *Statistical Fluid Mechanics* (Courier Corporation, USA, 2013).
[82] J. Wang, T. Gotoh, and T. Watanabe, Scaling and intermittency in compressible isotropic turbulence, Phys. Rev. Fluids **2**, 013403 (2017).
[83] S. Boldyrev, A. Nordlund, and P. Padoan, Scaling relations of supersonic turbulence in star-forming molecular clouds, Ap. J. **573**, 678 (2002).
[84] H. R. Pruppacher and J. D. Klett, *Microphysics of Clouds and Precipitation* (Springer, Berlin, 2010).
[85] P. Saffman and J. S. Turner, J. Fluid Mech. **1**, 16 (1956).
[86] I. Fouxon, Evolution to a singular measure and two sums of Lyapunov exponents, J. Stat. Mech. **201**, L02001 (2011).
[87] E. Balkovsky, A. Fouxon, and V. Lebedev, Turbulence of polymer solutions, Phys. Rev. E **64**, 056301 (2001).
[88] I. Fouxon, B. Meerson, M. Assaf, and E. Livne, Formation of density singularities in ideal hydrodynamics of freely cooling inelastic gases: A family of exact solutions, Phys. Fluids **19**, 093303 (2007).
[89] I. Fouxon, Finite-time collapse and localized states in the dynamics of dissipative gases, Phys. Rev. E **80**, 010301(R) (2009).
[90] I. Kolvin, E. Livne, and B. Meerson, Navier-Stokes hydrodynamics of thermal collapse in a freely cooling granular gas, Phys. Rev. E **82**, 021302 (2010).
[91] S. Luzzatto, Mixing and decay of correlations in non-uniformly expanding maps: A survey of recent results, arXiv:math/0301319 (unpublished).
[92] B. J. Bayly, C. D. Levermore, and T. Passot, Density variations in weakly compressible flows, Phys. Fluids A **4**, 945 (1992).
[93] D. Montgomery, M. R. Brown, and W. H. Matthaeus, Density fluctuation spectra in magnetohydrodynamic turbulence, J. Geoph. Res. **92**, 282 (1987).
[94] M. R. Brown and W. H. Matthaeus, Nearly incompressible magnetohydrodynamics at low Mach number, Phys. Fluids **31**, 3634 (1988).
[95] M. J. Lighthill, On sound generated aerodynamically. I. General theory, Proc. Royal Soc. London **211**, 564 (1952); On sound generated aerodynamically. II. Turbulence as a source of sound, **222**, 1 (1954).
[96] J. R. Ristorcelli, A pseudo-sound constitutive relationship for the dilatational covariances in compressible turbulence, J. Fluid Mech. **347**, 37 (1997).

[97] D. Terakado and Y. Hattori, Density distribution in two-dimensional weakly compressible turbulence, Phys. Fluids **26**, 085105 (2014).

[98] D. A. Donzis and S. Jagannathan, Fluctuations of thermodynamic variables in stationary compressible turbulence, J. Fluid Mech. **733**, 221 (2013).

[99] S. Jagannathan and D. A. Donzis, Reynolds and Mach number scaling in solenoidally-forced compressible turbulence using high-resolution direct numerical simulations, J. Fluid Mech. **789**, 669 (2016).

[100] L. Pan and E. Scannapieco, Mixing in supersonic turbulence, Ap. J. **721**, 1765 (2010).

[101] Y. Kifer, *Random Perturbations of Dynamical Systems* (Birkhauser, Boston, 1988).

[102] S.-K. Ma, *Statistical Mechanics* (World Scientific, Singapore, 1984).

[103] G. Falkovich and V. Lebedev, Nonlocal vorticity cascade in two dimensions, Phys. Rev. E **50**, 3883 (1994).

[104] R. H. Kraichnan, Inertial ranges in two-dimensional turbulence, Phys. Fluids **10**, 1417 (1967).

[105] R. H. Kraichnan, Inertial-range transfer in two- and three-dimensional turbulence, J. Fluid Mech. **47**, 525 (1971).

[106] R. H. Kraichnan, Statistical dynamics of two-dimensional flow, J. Fluid Mech. **67**, 155 (1975).

[107] G. K. Batchelor, High-speed computing in fluid dynamics, Phys. Fluids **12**, 233 (1969).

[108] G. Falkovich, K. Gawedzki, and M. Vergassola, in *New Trends in Turbulence* (Springer, Berlin, 2001).

[109] K. Gawedzki and P. Horvai, Sticky behavior of fluid particles in the compressible Kraichnan model, J. Stat. Phys. **116**, 1247 (2004).

[110] W. E. Vanden Eijnden and E. Vanden Eijnden, Generalized flows, intrinsic stochasticity, and turbulent transport, Proc. Natl. Acad. Sci. USA **97**, 8200 (2000).

[111] C. Federrath and S. Banerjee, The density structure and star formation rate of non-isothermal polytropic turbulence, Mon. Not. R. Astron. Soc. **448**, 3297 (2015).

[112] M. R. Maxey, The gravitational settling of aerosol particles in homogeneous turbulence and random flow fields, J. Fluid Mech. **174**, 441 (1987).

[113] M. Vucelja, G. Falkovich, and I. Fouxon, Clustering of matter in waves and currents, Phys. Rev. E **75**, 065301(R) (2007).

[114] L. Biferale, G. Boffetta, A. Celani, B. J. Devenish, A. Lanotte, and F. Toschi, Multifractal Statistics of Lagrangian Velocity and Acceleration in Turbulence, Phys. Rev. Lett. **93**, 064502 (2004).

[115] D. Bernard, K. Gawedzki, and A. Kupiainen, Slow modes in passive advection, J. Stat. Phys. **90**, 519 (1998).